

C 343-(04)

F-97

ISINN-29

**XXIX International Seminar
on Interaction of Neutrons with Nuclei**



**Fundamental Interactions &
Neutrons,
Nuclear Structure,
Ultracold Neutrons,
Related Topics**

Dubna, 2023

Abstracts

Экз. чит. зала

Joint Institute for Nuclear Research

0343Г(04)

F-97

**FUNDAMENTAL
INTERACTIONS & NEUTRONS,
NUCLEAR STRUCTURE,
ULTRACOLD NEUTRONS,
RELATED TOPICS**

*XXIX International Seminar
on Interaction of Neutrons with Nuclei*

Organized by

Frank Laboratory of Neutron Physics, JINR, Dubna

State Key Laboratory of Intense Pulsed Radiation Simulation
and Effect, NINT, China

School of Nuclear Science and Technology, Lanzhou
University, China

Dubna, May 29 – June 2, 2023

Abstracts

Научно-техническая

библиотека

Dubna 2023

ОИЯИ

155242

УДК 539.125.5(042)
ББК 22.383.2я431+22.383.5я431+22.383.25я431
F97

Organizing Committee

Conference Chair

Valery Shvetsov (JINR) Dongwei Hei (NINT) Ximeng Chen (LZU)

Director of Local Organizing Committee

Walter Furman (JINR) Mengtong Qiu (NINT) Ze'en Yao (LZU)

Scientific Secretary

Alexander Nezvnanov (JINR) Liang Sheng (NINT) Zheng Wei (LZU)

Committee Members

Marina Frontasyeva (JINR)	Xinjian Tan (NINT)	Lei Yang (IMP)
Yuri Kopatch (JINR)	Zhiming Li (NINT)	Guohui Zhang (PKU)
Egor Lychagin (JINR)	Zhongming Wang (NINT)	Yigang Yang (THU)
Ludmila Mitsyna (JINR)	Tianjiao Liang (CSNS)	Liangzhi Cao (XJTU)
Pavel Sedyshev (JINR)	Ruirui Fan (CSNS)	Sheng Wang (XJTU)
Inga Zinicovscaia (JINR)	Jian Gong (CAEN)	Wenbao Jia (NUAA)
Liang Sheng (NINT)	Shilong Liu (CIAE)	Bin Tang (ECUT)
Wei Chen (NINT)	Xichao Ruan (CIAE)	Ze'en Yao (LZU)
Quanlin Shi (NINT)	Zhiqiang Chen (IMP)	Zheng Wei (LZU)

Secretariat

Elena Rusakovich (JINR)	Changlin Lan (LZU)	Xiufeng Weng (NINT)
Tatiana Pikelner (JINR)	Junrun Wang (LZU)	Keqing Gao (NINT)
Elena Kopach (JINR)	Xiaolong Lu (LZU)	Jianxin Zhang (NINT)
Zheng Wei (LZU)	Dan Lin (LZU)	Xiao Liu (NINT)
Daqian Hei (LZU)	Min Zhang (LZU)	Bingjun Li (XJTU)
Dapeng Xu (LZU)	Jiatong Li (LZU)	Yihong Yan (XJTU)

The contributions are reproduced directly from the originals presented by the Organizing Committee.

Fundamental Interactions & Neutrons, Nuclear Structure, Ultracold Neutrons, F79 Related Topics: Abstracts of the XXIX International Seminar on Interaction of Neutrons with Nuclei (Dubna, May 29 – June 2, 2023). — Dubna: JINR, 2023. — 126 p.

ISBN 978-5-9530-0591-3

Фундаментальные взаимодействия и нейтроны, структура ядра, ультрахолодные нейтроны и связанные вопросы: Тезисы докладов XXIX Международного семинара по взаимодействию нейтронов с ядрами (Дубна, 29 мая – 2 июня 2023 г.). — Дубна: ОИЯИ, 2023. — 126 с.

ISBN 978-5-9530-0591-3

ISBN 978-5-9530-0591-3

© Joint Institute for Nuclear Research, 2023

CONTENTS

ISINN-29 Agenda	13
A Follow-up Assessment of Heavy Metal Pollution Recorded in Scleractinian Corals in Southern Red Sea, Hodeidah, Yemen <i>Abdo S.Y., Zinicovscaia I., Yushin N., Dului O.G.</i>	23
Angular Distribution of Prompt Fission γ-Rays <i>Ahmadov G., Berikov D., Kopatch Yu.</i>	24
Ternary Particles of Z from 1 to 6 Emitted in Spontaneous Fission of ^{252}Cf <i>Ahmadov G., Berikov D., Holik M., Kopatch Yu., Ahmadov F., Ajarli K., Nuruyev S., Sadigov A., Madadzada A.</i>	25
Modelling of the Setup for Carbon Analysis of Soil Sample <i>Andreev A.V., and TANGRA Collaboration</i>	26
Transition States, K Number and Mechanism of Nuclear Fission <i>Barabanov A.L., Filonchik P.G.</i>	27
Accelerator-Based Neutron Source VITA for Measuring Nuclear Reaction Cross Sections and for Irradiating Advanced Materials <i>Bikchurina M., Bykov T., Kasatov D., Kolesnikov I., Koshkarev A., Ostreinov G., Savinov S., Shchudlo I., Sokolova E., Sorokin I., Verkhovod G., Taskaev S.</i>	28
Measurement of Cross Sections for Nuclear Reactions of Interaction of Protons and Deuterons with Lithium at Ion Energies 0.4–2.2 MeV <i>Bikchurina M., Bykov T., Kasatov D., Kolesnikov I., Koshkarev A., Ostreinov G., Savinov S., Sokolova E., Taskaev S.</i>	29
Measurement and Calculation of D-T Neutron Induced Reaction Cross Sections <i>Bingyan Liu, Guoyu Tian, Rui Han, Fudong Shi, Zhiqiang Chen</i>	30
Study on Coupled Method of Monte Carlo Code and Discrete Ordinates Code <i>Bo Rong, Zhifeng Li, Wentao Peng, Qi Zheng, Sheng Wang</i>	31
Measurements and Estimates of the Fundamental Symmetry Breaking Effects <i>Bunakov V.E.</i>	32

Investigation of Biomass Waste Catalyst Treated with Sulphuric Acid for Hydrogen Generation <i>Canpolat G.</i>	33
Moss Biomonitoring of Atmospheric Deposition of Trace Elements in Georgia in 2019–2022 <i>Chaligava O., Zinicovscaia I., Peshkova A., Yushin N., Frontasyeva M.V., Vergel K., Grozdov D., Cepoi L.</i>	34
Neutron Reaction Data for Neutron Irradiation Damage Estimation <i>Shengli Chen</i>	35
The Covariance Analysis of $^{nat}\text{Sn}(\alpha, x)^{122}\text{Sb}$ Nuclear Reaction Cross Sections <i>Choudhary M., Singh N., Sharma A., Gandhi A., Upadhyay M., Dasgupta S., Datta J., Kumar A.</i>	36
The Variation of Elemental Content and Bioactive Compounds of <i>Lactuca Sativa L.</i> Grown in the Presence of Multiwall Carbon Nanotubes Functionalized with Fe and Mn Oxides <i>Culicov O., Podar D., Boza C.-L., Lung I., Soran M.-L., Stegarescu A., Opreş O., Ciorîţă A., Nekhoroshkov P.</i>	37
TOF Method Measurements of Neutron Cross Sections in 299 Energy Intervals of the ABBN-93 Group Constants <i>Djilkibaev R.M., Khliustin D.V.</i>	38
A Promising Neutron Source Based on the EG-5 Accelerator at FLNP JINR <i>Doroshkevich A.S., Isayev R.Sh., Mezentseva Zh.V., Kruglyak A.I., Hramco C., Alekseenok Yu.V., Didenko E.A., Chepurchenko I.A., Lichachev A.N., Balasoiu M.A., Popov E., Khiem L.H., Phuc T.V., Tuan P.L., Teofilović V., Ristić I., Balvanović R., Jovanović Z., Mirzayev M.N., Volgina V.S., Mita C., Mardare D., Ksenevich V.K., Appazov N.O., Bakiruly K.B., Chicea D., Oksengendler B.L., Taskaev S.Yu.</i>	39
Study of Neutron Multiplicity in $^{232}\text{Th} (n, f)$ Reaction Using TALYS-1.96 <i>Dubey P., Kumar A.</i>	40
Radioactivity Measurements in Coastal Sediments along the Mediterranean Sea — Egypt <i>Elsenbawy A., Badawy W., Dmitriev A., Kamel N., El-Gamal A., Moussa N.A., Mekewi M.</i>	41

Characteristics of Isotope Distributions Produced in Peripheral Collisions at Fermi Energies as a Function of the Projectile Mass <i>Erdemchîneg B., Klygin S.A., Kononenko G.A., Sereda Yu.M., Vorontsov A.N., Mikhailova T.I.</i>	42
The Development of Setup for a Study of p-Even Correlations in p-Wave Resonances <i>Ergashov A., Kopatch Yu.N., Kuznetsov V.L., Mitsyna L.V., Rebrova N.V., Sedyshev P.V.</i>	43
New Developments in TalysLib Library <i>Fedorov N.A., Pampushik G.V., Tretyakova T.Yu., Grozdanov D.N., Kopatch Yu.N., Ruskov I.N., Skoy V.R., and TANGRA Collaboration</i>	44
On the Significant Enhancement of the Stern-Gerlach Effect for Neutron, Diffracting in a Crystal at Bragg Angles Close to the Right One <i>Fedorov V.V., Voronin V.V., Semenikhin S.Yu.</i>	45
Angular Correlation (n', γ) in Reaction of Neutron's Inelastic Scattering on ^{12}C <i>Filonchik P.G., Kopatch Yu.N., Barabanov A.L., Fedorov N.A., Grozdanov D.N.</i>	46
Measurement of Fission Cross Section and Angular Distributions of Fission Fragments from Neutron-Induced Fission of ^{243}Am in the Energy Range 1–500 MeV <i>Gagarski A.M., Vorobyev A.S., Shcherbakov O.A., Vaishnene L.A., Barabanov A.L., Kuz'mina T.E.</i>	47
Programming of Robotic Arms for Automatic Sample Change on the REGATA Facility of the IBR-2 Reactor <i>Galustov V.A., Grozdov D.S.</i>	48
Investigation of Gamma Dose Changes of High-Degree Occupation Hall of Tehran Research Reactor up to a Few Days after the LOCA Accident <i>Gholamzadeh Z.</i>	49
Technical and Technological Features and Analysis of Painting Specifics from the Resurrection Church of the Derevyanitsky Monastery in Veliky Novgorod (Russia) <i>Glombotskaya N.V., Philippova O.S., Dmitriev A.Yu., Tsarevskaya T.J., Strokovskaya T.E., Lennik S.G.</i>	50
Possibility to Decrease the Losses of Ultracold Neutrons in Material Traps Covered by Liquid Helium <i>Grigoriev P.D., Dyugaev A.M., Sadovnikov A.V., Kochev V.D.</i>	51

Measurement of Yields and Angular Distributions of γ-Quanta from the Interaction of 14.1 MeV Neutrons with Oxygen, Phosphorus and Sulfur Nuclei <i>Grozdanov D.N., Fedorov N.A., Kopatch Yu.N., Skoy V.R., Ruskov I.N., Tretyakova T.Yu., Dabylova S.B., and TANGRA Collaboration</i>	52
Calculation and Simulation of Scattering Intensity Distribution in Neutron Pinhole Image in the Presence of Air <i>Guoguang Li</i>	53
Pulse Research Reactor IBR-3 – New Reflector Concept <i>Hassan A.A., Shabalin E.P.</i>	54
Assessment of Heavy Metal Absorption by Rice Plants in Contaminated Water <i>Hussein M., Badawy W., Dmitriev A.</i>	55
Natural-Based Microspheres for Heavy Metal Remediation from Industrial Wastewater <i>Ibrahim M.A.</i>	56
Characterization of Nano-Sized Titanium Dioxide <i>Imanova G., Melikova S., Aliyev A., Mansimov Z., Mirzayev M., Aliyev S.</i>	57
Determination of the Efficiency of Neutron Detectors in the Experiment of Inelastic Neutron Scattering on ^{12}C <i>Ionkin V.K., and TANGRA Collaboration</i>	58
Sample Analysis by Laser Spectroscopy, ICP-MS, RIMS and INAA <i>Izosimov I.N., Saidullaev B.D., Strashnov I., Vasidov A.</i>	59
Production of Molecular Hydrogen (an Environmentally Friendly Fuel) by the Interaction of γ-Rays with the BeO/H₂O System <i>Jafarov Y.D., Abbasova N.K.</i>	60
Investigation of Molecular Hydrogen in the Nano-SiO₂ (d=15–20 nm)/H₂O System under the Influence of γ-Quanta <i>Jafarov Y.D., Bashirova S.M., Imanova G.T., Aliyev S.M.</i>	61
Natural and Anthropogenic Contamination Analysis of the Sediments Collected around Novaya Zemlya <i>Jakhu R., Yushin N., Chaligava O., Grozdov D., Zinicovscaia I.</i>	62

Theoretical Approach That Simultaneously Describes P-Even T-Odd Asymmetries in Nuclear Fission Reactions by Polarized Neutrons with the Emission of Different Light Particles <i>Kadmensky S.G., Lubashevsky D.E.</i>	63
Status and Prospects of Studies of (γ, f) Reactions at MT-25 Microtron <i>Kamanin D.V., Pyakov Yu.V., Solodov A.N., Zhuchko V.E., Goryainova Z.I., Strekalovsky O.V., Kuznetsova E.A., Zhukova A.O.</i>	64
Revision of the Analytical Properties of Reaction Amplitude near Thresholds on the Example of Muon-Induced Prompt Fission <i>Karpeshin F.F.</i>	65
Observation of Structural Gamma Quanta in Neutron Radiative Decay <i>Khafizov R.U., Kolesnikov I.A., Nikolenko M.V., Tarnovitsky S.A., Tolokonnikov S.V., Torokhov V.D., Trifonov G.M., Solovei V.A., Kolkhidashvili M.R., Konorov I.V.</i>	66
Chromium and Zinc Accumulation and Translocation in Root and Leafy Vegetables Irrigated with Industrial Effluents — a Laboratory Study <i>Kravtsova A.V., Zinicovscaia I.I., Peshkova A.A., Yushin N.S.</i>	67
The Cross-Section Function for the $^{115}\text{In}(\gamma, 2n)^{113\text{m}}\text{In}$ Reaction Determined in the Energy Range up to 23 MeV <i>Krmar M., Jovancevic N., Maletic D., Teterov Y., Mitrofanov S., Knezevic D., Medic Z.</i>	68
Obtaining of Initial Forms for Synthetic Selection of Drought-Resistant Rice Crops Using Radiation Mutagenesis on Fast Neutrons <i>Kruglyak A.I., Aleksiyaynak Y.V., Bakiruly K.B., Appazov N.O., Doroshkevich A.S.</i>	69
Evaluation of a Mistaken Asymmetry in the Projected Experimental Search of Spatial Anisotropy of Gammas from $^{109}\text{Ag}(n, \gamma)$ Reaction at Neutron Energies near 32-eV p-Wave Resonance <i>Kuznetsov V.L., Mitsyna L.V., Rebrova N.V., Sedyshev P.V.</i>	70
Theoretical Study of Resonance Elastic Scattering of Thermal Neutrons on Atomic Nuclei <i>Kuznetsova L.S., Bazhin A.S., Naumenko M.A., Samarin V.V.</i>	71
The Production of the Industrially Significant ^{210}Po Radionuclide Irradiating ^{209}Bi by Neutrons <i>Lim S.</i>	72

Neutronic Chain Reactions in Bismuth Salts <i>Lim S.</i>	73
Pneumatic Transport System REGATA-2 for Neutron and Gamma-Activation Analysis at the IREN Facility at FLNP JINR: Implementation and First Results <i>Lobachev V.V., Dmitriev A.Yu., Borzakov S.B., Smirnov A.A., Zhironkin I.S., Golubkov E.A., Shvetsov V.N.</i>	74
Accelerator Version of the Intensive Lithium Antineutrino Source <i>Lyashuk V.I.</i>	75
The Effect of Gamma-Irradiation on VAC of GaS Monocrystal Doped with Yb <i>Madatov R.S., Tagiyev T.B., Khaliqzadeh A.Sh., Madadzada A.I.</i>	76
Anisotropy in Pre-Fission Neutron Spectra of $^{235}\text{U}(n,f)$ <i>Maslov V.M.</i>	77
Angular Anisotropy of Secondary Neutron Spectra in $^{232}\text{Th}+n$ <i>Maslov V.M.</i>	78
Effect of Angular Momentum Variation in Heavy-Ion Induced Fusion Reaction <i>Mishra U., Dubey P., Choudhary M., Sharma A., Singh N., Dubey N., Kumar A.</i>	79
Environmental Study for Mediterranean Sea Ecosystem Using Seagrass and Algae Samples with Neutron Activation Analysis <i>Nassar N., Kravtsova A., Frontasyeva M., Sherif M.</i>	80
Elemental Ratios in Marine Mussels for Assessment of Ecological Characteristics <i>Nekhoroshkov P.</i>	81
Electrophysical Properties of Thin Films Mn_4Si_7 <i>Normuradov M.T., Dovranov K.T., Imanova G.T., Bekpulatov I.R., Normurodov D.A.</i>	82
Angular Distribution in Fast Neutrons Induced Reactions on ^{64}Zn Isotope <i>Oprea C., Oprea A.I.</i>	83
Applying TalysLib Library for Optimization of Optical Potential Parameters for Neutron Scattering on ^{24}Mg and ^{32}S <i>Pampushik G.V., Fedorov N.A.</i>	84

Examination of Weisskopf–Ewing Approximation for the Determination of (n,α) Reaction Cross-Sections <i>Pandey J., Pandey B., Agrawal H.M., Suryanarayana S.V.</i>	85
Accumulation and Translocation of Copper and Gold Nanoparticles in <i>Petroselinum Crispum</i> Segments under Root Irrigation Conditions <i>Peshkova A., Zinicovscaia I., Cepoi L., Rudi L., Chiriac T., Yushin N.</i>	86
Measurement and Analysis of the Total Thick Target Yield from $^{13}\text{C}(\alpha,n_0)^{16}\text{O}$ Reaction <i>Prusachenko P.S., Bobrovsky T.L., Bokhovko M.V., Gurbich A.F.</i>	87
Observation of New Modes of Multi-Body Decays of $^{252}\text{Cf}(sf)$ <i>Pyatkov Yu.V., Kamanin D.V., Goryainova Z.I., Kuznetsova E.A., Solodov A.N., Strekalovsky O.V., Zhuchko V.E., Zhukova A.O., Wyngaardt S.M.</i>	88
Investigation of Rhenium by Neutrons <i>Ruskov I.N., Kopatch Yu.N., Tretyakova T.Yu., Skoy V.R., Fedorov N.A., Grozdanov D.N., Gundorin N.A., Shvetsov V.N., Sirakov I.A., Jovančević N., Knežević D., Badawi M.S., Thabet A.A., Kumar A., Gandhi A., Sharma A., Dongming W., Hramco C., Borzakov S.B., Zinicovscaia I., Tzvetkova Ch., and TANGRA Collaboration</i>	89
Forward-Backward Asymmetry Effect in the Slow Neutrons Capture by Silver Nucleus <i>Sedyshchev P.V., Oprea A.I., Oprea C., Kuznetsov V.L.</i>	90
Theoretical Works of G.C. Wick in Neutron Physics of 30-ies <i>Sharapov E.I.</i>	91
Experimental Validation of Surrogate Ratio Method for the (n, xp) Cross Sections <i>Sharma A., Pandey J., Dubey P., Mishra U., Dubey N., Gandhi R., Pal A., Baishya A., Sathosh T., Rout P.C., Santra S., Nayak B.K., Chakraborty A., Kumar A.</i>	92
Modified Collimator for Neutron Therapy Applications: Enhancing Narrow Beam Detection of Fast Neutrons <i>Shehada A.M.</i>	93
Monitoring of Airborne Potentially Toxic Elements Using Moss Bag Technique on Territory of Moscow Parks <i>Shvetsova M., Zinicovscaia I.I., Kamanina I.Z., Chaligava O., Nekhoroshkov P.S., Yushin N.S.</i>	94

PFN Multiplicity Variations Measurement at the IREN Facility <i>Sidorova O.V., Zeynalov Sh.</i>	95
Non-Destructive Investigation of Fragments of Mirrors (6th–3th Centuries BCE) from the Necropolis Volna 1 on the Taman Peninsula by Neutron Resonance Capture Analysis <i>Simbirtseva N., Mazhen S., Yergashov A., Sedyshev P.V., Saprykina I.A., Mimokhod R.A.</i>	96
Activation Study of the Metal-Organic Composite Using DT Neutrons <i>Skorkin V.M.</i>	97
A Study of Selected Rurik Dynasty Burials by the NAA Method <i>Strokovskaya T.E., Glombotskaya N.V., Dmitriev A.Yu., Philippova O.S., Lennik S.G.</i>	98
Grouping of Neutron Resonance Positions <i>Sukhoruchkin S.I., Soroko Z.N., Sukhoruchkina M.S.</i>	99
Electron Mass as the Base Parameter of the Standard Model <i>Sukhoruchkin S.I.</i>	100
Thermal Model of the IGR Research Reactor <i>Surayev A.S., Vityuk V.A., Vityuk G.A., Irkimbekov R.A., Zhanbolatov O.M.</i>	101
Ab Initio Study of Energies and Decay Widths of Neutron Resonances <i>Tchuvil'sky Yu. M., Rodkin D. M.</i>	102
Neutron Facilities and Their Applications at China Advanced Research Reactor <i>Tianfu Li, Kai Sun, Dongfeng Chen</i>	103
Accompanied by Alpha-Particles Ternary Fission of Actinides Induced by Thermal Neutrons <i>Titova L.V., Kadmensky S.G., Petrykina E.S.</i>	104
Determining of Thermal and Resonance Neutron Fluxes Distribution for Research of Nuclear Data of Isotopes at the IREN Facility <i>Tran Minh Nhat Le, Borzakov S.B., Dmitriev A.Yu., Hong Khiem Le, Duc Cong Vu, Ngoc Toan Tran</i>	105

Optical Properties and Chemical Composition of Native-Oxide Layer on the Surface of GaAs Irradiated with Noble Gases <i>Tuan P.L., Madadzada A.I., Kulik M., Khaligzadeh A.Sh., Phuc T.V., Kolodynska D., Khiem L.H., Siemek K.</i>	106
Using Rutherford Backscattering Spectroscopy to Investigate ErF₃ Doped CaF₂ Samples <i>Tuan P.L., Kulik M., Stef M., Phuc T.V., My N.T.B., Anh N.N., Zelenyak T.Y., Buse G., Racu A., Doroshkevich A., Khiem L.H., Cong V.D.</i>	107
Moss Survey-2020/2021 in the Regions of Central Russia <i>Vergel K., Zinicovscaia I., Yushin N., Chaligava O., Cepoi L.</i>	108
Experimental Measurement of Neutronic Performance at Neutron Beam Line in CSNS <i>Wang S.L., Zhou B., Yi T.Ch., Shen F., Liang T.J.</i>	109
Neutron Fields Measurements at IREN Facility behind Biological Shielding <i>Yakubov T.R., Timoshenko G.N., Shvetsov V.N.</i>	110
Application of the Yeast <i>Saccharomyces cerevisiae</i> for the Removal of Heavy Metals from Industrial Wastewater <i>Yushin N., Zinicovscaia I.</i>	111
Neutron Activation Analysis in Medical Diagnosis: Current State and Prospects for the Future <i>Zaichick V., Kolotov V.</i>	112
A New Experiment on Study Non-Stationary Neutron Diffraction by Surface Acoustic Waves <i>Zakharov M.A., Kulin G.V., Frank A.I., Rebrova N.V., Gutfreund Ph., Khaydukov Yu.N., Ortega L., Roshchupkin D.V.</i>	113
Study of Discrepancy Phenomenon for Excitation Function of ¹⁹¹Ir(n,2n)^{190g+m1+m2+8.6%^{m3}Ir} <i>Zhang Changfan, Hu Guangchun, Xiang Yongchun, Wenjie, Zhou Haojun, Heyao, Gong Jian</i>	114
Experimental Introduction to Parity Violation and Time Reversal Asymmetry in NOPTREX <i>Zhang M., Snow W.M., Fan R., Tong X.</i>	115

Measurement of the $^{159}\text{Tb}(n, \gamma)$ Cross Section at the CSNS Back-n Facility
Zhang S., Huang M., Wang D.X., Niu D.D., Li X., Li G., Gu M., Huang Y.S., Bai Y., Wang Z.L. 116

Design and Calibration of Large Field of View Dual-Particle Time-Encoded Imager Based on Depth of Interaction Detector
Zhao Dong, Liang Xuwen, Hei Daqian, Jia Wenbao 117

Assessment of Air Pollution in Ulaanbaatar Using Active Moss Biomonitoring Technique
Zinicoyscaia I., Narmandakh J., Yushin N., Peshkova A., Chaligava O., Tsendsuren T., Tserendorj B., Tsogbadrakh Ts. 118

Research on Position Resolution Method of Scintillation Signal Based on CNN+LSTM Network
Wei Cheng, Chengfeng Liu, Wenbao Jia, Weiwei Qu, Yongsheng Lin 119

Group Delay Time in Neutron Optics and Neutron Wave Reflection Time
Frank A.I., Bushuev V.A. 120

The Concept of an UCN Source for Periodic Pulsed Reactor
Frank A.I., Kulin G.V., Kurylev V.A., Popov A.A., Zakharov M.A. 121

The Virtual Character of Spontaneous and Induced (with the Participation of Thermal Neutrons) Ternary Fission of Nuclei with the Emission of Precission Nucleons and Light Nuclei
Kadmensky S.G., Otvodenko Y.O. 122

Active Bryomonitoring of Industrial Atmospheric Fallout Using Different Species of Mosses
Gorelova S.V., Yushin N., Peshkova A., Vergel K., Zinicoyscaia I. 123

Analysis of Multichannel Resonances with Unitary Breit-Wigner and K-Matrix Approaches and with Effective Range M-Matrix Method
Henner V. 124

Status and Prospects of China Spallation Neutron Source CSNS
Tianjiao Liang 125

The Application of Tagged Neutron Method for Elemental Analysis of Material on Conveyors
Alexakhin V.Yu., Komarov I.K., Lichkunova A.I., Razinkov E.A., Rogov Yu.N., Sapozhnikov M.G., Chirikov-Zorin I.E. 126

ISINN-29 Agenda

May 28, Sunday DUBNA Hotel

18:00 – 20:00 Registration

20:00 – 23:00 Welcome party

May 29, Monday International Conference Hall

8:30 – 9:00 Registration

Advanced neutron sources and perspective experiments

	09:00 – 09:15	Welcome/Introduction/Greetings	15 min
1	09:15 – 09:40	Hassan Ahmed Pulse research reactor IBR-3 – new reflector concept.	25 min
2	09:40 – 10:05	Tianfu Li Neutron facilities and their applications at China Advanced Research Reactor.	25 min
3	10:05 – 10:30	Tianjiao Liang Status and prospects of China Spallation Neutron Source CSNS.	25 min
4	10:30 – 10:55	Liang Sheng Discussion on application of High Repetitive Frequency Pulsed Neutron Sources.	25 min

10:55 – 11:25 Coffee break & Conference photo

5	11:25 – 11:50	Jijun Zou Accelerator-driven neutron source and its application prospect.	25 min
6	11:50 – 12:15	Sheng Wang Development status and prospect of Boron Neutron Capture Therapy (BNCT).	25 min
7	12:15 – 12:40	Yigang Yang Neutron and photon bimodal imaging method driven by a single accelerator driven neutron source.	25 min
8	12:40 – 13:05	Kolesnikov Iaroslav Accelerator-based neutron source VITA for measuring nuclear reaction cross sections and for irradiating advanced materials.	25 min

13:05 – 14:00 Lunch

9	14:00 – 14:25	Doroshkevich Aleksandr A promising neutron source based on the EG-5 accelerator at FLNP JINR.	25 min
10	14:25 – 14:45	Yakubov Timur Neutron fields measurements at IREN facility behind biological shielding.	20 min
11	14:45 – 15:05	Shehada Abdullah Modified collimator for neutron therapy applications: enhancing narrow beam detection of fast neutrons.	20 min
12	15:05 – 15:25	Shvedunov Vasily Development of electron accelerators for fundamental research and applied purposes at SINP MSU.	20 min
13	15:25 – 15:45	Lyashuk Vladimir Accelerator version of the intensive lithium antineutrino source.	20 min

15:45 – 16:15 Coffee break

Properties of compound states, nuclear structure

14	16:15 – 16:40	Tchuvil'sky Yury Ab initio study of energies and decay widths of neutron resonances.	25 min
15	16:40 – 17:00	Sukhoruchkin Sergey Electron mass as the base parameter of the Standard Model.	20 min
16	17:00 – 17:20	Soroko Zoya Grouping of neutron resonance positions.	20 min
17	17:20 – 17:40	Kuznetsova Lyubov Theoretical study of resonance elastic scattering of thermal neutrons on atomic nuclei.	20 min
18	17:40 – 18:00	Henner Victor Analysis of multichannel resonances with unitary Breit–Wigner and K-matrix approaches and with effective range M-matrix method.	20 min

May 30, Tuesday International Conference Hall

Nuclear reactor physics

19	09:00 – 09:25	Liangzhi Cao Progresses in advanced computational methods for thermal neutron scattering law data.	25 min
20	09:25 – 09:50	Jingen Chen Th-U fuel cycle in MSR and its simulation methods.	25 min
21	09:50 – 10:10	Surayev Artur Thermal model of the IGR research reactor.	20 min
22	10:10 – 10:35	Lim Solomon The production of the industrially significant ²¹⁰ Po radionuclide irradiating ²⁰⁹ Bi by neutrons.	25 min
23		Neutronic chain reactions in bismuth salts.	
24	10:35 – 10:55	Hoang Thanh-Phi Hung Improving neutronic characteristics of nuclear fuel using burnable particles.	20 min
25	10:55 – 11:15	Gholamzadeh Zohreh Investigation of gamma dose changes of high-degree occupation hall of Tehran research reactor up to a few days after the LOCA accident.	20 min

11:15 – 11:30 Coffee break

Nuclear and related analytical techniques in environmental and material science

26	11:30 – 11:55	Bin Tang Research advances in neutron-gamma fusion logging.	25 min
27	11:55 – 12:20	Zinicovsaia Inga Application of nuclear and related analytical techniques in environmental studies.	25 min
28	12:20 – 12:45	Daqian Hei Research progress on in situ on-line measurement technology of elemental composition of PGNAA.	25 min

12:45 – 13:00 Online poster session #1

13:00 – 14:00 Lunch

Nuclear fission

29	14:00 – 14:25	Zheng Wei Physics study of neutron-induced actinide fission and applications.	25 min
30	14:25 – 14:45	Wengang Jiang Research progress of E-STONE.	20 min
31	14:45 – 15:05	Gagarski Alexei Measurement of fission cross section and angular distributions of fission fragments from neutron-induced fission of ²⁴³ Am in the energy range 1–500 MeV.	20 min
32	15:05 – 15:25	Barabanov Alexey Transition states, K number and mechanism of nuclear fission.	20 min

Fundamental properties of the neutron

33	15:25 – 15:50	Ezhov Victor Neutron lifetime measurements: status and prospects.	25 min
34	15:50 – 16:15	Frank Alexander Group delay time in neutron optics and neutron wave reflection time.	25 min

16:15 – 16:30 Coffee break

Physics of ultracold neutrons

35	16:30 – 16:50	Grigoriev Pavel Possibility to decrease the losses of ultracold neutrons in material traps covered by liquid helium.	20 min
36	16:50 – 17:10	Kulin German The concept of an UCN source for a periodic pulsed reactor.	20 min
37	17:10 – 17:30	Zakharov Maxim A new experiment on study non-stationary neutron diffraction by surface acoustic waves.	20 min

Radiation transportation and simulation

38	17:30 – 18:00	Zhivkov Petar Influence of the high energy neutron cross section data of neutron induced reactions in massive targets.	30 min
39		Fission induced by high energy particles and energy release in massive fissionable targets applied for ADS.	

19:00 – 20:30 Concert

May 31, Wednesday International Conference Hall

9:00 – 10:50 Parallel session #1 (Green Hall, see details below)
“Nuclear data for applied and scientific purposes”

11:15 – 12:35 Parallel session #2 (Green Hall, see details below)
“Neutron radiation effects & Intermediate and fast neutron induced reactions”

14:00 – 17:30 Parallel session #3 (Green Hall, see details below)
“Nuclear and related analytical techniques in environmental and material science”

Fundamental interactions & Symmetries in neutron induced reactions

40	09:00 – 09:20	Ruirui Fan Neutron Optics Time Reversal Experiment (NOPTREX): search for T-violation in polarized neutron transmission through polarized nuclei.	20 min
----	---------------	--	--------

41	09:20 – 9:40	Zhang Mofan Experimental introduction to parity violation and time reversal asymmetry in NOPTREX.	20 min
42	9:40 – 10:00	Bunakov Vadim Measurements and estimates of the fundamental symmetry breaking effects.	20 min
43	10:00 – 10:20	Fedorov Valery On the significant enhancement of the Stern–Gerlach effect for neutron, diffracting in a crystal at Bragg angles close to the right one.	20 min
44	10:20 – 10:40	Xiaojun Sun Statistical theory of light-nucleus reactions and applications.	20 min

10:40 – 11:00 Coffee break

Neutron detection & Methodical aspects

45	11:00 – 11:20	Weixin Zhou Measurement of wide energy range neutrons with a CLYC(Ce) scintillator.	20 min
46	11:20 – 11:40	Wei Cheng Research on position resolution method of scintillation signal based on CNN+LSTM Network.	20 min
47	11:40 – 12:00	Dong Zhao Design and calibration of large field of view dual-particle time-encoded imager based on depth of interaction detector.	20 min
48	12:00 – 12:20	Lipeng Wang Investigation on thermal neutron scattering for Al ₂ O ₃ filter in support of PGNAA in Xi'an Pulsed Reactor.	20 min

12:20 – 13:00 Online poster session #2

13:00 – 14:00 Lunch

49	14:00 – 14:20	Khliustin Denis TOF method measurements of neutron cross sections in 299 energy intervals of the ABBN-93 group constants.	20 min
50	14:20 – 14:40	Skoy Vadim Neutron spin filter based on spin-exchange interaction of ³ He nuclei with the atoms of saturated ferromagnetic.	20 min
51	14:40 – 15:00	Bredikhin Ivan Russian high speed multi-channel digitizers and their possible applications for the neutron detectors research.	20 min

Intermediate and fast neutron induced reactions

52	15:00 – 15:20	Oprea Alexandru Ioan Angular distribution in fast neutrons induced reactions on ⁶⁴ Zn isotope.	20 min
53	15:20 – 15:40	Grozdanov Dimitar Measurement of yields and angular distributions of γ -quanta from the interaction of 14.1 MeV neutrons with oxygen, phosphorus and sulfur nuclei.	20 min
54	15:40 – 16:00	Singh Nand Lal Measurement of ⁸⁵ Rb(n,2n) ^{84m} Rb reaction cross section at different neutron energies.	20 min

16:00 – 16:20 Coffee break

16:20 – 17:15 Online poster session #3

9:00 – 10:50 Parallel session #1 (Wednesday May 31, Green Hall)

“Nuclear data for applied and scientific purposes”

55	9:00– 9:25	Yonghao Chen Measurement of the key cross sections in the Th–U fuel cycle at CSNS Back-n.	25 min
56	9:25 – 9:50	Rong Liu Progress in measurement of fission cross sections at CSNS Back-n white neutron source.	25 min
57	9:50 – 10:10	Changfan Zhang Study of discrepancy phenomenon for excitation function of ¹⁹¹ Ir(n,2n) ^{190g+m1+m2+8.6%^{m3}} Ir.	20 min
58	10:10 – 10:30	Fedorov Nikita New developments in TalysLib library.	20 min
59	10:30 – 10:50	Zhang S. Measurement of the ¹⁵⁹ Tb(n, γ) cross section at the CSNS Back-n facility.	20 min

11:15 – 12:35 Parallel session #2 (Wednesday May 31, Green Hall)

“Neutron radiation effects & Intermediate and fast neutron induced reactions”

60	11:15 – 11:35	Zujun Wang Experiment and simulation research of the displacement damage effects in CMOS image sensors irradiated by neutrons.	20 min
61	11:35 – 11:55	Yuanyuan Xue Single event transient in the pixel array of CMOS image sensor induced by neutrons.	20 min
62	11:55 – 12:15	Shengli Chen Neutron reaction data for neutron irradiation damage estimation.	20 min
63	12:15 – 12:35	Bingyan Liu Measurement and calculation of D–T neutron induced reaction cross sections.	20 min

14:00 – 17:30 Parallel session #3 (Wednesday May 31, Green Hall)

“Nuclear and related analytical techniques in environmental and material science”

64	14:00 – 14:20	Glombotskaya Natalya Technical and technological features and analysis of painting specifics from the Resurrection Church of the Derevyanitsky Monastery in Veliky Novgorod (Russia).	20 min
65	14:20 – 14:40	Strokovskaya Tatiana A study of selected Rurik dynasty burials by the NAA method.	20 min
66	14:40 – 14:55	Simbirtseva Nina Non-destructive investigation of fragments of mirrors (6th–3th centuries BCE) from the necropolis Volna 1 on the Taman Peninsula by neutron resonance capture analysis.	15 min
67	14:55 – 15:10	Canpolat Gurbet Investigation of biomass waste catalyst treated with sulphuric acid for hydrogen generation.	15 min
68	15:10 – 15:25	Izosimov Igor Sample analysis by laser spectroscopy, ICP-MS, RIMS and INAA.	15 min
69	15:25 – 15:45	Lichkunova Albina The application of tagged neutron method for elemental analysis of material on conveyors.	20 min
70	15:45 – 16:00	Phan Luong Tuan Using Rutherford backscattering spectroscopy to investigate ErF ₃ doped CaF ₂ samples.	15 min

155272

Научно-техническая
библиотека
ОИЯИ

16:00 – 16:20 Coffee break

71	16:20 – 16:40	Zaichick Vladimir Neutron activation analysis in medical diagnosis: current state and prospects for the future.	20 min
72	16:40 – 17:00	Skorkin Vladimir Activation study of the metal-organic composite using DT neutrons.	20 min
73	17:00 – 17:15	Madadzada Afag Optical properties and chemical composition of native-oxide layer on the surface of GaAs irradiated with noble gases.	15 min
74	17:15 – 17:30	Ibrahim Medhat A. Natural-based microspheres for heavy metal remediation from industrial wastewater.	15 min

June 1, Thursday International Conference Hall

Intermediate and fast neutron induced reactions

75	09:00 – 09:25	Maslov Vladimir ^{236}Np isomer yields in $^{237}\text{Np}(n,2n)$ and $^{238}\text{U}(p,3n)$ reactions.	25 min
76	09:25 – 09:50	Khryachkov Vitaly Experimental study of the fine structure in the $^{10}\text{B}(n,\alpha)^7\text{Li}$ reaction cross section.	25 min
77	09:50 – 10:10	Choudhary Mahesh The covariance analysis of $^{nat}\text{Sn}(\alpha,x)^{122}\text{Sb}$ nuclear reaction cross sections.	20 min
78	10:10 – 10:30	Sharma Aman Experimental validation of surrogate ratio method for the (n, xp) cross sections.	20 min
79	10:30 – 10:50	Pandey Jyoti Examination of Weisskopf–Ewing approximation for the determination of (n,α) reaction cross-sections.	20 min

10:50 – 11:20 Coffee break

80	11:20 – 11:40	Bikchurina Marina Measurement of cross sections for nuclear reactions of interaction of protons and deuterons with lithium at ion energies 0.4–2.2 MeV.	20 min
81	11:40 – 12:00	Prusachenko Pavel Measurement and analysis of the total thick target yield from $^{13}\text{C}(\alpha,n_0)^{16}\text{O}$ reaction.	20 min
82	12:00 – 12:20	Ruskov Ivan Investigation of rhenium by neutrons.	20 min
83	12:20 – 12:40	Jovancevic Nikola The cross-section function for the $^{115}\text{In}(\gamma,2n)^{113}\text{In}$ reaction determined in the energy range up to 23 MeV.	20 min

12:40 – 14:00 Lunch

14:00 – 15:30 On-site poster session #1

15:30 – 16:00 Coffee

16:00 Picnic (the buses will start from “Dubna” Hotel, Moscovskaya str. 2)

June 2, Friday International Conference Hall

9:00 – 14:45 Parallel session #2 (Friday June 2, Green Hall)

“Nuclear and related analytical techniques in environmental and material science”

Nuclear fission

84	9:00 – 9:30	Pyatkov Yuri Observation of new modes of multi-body decays of $^{252}\text{Cf}(sf)$.	30 min
85	9:30 – 9:55	Solodov Alex Status and prospects of studies of (γ,f) reactions at MT-25 microtron.	25 min
86	9:55 – 10:15	Dubey Punit Study of neutron multiplicity in $^{232}\text{Th}(n,f)$ reaction using TALYS-1.96.	20 min
87	10:15 – 10:50	Maslov Vladimir Angular anisotropy of secondary neutron spectra in $^{232}\text{Th}+n$.	35 min
88		Anisotropy in pre-fission neutron spectra of $^{235}\text{U}(n,f)$.	
89	10:50 – 11:20	Kadmensky Stanislav The virtual character of spontaneous and induced (with the participation of thermal neutrons) ternary fission of nuclei with the emission of pre-scission nucleons and light nuclei.	30 min

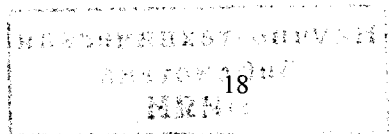
11:20 – 11:40 Coffee break

90	11:40 – 12:10	Lubashevsky Dmitry Theoretical approach that simultaneously describes P-even T-odd asymmetries in nuclear fission reactions by polarized neutrons with the emission of different light particles.	30 min
91	12:10 – 12:35	Titova Larisa Accompanied by alpha-particles ternary fission of actinides induced by thermal neutrons.	25 min
92	12:35 – 13:00	Ahmadov Gadir Ternary particles of Z from 1 to 6 emitted in spontaneous fission of ^{252}Cf .	25 min

13:00 – 14:00 Lunch

93	14:00 – 14:25	Karpeshin Feodor Revision of the analytical properties of reaction amplitude near thresholds on the example of muon-induced prompt fission.	25 min
94	14:25 – 14:45	Berikov Daniyar Angular distribution of prompt fission γ -rays.	20 min

14:45 – 15:00 Closing ceremony



Parallel session #2 (Friday June 2, Green Hall)

“Nuclear and related analytical techniques in environmental and material science”

95	9:00 – 9:15	Yushin Nikita Application of the yeast <i>Saccharomyces cerevisiae</i> for the removal of heavy metals from industrial wastewater.	15 min
96	9:15 – 9:30	Nekhoroshkov Pavel Elemental ratios in marine mussels for assessment of ecological characteristics.	15 min
97	9:30 – 9:50	Elsenbawy Ahmed Radioactivity measurements in coastal sediments along the Mediterranean Sea – Egypt.	20 min
98	9:50 – 10:10	Nassar Noha Environmental study for Mediterranean Sea ecosystem using seagrass and algae samples with neutron activation analysis.	20 min
99	10:10 – 10:30	Abdo Safa A follow-up assessment of heavy metal pollution recorded in scleractinian corals in southern Red Sea, Hodeidah, Yemen.	20 min
100	10:30 – 10:50	Jakhu Rajan Natural and anthropogenic contamination analysis of the sediments collected around Novaya Zemlya.	20 min
101	10:50 – 11:20	Duliu Octavian Assessment of soil pollution with presumably contaminating elements in Moscow recreational areas using instrumental neutron activation analysis.	30 min
102		On the geochemistry of the Danube River sediments (Serbian sector).	

11:20 – 11:40 Coffee break

103	11:40 – 12:00	Nguyen Thi Bao My Evaluation of metal content in BP plants grown on 23 soil samples collected from northern Vietnam.	20 min
104	12:00 – 12:20	Culicov Otilia The variation of elemental content and bioactive compounds of <i>Lactuca sativa L.</i> grown in the presence of multiwall carbon nanotubes functionalized with Fe and Mn oxides.	20 min
105	12:20 – 12:40	Tran Quang-Thien Development of a methodology for analyzing organic carbon and ¹³ C in soil and sediment samples through EA-IRMS.	20 min
106	12:40 – 13:00	Mustafa Hussein Assessment of heavy metal absorption by rice plants in contaminated water.	20 min

13:00 – 14:00 Lunch

107	14:00 – 14:15	Kruglyak Anastasiya Obtaining of initial forms for synthetic selection of drought-resistant rice crops using radiation mutagenesis on fast neutrons.	15 min
108	14:15 – 14:30	Kravtsova Aleksandra Chromium and zinc accumulation and translocation in root and leafy vegetables irrigated with industrial effluents – a laboratory study.	15 min
109	14:30 – 14:45	Chaligava Omari Moss biomonitoring of atmospheric deposition of trace elements in Georgia in 2019–2022.	15 min

Online poster session #1 (Tuesday May 30, 12:45 – 13:00 MSK)

110	12:45 – 12:50	Jianfeng Liang Measurement of cross section of ¹²⁴ Xe(n,p) induced by 14.8 MeV neutron.	5 min
111	12:50 – 12:55	Xianglei Wang Measurement of ²⁵² Cf fission fragment’s mass.	5 min
112	12:55 – 13:00	Chenhui Wang SPICE modeling of neutron displacement damage in bipolar amplifier.	5 min

Online poster session #2 (Wednesday May 31, 12:20 – 13:00 MSK)

113	12:20 – 12:25	Guoguang Li Calculation and simulation of scattering intensity distribution in neutron pinhole image in the presence of air.	5 min
114	12:25 – 12:30	Wang Song Lin Experimental measurement of neutronic performance at neutron beam line in CSNS.	5 min
115	12:30 – 12:35	Yapeng Zhang Influence of different parameters on the performance of Si-PIN detector.	5 min
116	12:35 – 12:40	Xiaodong Zhang Neutron detector based on SiPM and CLYC.	5 min
117	12:40 – 12:45	Zhisheng Huang Study on the energy response of Au–Si surface-barrier detector based on LEAF.	5 min
118	12:45 – 12:50	Upadhyay Mahima Neutron induced reaction cross section measurement for silver with detailed uncertainty quantification.	5 min
119	12:50 – 12:55	Mishra Utkarsha Effect of angular momentum variation in heavy-ion induced fusion reaction.	5 min
120	12:55 – 13:00	Shrivastava Abhinav Kumar Mechanization for reshaping of ancient archeological design into modern structures for “safe restoration of radioactive nuclear fuel” and residue of used nuclear fuel.	5 min

Online poster session #3 (Wednesday May 31, 16:20 – 17:15 MSK)

121	16:20 – 16:25	Khafizov Rashid Observation of structural gamma quanta in neutron radiative decay.	5 min
122	16:25 – 16:30	Oprea Alexandru Ioan Forward-backward asymmetry effect in the slow neutrons capture by silver nucleus.	5 min
123	16:30 – 16:35	Sidorova Olga PFN multiplicity variations measurement at the IREN facility.	5 min
124	16:35 – 16:40	Imanova Gunel Characterization of nano-sized titanium dioxide.	5 min
125	16:40 – 16:50	Jafarov Y.D. Investigation of molecular hydrogen in the nano-SiO ₂ (d=15–20 nm)/H ₂ O system under the influence of γ-quanta.	10 min
126		Production of molecular hydrogen (an environmentally friendly fuel) by the interaction of γ-rays with the BeO/H ₂ O system.	
127	16:50 – 16:55	Khaligzade Aydan The effect of gamma-irradiation on VAC of GaS monocrystal doped with Yb.	5 min

128	16:55 – 17:00	Bekpulatov Ilkhom Electrophysical properties of thin films Mn_4Si_7 .	5 min
129	17:00 – 17:05	Filonchik Polina Angular correlation (n',γ) in reaction of neutron's inelastic scattering on ^{12}C .	5 min
130	17:05 – 17:10	Ionkin Vyacheslav Determination of the efficiency of neutron detectors in the experiment of inelastic neutron scattering on ^{12}C .	5 min
131	17:10 – 17:15	Pampushik Grigory Applying TalysLib library for optimization of optical potential parameters for neutron scattering on ^{24}Mg and ^{32}S .	5 min

On-site poster session #1 (Thursday June 1, 14:00 – 15:30 MSK)

132	Andreev Alexander Modelling of the setup for carbon analysis of soil sample.
133	Batchuluun Erdemchimeg Characteristics of isotope distributions produced in peripheral collisions at Fermi energies as a function of the projectile mass.
134	Ergashov Almat The development of setup for a study of p-even correlations in p-wave resonances.
135	Galustov Vladimir Programming of robotic arms for automatic sample change on the REGATA facility of the IBR-2 reactor.
136	Gorelova Svetlana Active bryomonitoring of industrial atmospheric fallout using different species of mosses.
137	Goryainova Zoya New time pick-off algorithm for time-of-flight measurements with PIN diodes.
138	Kurylev Vladimir A high-field adiabatic spin flipper for strong neutron deceleration.
139	Le Tran Minh Nhat Determining of thermal and resonance neutron fluxes distribution for research of nuclear data of isotopes at the IREN facility.
140	Lobachev Valery Pneumatic transport system REGATA-2 for neutron and gamma-activation analysis at the IREN facility at FLNP JINR: implementation and first results.
141	Makhaldiani Nugzar Long range quarkonium potential for exotic hadrons and nuclei.
142	Mitsyna Liudmila Evaluation of a mistaken asymmetry in the projected experimental search of spatial anisotropy of gammas from $^{109}Ag(n,\gamma)$ reaction at neutron energies near 32-eV p-wave resonance.
143	Peshkova Alexandra Accumulation and translocation of copper and gold nanoparticles in <i>Petroselinum crispum</i> segments under root irrigation conditions.
144	Popov Alexander The problem of neutron transport for a time-focused UCN source.
145	Prozorova Irina Definition of thermophysical parameters of the IGV.1M reactor core with LEU fuel.
146	Sharapov Eduard Theoretical works of G.C. Wick in neutron physics of 30-ies.
147	Shvetsova Margarita Monitoring of airborne potentially toxic elements using moss bag technique on territory of Moscow parks.
148	Vergel Konstantin Moss survey-2020/2021 in the regions of Central Russia.

A FOLLOW-UP ASSESSMENT OF HEAVY METAL POLLUTION RECORDED IN SCLERACTINIAN CORALS IN SOUTHERN RED SEA, HODEIDAH, YEMEN

Safa Y. Abdo^{1,2}, Inga Zinicovscaia¹, Nikita Yushin¹, Octavian G. Duliu^{1,3}

¹Frank Laboratory of Neutron Physics, JINR, Dubna

²Cairo University, Egypt

³University of Bucharest, Faculty of Physics, Romania

This is a continuing study, which provides a representative data on the pollution status of two important harbors in Hodeidah, Yemen, southern Red Sea Al-Luhaya and Al-Saleef. The aim of study was to assess the potential effects of the current war on the studies area, which had been investigated eight years ago before the war has been started. Five species of corals were collected from each harbor and transferred to FLNP at JINR for ICP-AES analysis. Measurements of twelve trace elements (Al, Ba, Cd, Co, Cr, Cu, Fe, Mn, Ni, Pb, Zn, V) the major dominant element Sr and the nonmetal S were conducted. The Preliminary observations showed the order of the trace elements in the samples from Al-Luhaya harbor is Al> Fe > Ba> Mn> Zn> V> Cu> Ni> Cr> Cd> Pb> Co, whereas the order in Al-Saleef is Al> Fe> Ba> Mn> Zn> V> Ni> Cu> Cr> Pb> Co> Cd. The ICP-AES this time allowed to detect Pb and Cd which were not examined in the previous study by INAA. Pb and Cd average values were 0.22±0.07 and 0.45±0.24 µg/g in coral samples from Al-Luhaya and 0.53±0.49 and 0.21±0.27 µg/g in samples from Al-Saleef. Both elements can be derived from anthropogenic sources i.e. sewage input, municipal pipeline, and wastewater. In current study, Fe recorded significantly elevated value in both harbors (195±245 and 233±205 µg/g). These values are higher than values recorded for the same sites eight years ago also higher than values recorded in northern Red Sea and worldwide i.e., Japan, India, and Jordan. These high values may directly result from sunken boats and low surveillance on the old boats and their maintenance. Also, the (Co, Mn, and Zn) elements recorded increased values compared to the previous study (0.14±0.03, 6.8±2.35, 1.85±0.93 µg/g and 0.37±0.33, 11.31±4.56, 4.93±22.39 µg/g) for Al-Luhaya and Al-Saleef respectively. Statistical analyses outputs showed strong correlation between Al, Cr, Fe and V, indicating a sign of anthropogenic pollution level. The concentrations of those elements are higher than the levels of these heavy metals worldwide, i.e. Gulf of Aqaba, Jordan, India and Japan, although this level still lesser than other sites from northern Red Sea, Egypt. As conclusion there is upward increase pollution in the studied areas.

Key words: Red Sea, Yemen, scleractinian corals, Pollution ICP-AES

Angular Distribution of Prompt Fission γ -Rays

Ahmadov G.¹, Berikov D.^{1,2}, Kopatch Yu.¹

¹Joint Institute for Nuclear Research, Dubna, Russia

²Institute of Nuclear Physics of the National Nuclear Center of Kazakhstan, Almaty, Kazakhstan

A more detailed analysis was carried out of the previously obtained experimental data on the measurement of angular correlations of prompt γ -rays emitted by fragments of ^{235}U fission induced by monochromatic polarized neutrons with the energy of 60 meV. Experimental measurements were carried out at the POLI facility of the FRM II reactor (Garching, Germany). The work was published in the journal Romanian Reports in Physics [1].

In our previous studies, using the angular distribution of prompt gamma-rays from binary fission, we studied the effect of rotation of the fission axis, the so-called ROT effect. This effect is expressed in the shift of the anisotropic angular distribution of γ -quanta emitted by excited fission fragments by some small angle $\delta\theta$ relative to the fission axis when the neutron beam polarization direction is reversed. Results on the ROT effect have been published in [2]. As a result of processing these data, in parallel, results were obtained on the angular distribution of gamma quanta relative to the fission axis, which are also of scientific value.

The paper describes a technique for determining the efficiency of gamma radiation detectors by analysis of all possible combinations of angles between the sectors of the fragment detector and all gamma detectors. Such an operation is analogous to rotating a clip of eight detectors and measuring the number of γ -quanta of each detector at the same angle per unit time. As a result, the gamma-ray emission angular anisotropy coefficient relative to the fission axis was $A = 0.1570 \pm 0.0053$, which is in good agreement with the results obtained by other authors for thermal neutrons.

1. G. Ahmadov, D. Berikov, Yu. Kopatch, Angular distribution of prompt fission γ -rays // Romanian Reports in Physics, 75(1), (2023), 202.
2. D. Berikov, G. Ahmadov, Yu. Kopatch, A. Gagarski et. al., Effect of rotation in the gamma-ray emission from 60 meV polarized neutron-induced fission of the ^{235}U isotope // Phys. Rev. C, 104(2), (2021), 024607.

Ternary Particles of Z from 1 to 6 Emitted in Spontaneous Fission of ^{252}Cf

G. Ahmadov^{1,4,5*}, D. Berikov^{1,6}, M. Holik^{2,3}, Yu. Kopatch¹, F. Ahmadov^{4,5}, K. Ajdarli⁴, S. Nuruyev^{1,5}, A. Sadigov^{4,5}, A. Madadzada^{1,4}

¹Joint Institute for Nuclear Research, Dubna, Russia

²Faculty of Electrical Engineering, UWB in Pilsen, Czech Republic

³Institute of Experimental and Applied Physics, CTU, Prague, Czech Republic

⁴Innovation and Digital Development Agency Nuclear Research Department, Baku, Azerbaijan

⁵Institute of Radiation Problems under Ministry of Science and Education, Baku, Azerbaijan

⁶Institute of Nuclear Physics, I Ibragimova, Almaty, Kazakhstan

In this study, ternary particles of Z from 1 to 6 were measured from spontaneous fission of ^{252}Cf using a position sensitive ΔE -E telescope in which the ΔE -E method was used employed to identify the particles. Specific energy loss (ΔE) was measured using transmission type ΔE detectors of thicknesses 16 μm and 150 μm from Micron Semiconductors, while residual energy (E) was measured using a Timepix detector with thicknesses of 300 and 600 μm . It was possible to measure partial-energy spectra of the various ternary particle types due to the thicknesses of Al foil (30 μm) and ΔE detector (16 μm and 150 μm) placed in front of E detectors. The detector system resolution was sufficient for clear separation of ^1H , ^2H , ^3H , ^6He , and ^8He from ^4He . Gaussian function fitting was used to estimate the yields and energy of various particle types from the measured partial-energy spectra. The energy spectrum of ^1H was different from the spectra of other particles because ^1H from $\text{Al}(\alpha, p)$, $\text{Al}(n, p)$, and $\text{Si}(n, p)$ reactions could contribute to the spectra. Talys calculation was used to estimate the contributions of these reactions for H isotopes. The calculations confirmed the presence of ^1H from $\text{Al}(\alpha, p)$ in the ternary ^1H spectrum within the measured energy range. The background-free energy spectra were obtained by subtracting the calculated spectra from the experimental data. The yields and energies of the various ternary particles, including ^1H , ^2H , ^3H , ^4He , ^6He , ^8He , Li, Be, B, and C, were estimated.

Modelling of the Setup for Carbon Analysis of Soil Sample

A.V. Andreev^{1,2*}, and TANGRA Collaboration

¹Joint Institute for Nuclear Research (JINR), Dubna, Russia

²Faculty of Physics, Lomonosov Moscow State University (MSU), Moscow, Russia

* Corresponding author email: andreev.av20@physics.msu.ru

Accurate determining the concentration of carbon in soil today remains an important task for various fields of science. The special role of soil in food production, as well as its participation in regulating the chemical composition of the atmosphere, makes it necessary to research it. Chemical methods are commonly used to determine carbon concentration in soil, but they require specific preparations. Nowadays, nuclear physics offers new methods of soil research, based on so-called neutron gamma analysis. This method involves irradiating the material with neutrons and measuring the characteristic gamma peaks' energies for a particular isotope. By the area of gamma peaks, it is possible to determine the amount of a substance in a sample.

There are two different types of typical system for neutron gamma analysis: mobile setup [1], which can move on field collecting data and stationary setup researching a specimen of material[2]. These configurations consist of a neutron source, a gamma detector (detectors), electronics, and a data acquisition system.

When substances are irradiated with neutrons with the energy of 14 MeV, characteristic gamma peaks occur. The gamma spectrum provides information about the chemical composition of the substance. To determine carbon, a peak corresponding to neutron inelastic scattering on ¹²C with energy of 4440 keV is used.

Calculations of the spectra and installation simulation are done in the Geant4, a toolkit that models the passage of elementary particles through matter using the Monte Carlo method, developed at CERN.[3] Modelled spectra in Geant4 sometimes demonstrate notable deviation from the experimental data. However, this issue can be resolved by separately modeling neutron transport and generating gamma-quantum. This work involves computer modelling of the setup for carbon analysis of soil sample in toolkit Geant4.

1. A. Kavetskiy, G. Yakubova, S. A. Prior et al. //Applied Radiation and Isotopes.–2019.– Vol. 150.–P. 127-134.
2. E.A. Razinkov, V.Y. Aleksakhin, Yu.N. Rogov et al.// Mining Journal.– 2022. No. 2. –P. 51-56.
3. Geant4 v. 10.01, p. 2. https://geant4.web.cern.ch/support/download_archive?page=3.

Transition states, K number and mechanism of nuclear fission

A.L. Barabanov^{1,2,3}, P.G. Filonchik^{1,3}

¹NRC "Kurchatov Institute", Moscow, Russia

²National Research Nuclear University MEPhI, Moscow, Russia

³Moscow Institute of Physics and Technology, Dolgoprudny, Moscow Region, Russia

The spectrum of nuclear transition states at the top of the fission barrier determines many essential features of the fission process. In particular, for a nucleus with spin J and parity π with sufficiently high excitation energy, the greater the density of transition states with the same J and π , the higher the probability of fission. If the fissioning nuclei have a spin orientation, then the angular anisotropy of the fragments relative to the orientation axis is determined by the dependence of the fission probability on the projection K of the nuclear spin onto the deformation axis. Thus, the angular distribution of fragments in fission of highly excited nucleus is determined by the dependence of the density of transition states with given J and π on the additional quantum number K . This dependence is described by the Ericson formula [1] for the level density of deformed nuclei. Accounting for this dependence underlies the statistical approach to describing the angular anisotropy of fission fragments (see, for example, [2]). Ericson's result also explained the significant increase in the number of levels in deformed nuclei; this effect, described by the factor of collective enhancement of the level density, is critical for the correct reproduction of the fission probability.

Transition states are taken into account in the currently used methods for calculating fission cross sections (see, e.g., [3]). However, only in a narrow energy band adjacent to the top of the barrier, certain values of K are assigned to the transition states. At higher excitation energies, the density of transition states with given J and π is calculated with the factor of collective enhancement, but without taking into account the quantum number K . This makes it possible to calculate the cross section for nuclear fission, for example, by neutrons. It is this algorithm that is implemented in modern computer programs for nuclear reactions modelling [3]. However, as was shown (see, e.g., [4, 5]), the modification of such programs allows to reproduce the angular anisotropy of fragments with good accuracy at relatively high excitation energies, where the statistical approach is valid. But to do the same at low excitation energies, it is necessary to take into account the quantum number K , as an important characteristic of transition states, in the entire range of excitation energies of the fissioning nucleus.

We propose a method for such consistent consideration of the quantum number K . Its use will make it possible not only to describe numerous data on the angular distributions of fission fragments by neutrons, but also to reconstruct the characteristics of transition states from these data. This will open the way to increasing the reliability of the description of cross sections for nuclear fission by neutrons.

1. T. Ericson. Nucl. Phys. 1958. V. 6. P. 62.
2. R. Vandenbosch, J.R. Huizenga. Nuclear Fission. - New York, Academic Press, 1973.
3. R. Capote et al. Nucl. Data Sheets. 2009. V. 110. P. 3107.
4. A.S. Vorobyev et al. JETP Lett. 2020. V. 112. P. 323.
5. A. Barabanov et al. EPJ Web Conf. 2021. V.B 256. 00003.

Accelerator-Based Neutron Source VITA for Measuring Nuclear Reaction Cross Sections and for Irradiating Advanced Materials

Bikchurina M., Bykov T., Kasatov D., Kolesnikov I., Koshkarev A., Ostreinov G., Savinov S., Shchudlo I., Sokolova E., Sorokin I., Verkhovod G., Taskaev S.

Budker Institute of Nuclear Physics, ave. Lavrentiev 11, Novosibirsk, Russia

A compact accelerator-based neutron source has been proposed and created at the Budker Institute of Nuclear Physics in Novosibirsk, Russia [1]. An original vacuum insulated tandem accelerator (VITA) is used to provide a dc proton/deuteron beam. The ion beam energy can be varied within a range of 0.3–2.3 MeV, keeping a high-energy stability of 0.1 %. The beam current can also be varied in a wide range (from 1 nA to 10 mA) with high current stability (0.4 %). VITA is used to generate a neutron flux via the ${}^7\text{Li}(p,n){}^7\text{Be}$ or ${}^7\text{Li}(d,n)$ reactions, α -particles through ${}^7\text{Li}(p,\alpha)\alpha$ and ${}^{11}\text{B}(p,\alpha)\alpha$ reactions, 478 keV photons through ${}^7\text{Li}(p,p'\gamma){}^7\text{Li}$ reaction, and positrons through ${}^{19}\text{F}(p,\alpha e^+e^-){}^{16}\text{O}$ reaction. The facility provides a neutron beam of almost any energy range: cold, thermal, epithermal, monoenergetic, and fast. The facility is used to study radiation blistering of metals during ion implantation [2,3], for the development of boron neutron capture therapy [4–16] including use in clinics [17], for radiation testing of steel and boron carbide for ITER [18] and fibers for CERN, for studying the composition of films by back-scattered protons, for in-depth investigation of the ${}^{11}\text{B}(p,\alpha)\alpha$ neutronless fusion reaction, for measuring nuclear reaction cross sections [19–21], *etc.* The report will describe the VITA, present and discuss the results obtained, and declare plans.

This research was supported by Russian Science Foundation, grant No. 19-72-30005.

References

1. S. Taskaev *et al.* *Biology* **10** (2021) 350.
2. A. Badrutdinov *et al.* *Metals* **7** (2017) 558.
3. T. Bykov *et al.* *NIM B* **481** (2020) 62.
4. M. Dymova *et al.* *Cancer Communications* **40** (2020) 406.
5. M. Dymova *et al.* *Radiation Research* **196** (2021) 192.
6. T. Bykov *et al.* *JINST* **16** (2021) P10016.
7. T. Popova *et al.* *Molecules* **26** (2021) 6537.
8. M. Vorobyeva *et al.* *Intern. J. Mol. Sciences* **22** (2021) 7326.
9. V. Kanygin *et al.* *Biology* **11** (2022) 138.
10. A. Zaboronok *et al.* *Pharmaceutics* **14** (2022) 761.
11. K. Aiyyzhy *et al.* *Laser Physics Letters* **19** (2022) 066002.
12. E. Byambatseren *et al.* *JINST* **18** (2023) P02020.
13. D. Novopashina *et al.* *Intern. J. Mol. Sciences* **24** (2023) 306.
14. I. Taskaeva *et al.* *Life* **13** (2023) 518.
15. V. Raskolupova *et al.* *Molecules* **28** (2023) 2672.
16. V. Kanygin *et al.* *Veterinary Sciences* **10** (2023) 274.
17. <https://isnct.net/bnct-boron-neutron-capture-therapy/accelerator-based-bnct-projects-2021/>
18. A. Shoshin *et al.* *Fusion Engineering and Design* **178** (2022) 113114.
19. S. Taskaev *et al.* *NIM B* **502** (2021) 85.
20. M. Bikchurina *et al.* *Biology* **10** (2021) 834.
21. S. Taskaev *et al.* *NIM B* **525** (2022) 55.

Measurement of Cross Sections for Nuclear Reactions of Interaction of Protons and Deuterons with Lithium at Ion Energies 0.4–2.2 MeV

Bikchurina M., Bykov T., Kasatov D., Kolesnikov I., Koshkarev A., Ostreinov G., Savinov S., Sokolova E., and Taskaev S.

*Budker Institute of Nuclear Physics, Novosibirsk, Russia
Novosibirsk State University, Novosibirsk, Russia*

An accelerator based epithermal neutron source for the development of boron neutron capture therapy (BNCT), a promising method for the treatment of malignant tumors, and other various applications is proposed, created and is functioning at the Budker Institute of Nuclear Physics. The neutron source consists of a tandem accelerator of charged particles of an original design, a lithium neutron-generating target for generating neutrons as a result of the ${}^7\text{Li}(p,n){}^7\text{Be}$ or ${}^7\text{Li}(d,n)$ reaction, and a beam shaping assembly for forming a therapeutic beam of epithermal neutrons. The facility is capable of producing α -particles through different reactions.

Knowledge of the cross sections of the reactions $\text{Li}(p, \)$, $\text{Li}(d, \)$ is important both for nuclear data evaluation, as well as within the framework of BNCT and other applications. In this work, the cross sections of the following nuclear reactions were determined with good accuracy for proton/deuteron energies $E = 0.4\text{--}2.2$ MeV: ${}^7\text{Li}(d,n\alpha){}^4\text{He}$, ${}^7\text{Li}(d,\alpha){}^5\text{He} \rightarrow \alpha + n$, ${}^6\text{Li}(d,\alpha){}^4\text{He}$, ${}^6\text{Li}(d,p){}^7\text{Li}$, ${}^6\text{Li}(d,p){}^7\text{Li}^*$, ${}^7\text{Li}(p,\alpha){}^4\text{He}$. The measurements were made using a silicon-based semiconductor α -spectrometer by ion scattering spectroscopy. The energy distribution of alpha particles from a thick layer of boron carbide when irradiated with a proton beam with energies from 0.6 to 2.1 MeV was measured. The results show that it is possible to measure the cross sections of the nuclear reactions ${}^{11}\text{B}(p,\alpha){}^8\text{Be}$ and ${}^{11}\text{B}(p,\alpha)\alpha$ using the thin boron layer. For the deposition of a thin layer of boron on a metal substrate it is proposed to carry out a magnetron sputtering method with preheating of the thermally insulated target by a low-current high-voltage discharge. Measurement of the reaction cross section is important for both boron-proton-capture therapy and for neutron-free thermonuclear energy on the ${}^{11}\text{B}(p,\alpha)\alpha$ reaction.

This research was funded by Russian Science Foundation, grant number 19-72-30005, <https://rscf.ru/project/19-72-30005>.

Measurement and Calculation of D-T Neutron Induced Reaction Cross Sections

Bingyan Liu, Guoyu Tian, Rui Han, Fudong Shi, Zhiqiang Chen

Institute of Modern Physics, Chinese Academy of Sciences, Lanzhou, 730000, China

Radionuclides production cross sections have been measured by using the activation technique and off-line gamma spectrometry for D-T neutron induced reactions. The samples were composed with metal foils of Al, Ti, Mn, Fe, Ni, Zn, Zr, Nb, In, Sn, Ta, Au and Pb. Reactions of $^{90}\text{Zr}(n,2n)^{89}\text{Zr}$ and $^{93}\text{Nb}(n,2n)^{92m}\text{Nb}$ were used to determine the mean neutron energy by the method of cross section ratios. The reactions of $^{93}\text{Nb}(n,2n)^{92m}\text{Nb}$ and $^{27}\text{Al}(n,\alpha)^{24}\text{Na}$ were used to calculate the neutron intensity. Experimental data are compared with evaluated nuclear data of the CENDL-3.2, ENDF/B-VIII.0, JENDL-5, BROND-3.1 and JEFF-3.3 libraries. Besides, these excitation functions were calculated by using theoretical model of the TALYS-1.96 code from thresholds up to 20 MeV with adjusted parameters. And a group of parameters was obtained, which shows better consistency than the default parameters compared with the experimental data.

Study on Coupled Method of Monte Carlo Code and Discrete Ordinates Code

Bo Rong, Zhifeng Li[✉], Wentao Peng, Qi Zheng, Sheng Wang[✉]

School of Nuclear Science and Technology, Xi'an Jiaotong University, Xi'an, 710049, China

[✉]Corresponding author's email: lizhifengedu@163.com

[✉]Corresponding author's email: shengwang@mail.xjtu.edu.cn

Monte Carlo code NECP-MCX has the ability to construct the complex geometries accurately. But slow convergence speed is one of the disadvantages of NECP-MCX, especially for the deep-penetration problems. It usually takes a large amount of time to get a reliable calculation result. Marvin is a three-dimensional discrete ordinates code, which has employed the multi-group and discrete ordinates approximations to discretize the energy and angular variables, respectively. While poor geometric description is one of the disadvantages of Marvin. A method which coupled both the Monte Carlo and the discrete ordinates approaches has been proposed and applied to the transport calculations of beam shaping assembly for BNCT. The results demonstrated that the computing efficiency was significantly enhanced by using this coupled method.

Key words: Monte Carlo code; discrete ordinates code; coupled method

MEASUREMENTS AND ESTIMATES OF THE FUNDAMENTAL SYMMETRY BREAKING EFFECTS

Bunakov V.E.

*Petersburg Nuclear Physics Institute, National Research Center "Kurchatov Institute",
Gatchina, 188300 Russia
E-mail: vadim.bunakov@mail.ru*

All the enhancements of the P-violation effects in γ -transitions between the compound-nucleus states were analyzed in the classical paper [1] by I.S. Shapiro. The source of these effects is the weak interaction V_w leading to the fact that the wave function Ψ_i of this state contains, besides the wave function of a definite parity Ψ_1 , the small admixture Ψ_2 of the opposite parity state

$$\Psi_i = \Psi_1 + \Psi_2 \quad (1)$$

The effect is defined by the ratio of the P-forbidden transition normalized by the total transition value:

$$R = \frac{c(A_a \cdot A_f)}{(A_a + A_f)^2} \approx \frac{cA_f}{A_a} \equiv \frac{n}{d} \quad (2)$$

Here A_a and A_f are the amplitudes of the P-allowed and P-forbidden transitions. The review [1] indicates 3 types of enhancement: 1) kinematical enhancement, 2) structural enhancement and 3) dynamical enhancement. The kinematical enhancement appears when the allowed transition is the magnetic one which is smaller than the forbidden electric of the same multipolarity by the factor $c/v \approx 10$. The structural enhancement appears when the allowed transition amplitude A_a comes to be unusually small due to some suppression caused by the structure of the initial and final states.

One should point that both the kinematical and structural enhancements arise because of the decrease of the denominator d in Eq. (2). Only the dynamical enhancement is caused by the increase of the admixture coefficient:

$$c = \frac{\langle \Psi_2 | V_w | \Psi_1 \rangle}{|E_1 - E_2|} \equiv \frac{v_p}{D}$$

in the numerator n of (2). Here v_p is the weak interaction matrix element, while the enhancement of the admixture for the high-lying excited states is caused by their strongly decreased level spacing.

It is assumed that the largest magnitude of the symmetry-breaking effect allows to measure it with the largest accuracy (i. e. with the smallest relative error). This assumption is shown to be often misleading. Indeed, the experimentally measured value (2) is the ratio of the normally distributed numbers of numerators n to denominators d . Taking their absolute errors to be σ and neglecting the correlation between them, one obtains for the relative error of the measured effect:

$$\frac{\sigma_R}{R} = \sqrt{\frac{\sigma^2}{n^2} + \frac{\sigma^2}{d^2}} \approx \frac{\sigma}{n}$$

We see that the dynamical enhancement of n decreases the relative error and indeed leads to the enhanced accuracy of the effect's measurement. However, the other two enhancements lead only to the slight increase of the relative error and to the poorer accuracy of the effect's measuring. Usefulness of the relative error approach to transmission measurements is also discussed.

1. I.S. Shapiro, *Sov.Phys.Uspokhi*. **95**, 647 (1968).

Investigation of Biomass Waste Catalyst Treated with Sulphuric Acid for Hydrogen Generation

Gurbet CANPOLAT

Department of Chemistry, Faculty of Arts and Sciences, Siirt University, 56100 Siirt, Turkey

Hydrogen is a highly versatile and promising source of energy that has the potential to revolutionize various industries. It is a nature-friendly element that can be easily obtained and has a high calorific value, making it an attractive option for fuel. Moreover, it is portable, and its conversion into different forms of energy makes it a versatile choice for various applications [1-4]. This research aimed to investigate the potential of defatted spent coffee grounds (DSCG) as a catalyst for the generation of hydrogen through the methanolysis of sodium borohydride (NaBH₄). The DSCG was treated with sulphuric acid at a temperature of 75 °C for 24 hours, followed by burning in an oven to create the catalyst. Various acid ratios, burning temperatures, and burning times were assessed to determine the optimal conditions for synthesizing the DSCG-SO₄ catalyst. Results revealed that the optimal conditions were sulphuric acid ratio of 5M, burning temperature of 500 °C, and burning time of 90 minutes. The hydrogen generation rate via methanolysis was studied using different NaBH₄ ratios ranging from 1% to 7.5%, with catalyst concentrations ranging from 0.05 g to 0.25 g, and at various temperatures of 30 °C, 40 °C, 50 °C, and 60 °C. The highest hydrogen generation rate (HGR) using the novel DSCG-SO₄ catalyst was found to be 5278.7, 13002.4, 16325.5, and 28654.7 mLmin⁻¹gcat⁻¹ at temperatures of 30 °C, 40 °C, 50 °C, and 60 °C, respectively. The activation energy for this process was determined to be 33.7 kJmol⁻¹. Overall, the findings suggest that DSCG-SO₄ is a highly efficient catalyst for the methanolysis of NaBH₄ to produce hydrogen, and the optimal conditions for synthesizing the DSCG-SO₄ catalyst are sulphuric acid ratio of 5M, burning temperature of 500 °C, and burning time of 90 minutes. These results could provide insights for the development of more sustainable and cost-effective catalysts for the production of hydrogen.

Keywords: Defatted spent coffee ground, Sodium Borohydride, Methanolysis, Catalyst, Sulphuric Acid

References

1. Kaya, M., *Evaluating organic waste sources (spent coffee ground) as metal-free catalyst for hydrogen generation by the methanolysis of sodium borohydride*. International Journal of Hydrogen Energy, 2019.
2. Duman, F., et al., *A novel Microcystis aeruginosa supported manganese catalyst for hydrogen generation through methanolysis of sodium borohydride*. International Journal of Hydrogen Energy, 2020.
3. Liu, B. and Z. Li, *A review: hydrogen generation from borohydride hydrolysis reaction*. Journal of Power Sources, 2009. **187**(2): p. 527-534.
4. Kaya, M. and M. Bekiroglu, *Investigation of hydrogen production from sodium borohydride methanolysis in the presence of Al₂O₃/spirulina platensis supported Co catalyst*. Avrupa Bilim ve Teknoloji Dergisi, 2019(16): p. 69-76.

Moss Biomonitoring of Atmospheric Deposition of Trace Elements in Georgia in 2019–2022

Chaligava O.^{1,2}, Zinicovscaia I.¹, Peshkova A.^{1,2}, Yushin N.¹, Frontasyeva M.V.¹, Vergel K.^{1,2}, Grozdov D.¹, Cepoi L.^{2,3}

¹Sector of Neutron Activation Analysis and Applied Research, Division of Nuclear Physics, FLNP, Joint Institute for Nuclear Research, Dubna, Moscow Region, Russian Federation

²Doctoral School of Biological, Geonomic, Chemical and Technological Sciences, Moldova State University, Chisinau, Republic of Moldova

³Institute of Microbiology and Biotechnology, Technical University of Moldova, Chisinau, Republic of Moldova

*e-mail: chaligava@jinr.ru

The second moss survey in Georgia was performed between 2019 and 2022. During this survey 96 samples were collected, including 59 samples of *Hypnum cupressiforme* Hedw., 14 samples of *Abietinella abietina* (Hedw.) M. Fleisch., 13 samples of *Pleurozium schreberi* (Brid.) Mitt, and 10 samples of *Hylocomium splendens* (Hedw.) Schimp. A total of 16 elements, among them As, Al, Ba, Cd, Co, Cr, Cu, Fe, Mn, Ni, Pb, S, Sr, V, and Zn, were determined using inductively coupled plasma atomic emission spectroscopy and Hg was determined using direct mercury analyzer (DMA-80 Milestone). In order to assess the trend in elements deposition the obtained results were compared with the previous survey in Georgia [1-3]. Background concentrations were calculated for both surveys individually using iterative 2 σ -technique. Contamination Factor (CF) and Pollution load index (PLI) were calculated and mapped using GIS technology. Contaminated sites and potential sources of pollution were identified.

References

1. Shetekauri, S., Shetekauri, T., Kvlivdze, A., Chaligava, O., Kalabegishvili, T., Kirkesali, E.I., Frontasyeva, M.V., Chepurchenko, O.E., Preliminary Results of Atmospheric Deposition of Major and Trace Elements in the Greater and Lesser Caucasus Mountains Studied by the Moss Technique and Neutron Activation Analysis. In: *Annali di Botanica* 2015, 5, 89–95.
2. Shetekauri, S., Chaligava, O., Shetekauri, T., Kvlivdze, A., Kalabegishvili, T., Kirkesali, E., Frontasyeva, M.V., Chepurchenko, O.E., Tselmovich, V.A., Biomonitoring Air Pollution Using Moss in Georgia. In: *Polish Journal of Environmental Studies*, 2018, 27, 2259–2266.
3. Chaligava, O., Shetekauri, S., Badawy, W.M., Frontasyeva, M.V., Zinicovscaia, I., Shetekauri, T., Kvlivdze, A., Vergel, K., Yushin, N., Characterization of Trace Elements in Atmospheric Deposition Studied by Moss Biomonitoring in Georgia. In: *Archives of environmental contamination and toxicology*, 2021, 80, doi:10.1007/s00244-020-00788-x.

Neutron Reaction Data for Neutron Irradiation Damage Estimation

Shengli Chen

Sino-French Institute of Nuclear Engineering and Technology, Sun Yat-sen University, Zhuhai 519082, China

Neutron reaction data are essential to estimate the neutron irradiation damage. NJOY is the only open-source nuclear data processing code allowing calculating neutron-induced displacement damage cross sections from evaluated nuclear data. However, there are many issues related to NJOY and/or evaluated nuclear data for the damage cross section calculation, such as the inconsistent DPA cross sections and KERMA factors induced by neutron capture reaction with photon data given in MF6 vs. MF12-15, incorrect recoil nuclear data in MF6, and the discrepancy of DPA cross sections using different approaches/nuclear data. The present work briefly introduces the methods of calculating neutron irradiation-induced displacement damage cross sections, summarizes the aforementioned issues, and proposes the corresponding improvements.

The Covariance Analysis of $^{nat}\text{Sn}(\alpha, x)^{122}\text{Sb}$ Nuclear Reaction Cross Sections

Mahesh Choudhary¹, Namrata Singh¹, Aman Sharma¹, A. Gandhi¹,
Mahima Upadhyay¹, S. Dasgupta², J. Datta², and A. Kumar¹

¹Department of Physics, Banaras Hindu University, Varanasi-221005, India

²Analytical Chemistry Division, Bhabha Atomic Research Centre, Variable Energy Cyclotron Centre,
Kolkata-700064, India

E-mail: maheshchoudhary921@gmail.com

In nuclear medicine, a range of radioactive isotopes are employed for therapy and diagnosis. Several types of radioisotopes are produced by alpha-induced reactions with different types of targets. In this study, we have used ^{nat}Sn as a target material and alpha particle as a projectile. The radioisotopes ^{116}Te , ^{117}Te , ^{118}Te , ^{119}Te , ^{120}Te , ^{121}Te , ^{122}Te , ^{123}Te , ^{117}Sb , ^{120}Sb , ^{122}Sb , ^{124}Sb , ^{126}Sb , ^{117}Sn and ^{111}In are produced from $^{nat}\text{Sn}(\alpha, x)$ nuclear reactions. In this work, we have obtained the production cross sections for $^{nat}\text{Sn}(\alpha, x)^{122}\text{Sb}$ nuclear reaction in the incident alpha energy range of about 24–40 MeV. The experiment was performed at K-130 cyclotron, VECC, Kolkata, India for this study. The stacked foil activation technique followed by the offline gamma-ray spectrometry was used to measure the reaction cross-sections for the $^{nat}\text{Sn}(\alpha, x)^{122}\text{Sb}$ nuclear reaction. The uncertainty propagation in the measured cross-sections was calculated using covariance analysis by taking into account the micro-correlation between various variables such as particle number density, efficiency of the HPGe detector, decay constants and counts etc. [1-3]. The measured cross sections for the $^{nat}\text{Sn}(\alpha, x)^{122}\text{Sb}$ nuclear reaction are shown in Fig. 1 along with previous experimental results from EXFOR and theoretical calculations from the TALYS nuclear code. More details about the experimental setup and data analysis will be presented during the conference.

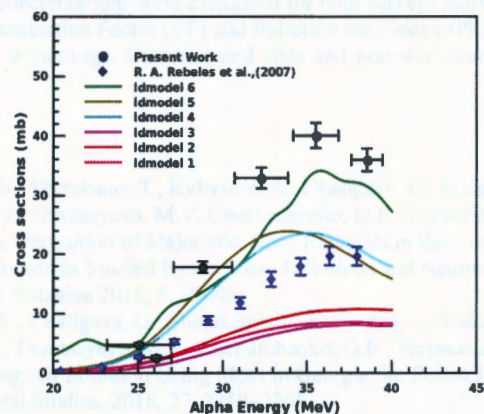


Fig. 1: The measured cross sections for the $^{nat}\text{Sn}(\alpha, x)^{122}\text{Sb}$ nuclear reaction along with previous experimental results from EXFOR and theoretical calculations from the TALYS nuclear code.

References

- [1] M Choudhary *et al.*, Eur. Phys. J. A **58** 95 (2022).
- [2] A. Gandhi *et al.*, Phys. Rev. C **102** 014603 (2020).
- [3] M. Choudhary *et al.*, Journal of Physics G: Nuclear and Particle Physics **50** 015103 (2022).

The Variation of Elemental Content and Bioactive Compounds of Lactuca Sativa L. Grown in the Presence of Multiwall Carbon Nanotubes Functionalized with Fe and Mn Oxides

Otilia Culicov^{1,2}, Dorina Podar³, Camelia-Loredana Boza³, Ildiko Lung⁴,
Maria-Loredana Soran⁴, Adina Stegarescu⁴, Ocsana Opris⁴, Alexandra Ciorita⁴,
and Pavel Nekhoroshkov¹

¹Joint Institute for Nuclear Research, 6 Joliot-Curie, 141980 Dubna, Russia;

culicov@nf.jinr.ru; nekoroshkov@jinr.ru

²National Institute for Research and Development in Electrical Engineering ICPE-CA, 313
Splaiul Unirii, 030138 Bucharest, Romania;

culicov@nf.jinr.ru

³Babeş-Bolyai University, Faculty of Biology and Geology, 1 Kogălniceanu St., 400084, Cluj-
Napoca, Romania;

dorina.podar@ubbcluj.ro; loredana.boza@stud.ubbcluj.ro

⁴National Institute for Research and Development of Isotopic and Molecular Technologies,
67-103 Donat, 400293 Cluj-Napoca, Romania;

ildiko.lung@itim-cj.ro; loredana.soran@itim-cj.ro; adina.stegarescu@itim-cj.ro;

ocsana.opris@itim-cj.ro; alexandra.ciorita@itim-cj.ro

The aim of this work was to evaluate the effect of six nanomaterials, namely CNT-COOH, CNT-MnO₂, CNT-Fe₃O₄, CNT-MnO₂-Fe₃O₄, MnO₂ and Fe₃O₄ on the lettuce. In order to determine the impact of nanomaterials on lettuce, the features of treated samples were compared with appropriate for the control plant, grown in the same conditions of light, temperature and humidity, but without the addition of nanomaterial. The physiological growth parameters, quantity of pigments (chlorophyll a, chlorophyll b, and carotenoids) and total polyphenols, as well as the antioxidant activity and elemental content in lettuce leaves was determined.

The study found that the amount of bioactive compounds varied in the treated plants compared to the control ones, depending on the type of nanomaterial. The same variation was observed in the case of antioxidant capacity. The use of CNTs functionalized with metal oxides increased the levels of wide number of elements in lettuce leaves. On the contrary, metal oxide nanoparticles and CNT functionalized with carboxyl groups induced decrease in content for more elements than increase. Soil amending with MnO₂ affects the content of more than ten elements in leaves of lettuce. Simultaneous application of CNT with MnO₂ and Fe₃O₄ may stimulate the elemental translocation of all elements from root to leaf.

TOF Method Measurements of Neutron Cross Sections in 299 Energy Intervals of the ABBN-93 Group Constants

Djilkibaev R.M., Khliustin D.V.

*Institute for Nuclear Research, Russian Academy of Sciences, Moscow, Russia
denhlustin@gmail.com*

Numerical Monte-Carlo codes, designed for calculation of fast breeder reactors and their radiation shields, in order to achieve high accuracy are currently being transformed to the use of 299-group ABBN-93 constants, instead of classical 28-group ABBN-78 system. The new system, having a smaller step of lethargy, puts forward increased requirements on performance of nuclear physics facilities. On which, in order to provide calculation codes with initial data, experimental measurements of the cross sections for interaction of neutrons with nuclei of fissile, raw and structural materials are carried out.

In this paper we review the possibility of measurements of the 299-group constants at the existing 50 meter, and at projected 500-meter, flight bases of the INES TOF spectrometer of a pulsed spallation neutron source RADEX, installed on the beam of the INR RAS linear proton accelerator.

Results of numerical calculations for the diffusion time of neutron spectrums from tungsten targets of various thicknesses are also presented, within the framework of the analysis for possibility to reduce the duration of neutron flashes.

A Promising Neutron Source Based on the EG-5 Accelerator at FLNP JINR

Doroshkevich A.S.^{1,2}, Isayev R.Sh.^{1,2,3}, Mezentseva Zh.V.¹, Kruglyak A.I.¹, Hramco C.¹, Alekseenok Yu.V.¹, Didenko E.A.⁴, Chepurchenko I.A.¹, Lichachev A.N.¹, Balasoiu M.A.^{1,5}, Popov E.^{1,6,7}, Khiem L.H.^{8,9}, Phuc T.V.^{8,9}, Tuan P.L.^{1,10}, Teofilović V.¹¹, Ristić I.¹¹, Balvanović R.^{12,13,14}, Jovanović Z.¹³, Mirzayev M.N.^{1,3}, Volgina V.S.¹⁵, Mita C.¹⁶, Mardare D.¹⁶, Ksenevich V.K.¹⁷, Appazov N.O.^{18,19}, Bakiruly K.B.¹⁹, Chicea D.²⁰, Oksengendler B.L.²¹, Taskaev S.Yu.^{1,22}

¹ Joint Institute for Nuclear Research, Dubna, Russia;

² NATIONAL RESEARCH NUCLEAR UNIVERSITY MEPhI, Moscow, Russia;

³ National Center for Nuclear Research, Baku, Azerbaijan;

⁴ University "Dubna", Dubna, Russia;

⁵ Horia Hulubei National Institute for R&D in Physics and Nuclear Engineering (IFIN-HH), Romania;

⁶ Institute of Solid-State Physics, Bulgarian Academy of Sciences, Sofia, Bulgaria;

⁷ Institute for Nuclear Research and Nuclear Energy, Bulgarian Academy of Sciences, Sofia, Bulgaria;

⁸ Graduate University of Science and Technology, Vietnam Academy of Science and Technology, Vietnam;

⁹ Institute of Physics, Vietnam Academy of Science and Technology, 10 Dao Tan, Ba Dinh, Ha Noi 10000, Vietnam;

¹⁰ Vietnam Atomic Energy Institute, 59 Ly ThuongKiet, HoanKiem, Hanoi, Vietnam;

¹¹ University of Belgrade, INN Vinča, Laboratory of Physics, Serbia;

¹² National Museum Belgrade, Serbia;

¹³ University of Belgrade- Archaeology Department, Serbia;

¹⁴ National Museum Požarevac, Serbia;

¹⁵ Pskov State University, Sovetskaya str., 21, Pskov, 180000, Pskov region, Russia;

¹⁶ "Alexandru Ioan Cuza" University of Iasi, Faculty of Physics, Iasi, Romania;

¹⁷ Belarusian State University, Minsk, Belarus;

¹⁸ Korkyt Ata Kyzylorda University, Kyzylorda, Kazakhstan;

¹⁹ Kazakh Research Institute of Rice named after I. Zhakhaev, Kyzylorda, Kazakhstan;

²⁰ Department of Environmental Sciences, Physics Group, "Lucian Blaga" University of Sibiu, Romania;

²¹ Ion-Plasma and Laser Technologies Institute after U. Arifov, Tashkent, Uzbekistan;

²² G.I. Budker Institute of Nuclear Physics SB RAS, Novosibirsk, Russia

E-mail: doroh@jinr.ru

In FLNP the project of modernization of the accelerator EG-5 and its experimental infrastructure implement (2024-2026). The purpose of the project: to provide technical feasibility for the implementation of the scientific program of the PTP JINR on the study of reactions with fast quasi-monoenergetic neutrons, the processes of interaction of accelerated charged particles with matter, the development of nuclear-physical methods for studying the elemental composition (Ion-Beam Analysis), inelastic interaction of neutrons with substances, solution of the problems of neutron radiation materials science, implementation of practical applications of neutron physics; provision of technical feasibility for the implementation of a tunable high-power quasi-monoenergetic neutron generator for two energy ranges (12-800 keV; 3.3-5.1 MeV). A relatively intense ion beam (up to 250 μ A) will make it possible to obtain relatively intense neutron fluxes (over 10^8 particles/s cm^2) on a solid-phase lithium target. The use of moderators will make it possible to obtain thermal neutrons. Neutron activation analysis methods are planned to be developed in the EG-5 facility group. With the use of powder nanotechnologies, it is planned to develop portable active neutron optics (bandpass reflectors, tunable notch filters). Neutron fluxes are planned to be used for the needs of reactor materials science. Imitation of atmospheric neutrons (1-5 MeV) will be used to study the mechanisms of radiation mutagenesis of Earth biological forms and the electronics industry (study of the radiation resistance of electronic devices to fast neutron fluxes, equipment calibration).

Study of Neutron Multiplicity in ^{232}Th (n,f) Reaction Using TALYS-1.96

Punit Dubey and Ajay Kumar

Banaras Hindu University, Varanasi, India

E-mail: punitdubey@bhu.ac.in

The nuclear scientific community views ^{232}Th as an option for fuel in the future nuclear energy program. Numerous experimental studies have been conducted to determine the cross-section; however, very few [1–3] have been performed to calculate the total neutron multiplicity above 10 MeV energy. In this work, we have compared the experimental data of average neutron multiplicity at different incident energies from EXFOR with the evaluated data from ENDF/B-VI, JENDL-4.0, and the calculated data from TALYS-1.96 [4], as shown in Fig. 1. The experimental data are in good agreement with the evaluated data from both the ENDF/B-VI and JENDL-4.0 libraries and at high incident energy (14.7 MeV), the TALYS data are also in agreement with the experimental data.

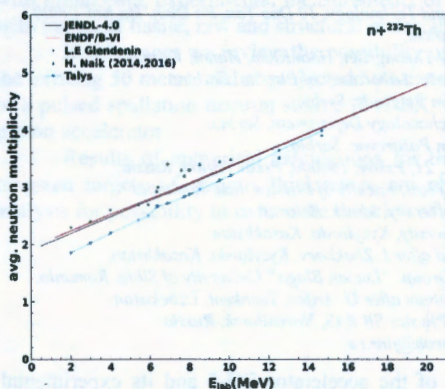


Fig.1: Comparison of experimental and evaluated data w.r.t TALYS calculated data for ^{232}Th (n,f) reaction.

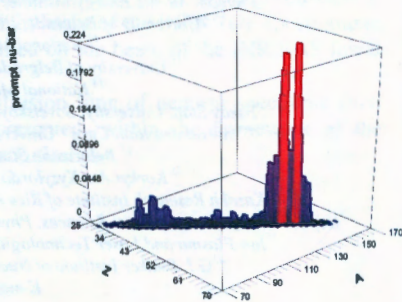


Fig.2: Prompt neutron multiplicity as a function of mass (A) and charge (Z) using TALYS code for ^{232}Th (n,f) reaction at 14.7 MeV.

As shown in Figure 2, we have also calculated the prompt neutron multiplicity at 14.7 MeV as a function of mass (A) and charge (Z). This figure reveals that neutron multiplicity is highly dependent on both Z and A fission fragments, as evidenced by the peaks at $^{54}\text{Xe}^{141,142,143,144}$ and $^{56}\text{Ba}^{146,147,148,149}$. Therefore, it is evident from the graph that neutron multiplicity varies with respect to Z and A. In order to understand the effect of neutron multiplicity, we require additional experimental data at high incident energies, and we intend to perform such experiment in the near future.

The author Punit Dubey is grateful to the Prime Minister Research Fellowship (PMRF) for the financial support for this work.

1. L.E Glendenin *et al.*, (1980), Phys. Rev. C **22**, 152.
2. H.Naik *et al.*, (2014), The European Physical Journal A, **50**, 144.
3. H.Naik *et al.*, (2016), Nuclear Physics A, **952**, 100-120.
4. Arjan Koning, D. Rochman, Nucl. Data Sheets **113**, 2841 (2012).

Radioactivity Measurements in Coastal Sediments along the Mediterranean Sea — Egypt

Ahmed Elsenbawy¹, Wael Badawy^{1,2}, Andrey Dmitriev², Nariman Kamel¹,
Ayman El-Gamal³, N. A. Moussa⁴, Mohammed Mekewi⁴

¹*Radiation Protection and Civil Defense Department, Nuclear Research Center, Egyptian Atomic Energy Authority, Cairo, Egypt*

²*Frank Laboratory of Neutron Physics, Joint Institute for Nuclear Research, 141980 Dubna, Russian Federation*

³*Marine Geology Department, Coastal Research Institute, National Water Research Center, 15, St. Elpharanaa, Elshalalat, 21514 Alexandria, Egypt*

⁴*Department of Chemistry, Faculty of Science, Ain Shams University, Cairo 11566, Egypt*

Naturally occurring radioactive material (NORM) is responsible for most of the radiation exposure of the population. Activity concentrations of naturally occurring U-238, Th-232, K-40, and in 99 sediment samples collected from Egyptian Mediterranean coasts were determined by neutron activation analysis. The average activity concentrations of U-238, Th-232, K-40 and were 10.35 ± 1.85 , 16.29 ± 4.35 , and 196.81 ± 10.25 Bq/kg, respectively. These concentrations are lower than in the upper continental crust (UCC) and shale. The highest levels of U-238 and Th-232 were observed at the Nile branches input to the Mediterranean Sea. The activities in the mouth of the Damietta branch estuary were 157.86 and 349.35 Bq/kg and in the mouth of the Rashid branch were 34.18 and 42.33 Bq/kg for U-238 and Th-232, respectively, which is higher than in the UCC and shale. The various hazard indices such as the radium equivalent, the gamma index, the external hazard as well as the internal hazard show a low radiological exposure with the exception of the area on the Damietta branch that discharges into the sea. The annual effective indoor dose is slightly higher than the dose limit (1 mSv) in the Damietta branch region was 1.428 mSv. The obtained results can serve as a baseline data for potential changes in the future.

Keywords: Radioactivity of NORM, sediments, Mediterranean Sea, hazard indices

Characteristics of Isotope Distributions Produced in Peripheral Collisions at Fermi Energies as a Function of the Projectile Mass

B. Erdemchimeg^{1,2*}, S.A. Klygin¹, G.A. Kononenko¹, Yu.M. Sereda¹,
A.N. Vorontsov¹, T.I. Mikhailova¹

¹Joint Institute for Nuclear Research, 141980, Dubna, Russia

²National University of Mongolia, Nuclear Research Center, Ulaanbaatar, Mongolia

Peripheral collisions at Fermi energies are a tool to obtain new neutron rich isotopes far from stability line and also to make further experiments with secondary beams of exotic projectiles. In this work analysis of characteristics of isotope distributions produced in peripheral collisions at Fermi energies as a function of the projectile mass is presented. Experiments were performed at COMBAS set-up at FLNR Laboratory. The experimental data obtained in reactions with different projectiles: ^{18}O , ^{22}Ne and ^{40}Ar on ^9Be and ^{181}Ta targets are shown. The energies of collisions vary from 35 to 40 MeV per nucleon. Yields of isotope distributions produced in the reactions with different projectiles are compared with each other. The influence of N/Z ratio of the projectile on the N/Z is discussed.

The Development of Setup for a Study of p-Even Correlations in p-Wave Resonances

Ergashov A., Kopatch Yu.N., Kuznetsov V.L., Mitsyna L.V., Rebrova N.V.,
Sedyshev P.V.

Frank Laboratory of Neutron Physics, JINR, Dubna

A design of a setup for studying p-even correlations in p-wave resonances on the 4th channel of the IREN resonant neutron source is presented, and a prototype of the setup is assembled. The ongoing research is aimed at searching for the violation of T-invariance in (n,γ) -reactions.

Time-of-flight spectra were measured for a number of nuclei. Preliminary measuring results have shown that there is a possibility to study p-even correlations in p-wave resonances of lanthanum, bromine, and silver.

New Developments in TalysLib Library

N.A. Fedorov^{1,2}, G.V. Pampushik^{1,2}, T.Yu. Tretyakova^{1,3}, D.N. Grozdanov^{1,4},
Yu.N. Kopatch¹, I.N. Ruskov⁴, V.R. Skoy¹, and TANGRA Collaboration

¹Joint Institute for Nuclear Research (JINR), Dubna, Russia

²Faculty of Physics, Lomonosov Moscow State University (MSU), Moscow, Russia

³Skobeltsyn Institute of Nuclear Physics (SINP), MSU, Moscow, Russia

⁴Institute for Nuclear Research and Nuclear Energy (INRNE), BAS, Sofia, Bulgaria

Two years ago the first report about TalysLib was made on ISINN-28 [1]. Since that moment a lot of new features were added. The main direction of work was implementation of the interfaces to EXFOR and ENDF databases. To do that we have analysed existed tabulated experimental data formats C4 [2] and EXFORTABLES [3] and found advantages and disadvantages of these data sets. Interaction with evaluated data bases in ENDF-VI [4] format was partially implemented for total, elastic and inelastic data.

Another direction of library development is a web-interface creation. Implemented testing version of the web-interface is based on the Flask [5] Python library and realizes optical model parameters changing and plotting of the calculation results.

In the proposed report results of the experimental data sources analysis as well as discussion about implementation of the interaction with the evaluated data library and web-interface development will be presented.

1. N.A. Fedorov, I.D. Dashkov, T.Yu. Tretyakova et al., TalysLib: a ROOT-based library for TALYS integration in data processing. ISINN-28, Book of abstracts.
2. V.V. Zerkin, B. Pritychenko. NIM A, 888 (2018) 31-43.
3. A. Koning. EXFORTABLES-1.0. IAEA NDS Document Series IAEA(NDS)-235, 2020
4. A. Trkov, M. Herman, D. A. Brown. ENDF-6 Formats Manual, National Nuclear Data Center, Brookhaven National Laboratory, 2018.
5. M. Grinberg. *Flask web development: developing web applications with python*. Reilly Media, Inc, 2018.

On the Significant Enhancement of the Stern–Gerlach Effect for Neutron, Diffracting in a Crystal at Bragg Angles Close to the Right One

V.V. Fedorov, V.V. Voronin, S.Yu. Semenikhin

NRC "Kurchatov Institute" – PNPI, Petersburg, Russia

The essential magnification of any external force, acting on a neutron under diffraction at the Bragg angles close to the $\pi/2$ for Laue diffraction case is discussed. Such enhancement is due, on the one hand, to the smallness of the Darwin width compared to the Bragg angle, and, on the other, to the significant slowing down of the neutron in the crystal at diffraction angles close to the right one. As well a neutron trajectory "curvature" in crystal is discussed. With taking into account of the Bormann effect of abnormal absorption it is shown that the Stern-Gerlach effect will be sharply displayed for diffracting neutron in a weak gradient of magnetic field. The enhancement factor for neutron in the crystal can reach magnitudes of about 7 orders in comparison with a "free" neutron in the same field gradient. The experimental results are demonstrated.

Angular Correlation (n', γ) in Reaction of Neutron's Inelastic Scattering on ^{12}C

P.G. Filonchik^{1,4}, Yu.N. Kopatch¹, A.L. Barabanov^{2,3}, N.A. Fedorov¹,
D.N. Grozdanov¹

¹Joint Institute for Nuclear Research, FLNP, Dubna, Russia

²NRC "Kurchatov Institute", Moscow, Russia

³National Research Nuclear University MEPhI, Moscow, Russia

⁴Moscow Institute of Physics and Technology, Dolgoprudny, Moscow Region, Russia

The knowledge about (n, γ) and ($n, n'\gamma$) correlations is very useful for understanding of the neutron inelastic scattering process and estimations of the impacts of direct and compound (CN) mechanisms on the nuclear reaction. A detailed review of the CN approach is presented in the paper [1], for direct - in [2]. Formalism described in [1] works quite well for low-energy particle scattering when CN is dominant but fails to describe 14 MeV neutrons scattering [3]. There are not too many experiments with ($n, n'\gamma$) correlation measurements with 14 MeV neutrons, and the largest part of them were made more than 40 years ago with a quite poor accuracy [4]. Thus, it is interesting to make new experiments to survey this correlation with higher statistics and angular resolution. At this moment the experiment with tagged neutrons is being carried out on TANGRA with a carbon target. It is planned to extract data about (n', γ) correlation from this experiment. To estimate the needed measurement time and optimize the experimental setup for future measurements we are working on the angular correlation (n', γ) modelling in Geant4's, since now there is no information about (n', γ) anisotropy. Modelling results are compared with experimental results.

In the future, the angular anisotropy of emitted γ relative to scattered neutron n' perpendicular to the plane reaction might become a question of interest.

1. E. Sheldon. Rev. Mod. Phys. 1963. V.35 P. 795.
2. A.B. Clegg and G.R. Satchler. Nucl. Phys. 1961. V. 27. P. 431.
3. N.A. Fedorov. Studying of 14.1 MeV neutrons scattering on light nuclei. Master thesis. MSU, Moscow, 2017.
4. J. Zamudio, L. Romero, R. Morales. Nuclear Physics. 1967. V. A96. P. 449.

Measurement of Fission Cross Section and Angular Distributions of Fission Fragments from Neutron-Induced Fission of ^{243}Am in the Energy Range 1–500 MeV

A.M. Gagarski¹, A.S. Vorobyev¹, O.A. Shcherbakov¹, L.A. Vaishnena¹,
A.L. Barabanov^{2,3,4}, T.E. Kuz'mina⁵

¹B.P. Konstantinov Petersburg Nuclear Physics Institute of National Research Centre "Kurchatov Institute", Gatchina, Russia;

²National Research Centre "Kurchatov Institute", Moscow, Russia;

³National Research Nuclear University "MEPhI", 115409, Moscow, Russia;

⁴Moscow Institute of Physics and Technology, 141701, Dolgoprudny, Moscow Region, Russia;

⁵V.G. Khlopin Radium Institute, St.-Petersburg, Russia

Fission cross sections and angular distributions of fission fragments from the neutron-induced fission of ^{243}Am have been measured in the energy range 1–500 MeV at the neutron time-of-flight spectrometer GNEIS based on the 1-GeV proton synchrocyclotron of the NRC KI - PNPI (Gatchina) used as pulsed neutron source. The description of the original experimental set-up consisted of two MWPC counters with targets of ^{243}Am and ^{235}U is given, as well as the some principal details of experimental data processing.

The fission cross section of ^{243}Am was obtained by ratio method using ^{235}U as a standard. The anisotropy of fission fragments $W(0^\circ)/W(90^\circ)$ was deduced from the experimental data on angular distributions of ^{243}Am . The anisotropy data are of particular interest because in the investigated energy range 1–500 MeV other experimental data are practically absent, despite the ever-growing interest in this field, stimulated by the creation of new nuclear technologies. This work is a part of the program dedicated to investigations of neutron-induced fission at intermediate energies.

Programming of Robotic Arms for Automatic Sample Change on the REGATA Facility of the IBR-2 Reactor

Galustov V.A, Grozdov D.S.

Joint Institute for Nuclear Research, Joliot-Curie Str., 6, Dubna, Moscow region, Russia

Performing of neutron activation analysis at the REGATA facility of the IBR-2 reactor is associated with irradiation and measurement of the large number of samples. In 2022, four robotic arms (KUKA KR10 R1100, Germany) were purchased in order to ensure simultaneously measurement of samples and to replace outdated sample changers. The replacement of the changing devices created the need for a new software since the current one does not support the introduction of new devices.

The new software is based on the object-oriented language (OOL) C# and the .NET Framework. The use of OOL allowed to create a separate class for manipulator control. This will make it easy to upgrade the program if the number of robots will change: objects of this class are created or deleted. The .Net Framework will avoid the problem of outdated software libraries by keeping them up to date. This ensures that the program will run on modern versions of Windows OS.

The created software allows users to simultaneously control the operation of all manipulators and set individual measurement parameters (measurement time and number of samples) for each robot. The program was designed as a graphical application for the convenience of users. The GUI was developed using the UI framework Windows Forms.

INVESTIGATION OF GAMMA DOSE CHANGES OF HIGH-DEGREE OCCUPATION HALL OF TEHRAN RESEARCH REACTOR UP TO A FEW DAYS AFTER THE LOCA ACCIDENT

Gholamzadeh Z.

*Reactor and Nuclear Safety Research School,
Nuclear Science and Technology Research Institute (NSTRI),
Tehran, Iran
Cadmium_109@yahoo.com, zgholamzadeh@aeoi.org.ir*

Loss Of Coolant Accident (LOCA) investigation of Tehran Research Reactor (TRR) exactly at the time when the reactor has been operating at its maximum power (5 MW) and the consequent impact of it on the reactor operators and other people in the vicinity of the reactor containment is a very important subject which should be carefully evaluated. The effects of the events have been there since the first nuclear reactor built in 1954. It should be noted that according to the documents, high dose rate (1–2 Sv/h) has been reported inside the rooms of the damaged Chernobyl nuclear power plant after the accident. Considering the different nuclear accidents and the regularity body concerns, the present work aimed to calculate the gamma dose rates in high-degree occupation portions from the TRR hall after LOCA accident. The main purpose of upgrading the technical documentation of the reactor is to ensure the safe operation of the reactor and to ensure the safety of the whole site in such accidents. In the present work, the dose rate received by the staff working in the TRR entrance room after the LOCA accident was investigated when the situation resulted in the complete baring of the nuclear core. MCNPX code was used to model the TRR containment with the most details.

Keywords: Gamma dose rate, LOCA, Tehran Research Reactor

Technical and Technological Features and Analysis of Painting Specifics from the Resurrection Church of the Derevyanitsky Monastery in Veliky Novgorod (Russia)

N.V. Glombotskaya¹, O.S. Philippova¹, A.Yu. Dmitriev^{1*}, T.J. Tsarevskaya²,
T.E. Strokovskaya¹, S.G. Lennik³

¹Frank Laboratory of Neutron Physics, Joint Institute for Nuclear Research, Dubna, Moscow Region, Russia

²State Institute for Art Studies, Moscow, Russia

³Institute of Nuclear Physics, Ibragimov str., 1, Almaty, Republic of Kazakhstan

* andmitriev@jinr.ru

The Resurrection Church of the Derevyanitsky Monastery in Veliky Novgorod (Russia) is a cultural heritage site of federal significance. It was built in 1335 at the direction of Novgorod Archbishop Moses and painted in 1348. During its existence, the monument was repeatedly rebuilt, and only the main part from the 17th century has survived to this day. Currently, the church building is rapidly going to decay and urgently needs professional restoration. In 2013-2015, an archaeological expedition from St. Petersburg State University worked on the site, where a lot of fragments of wall paintings were discovered, presumably dated 1348. Within this work, 71 archaeological fragments were studied at the Laboratory of Neutron Physics of the Joint Institute for Nuclear Research. Samples were analyzed using neutron activation and X-ray fluorescence analysis, infrared and Raman spectroscopy, stratigraphy, and polarized microscopy. In addition, statistical analysis was used. As a result of the study, the set of main pigments used was revealed: yellow and red ochres, cinnabar, green earth, azurite, carbon black and lime white. The presence of blue smalt pigment was unexpected and did not correspond to the preliminarily dating all fragments to 14th century. Also the structure of the wall painting was determined. In most cases, a levelling layer was applied over the plaster. The number of color layers varied from 1 to 3. Using neutron activation analysis, it was found out that lime is the main component of the plaster bases. The statistical analysis of the mass fraction of the main macrooxides clearly separated the "lower" and "upper" plaster layers. According to infrared spectroscopy, protein was found in the color layers as a binder. Thus, it was established that the painting was made in the tempera technique.

Possibility to Decrease the Losses of Ultracold Neutrons in Material Traps Covered by Liquid Helium

P.D. Grigoriev^{1,2}, A.M. Dyugaev¹, A.V. Sadovnikov³, V.D. Kochev²

¹L.D. Landau Institute for Theoretical Physics, 142432, Chernogolovka, Russia

²National University of Science and Technology "MISIS", 119049, Moscow, Russia

³Lomonosov Moscow State University, 119991, Russia

We propose a method to increase both the neutron storage time and the precision of its lifetime measurements by at least tenfold [1,2]. The storage of ultracold neutrons (UCN) in material traps now provides the most accurate measurements of neutron lifetime and is used in many other experiments. The precision of these measurements is limited by the interaction of UCN with the trap walls. We show that covering trap walls with liquid helium may strongly decrease the UCN losses from material traps. ⁴He does not absorb neutrons at all. Superfluid He covers the trap walls as a thin film, ≈ 10 nm thick, due to the van der Waals attraction. However, this He film on a flat wall is too thin to protect the UCN from their absorption inside a trap material. By combining the van der Waals attraction with capillary effects we show that surface roughness may increase the thickness of this film much beyond the neutron penetration depth, ≈ 33 nm. It is demonstrated that triangular roughness is more efficient than rectangular for the reduction of the rate of loss of ultracold neutrons [2]. Triangular roughness is more easily implemented technically, as such diffraction gratings are fabricated industrially. Thus, not only the bottom but also a rough side wall of UCN trap holds the required amount of ⁴He by the capillary effects. To increase the thickness of liquid He on the very edges of rough side walls and to cover the entire UCN trap surface by sufficiently thick helium films we also propose to apply an electric voltage to these rough side walls of UCN traps. This completely protects UCN from being absorbed inside the trap walls. We estimate the required electric field and voltage for several possible designs of UCN traps. This improvement may give rise to a new generation of ultracold neutron traps with very long storage time. Using liquid He for UCN storage requires low temperature, $T < 0.5$ K, to avoid neutron interaction with He vapor, while the neutron losses due to the interaction with surface waves are small and can be accounted for using their linear temperature dependence [4].

The work is supported by the Russian Science Foundation grant # 23-22-00312.

References

1. P.D. Grigoriev, A.M. Dyugaev, *Superfluid helium film may greatly increase the storage time of ultracold neutrons in material traps*, Phys. Rev. C **104**, 055501 (2021).
2. P.D. Grigoriev, A.M. Dyugaev, T.I. Mogilyuk, A.D. Grigoriev, *On the Possibility of a Significant Increase in the Storage Time of Ultracold Neutrons in Traps Coated with a Liquid Helium Film*, JETP Letters, **114**(8), 493 (2021).
3. P.D. Grigoriev, A.V. Sadovnikov, V.D. Kochev, A.M. Dyugaev, *Improving of ultracold neutron traps coated with liquid helium using capillarity and electric field*, arXiv:2303.04429.
4. P.D. Grigoriev, O. Zimmer, A.D. Grigoriev, T. Ziman, *Neutrons on a surface of liquid helium*, Phys. Rev. C **94**, 025504 (2016).

Measurement of Yields and Angular Distributions of γ -Quanta from the Interaction of 14.1 MeV Neutrons with Oxygen, Phosphorus and Sulfur Nuclei

D.N. Grozdanov^{1,2}, N.A. Fedorov¹, Yu.N. Kopatch¹, V.R. Skoy¹, I.N. Ruskov², T.Yu. Tretyakova^{1,3}, S.B. Dabylova¹, and TANGRA Collaboration

¹Joint Institute for Nuclear Research (JINR), Dubna, Russia

²Institute for Nuclear Research and Nuclear Energy (INRNE) of Bulgarian Academy of Sciences (BAS), Sofia, Bulgaria

³Skobeltsyn Institute of Nuclear Physics (SINP), MSU, Moscow, Russia

*Corresponding author E-mail: dimitar@nf.jinr.ru

The study of inelastic scattering of fast neutrons by atomic nuclei is of great importance for fundamental and applied neutron-nuclear physics. Reactions induced by neutrons are the unique source of information for describing the processes of strong interaction between nucleons. Inelastic scattering processes are used to study the characteristics of excited states of target nuclei [1]. The practical use of the $(n,n'\gamma)$ reaction requires the expansion and refinement of experimental data on this process. Research on the inelastic scattering of fast neutrons has recently become more active in connection with new prospects for the production of nuclear energy using fast neutron reactors.

The purpose of the experiment was to refine the available data on the yields and angular distributions of γ -rays from inelastic scattering of 14.1 MeV neutrons by natural composition of oxygen, phosphorus and sulfur nuclei. The work was carried out within the framework of the scientific program of the international TANGRA (TAGged Neutrons and Gamma RAys) project at Frank Laboratory of Neutron Physics of the Joint Institute for Nuclear Research in Dubna (Russia).

Inelastic scattering was studied by the Tagged Neutron Method [2], in which neutrons with an energy of 14.1 MeV produced in the $d(t,\alpha)n$ reaction are "tagged" by detecting alpha particles. Gamma quanta from the $(n,n'\gamma)$ reaction were recorded by the "Romashka" multidetector system [3]. Experimental data are shown and discussed in comparison with previously published data.

1. W. Hauser and H. Feshbach. The Inelastic Scattering of Neutrons, Phys. Rev., 1952, vol. 87, p. 366., <https://doi.org/10.1103/PhysRev.87.366>
2. I.N. Ruskov, Yu.N. Kopatch, V.M. Bystritsky et al. Physics Procedia, vol. 64, 2015, pp. 163-170, ISSN 1875-3892, <https://doi.org/10.1016/j.phpro.2015.04.022>.
3. D.N. Grozdanov, N.A. Fedorov, Yu.N. Kopatch et al. IJPAP vol. 58(05), pp. 427-430, 2020, <http://nopr.niscair.res.in/handle/123456789/54739>.

Calculation and Simulation of Scattering Intensity Distribution in Neutron Pinhole Image in the Presence of Air

Guoguang Li

Department of Engineering Physics, Tsinghua University, Beijing 100084, China

lgg20@mails.tsinghua.edu.cn

The intense pulsed neutron radiation image diagnostic system mainly consists of tungsten pinhole collimator, plastic scintillator and image recording system. In the existing literature, the scattering intensity distribution in neutron pinhole image is considered as a uniform background, and the neutrons attenuation and scattering in air are ignored. In this paper, we propose a novel program for calculating the scattering intensity distribution on the incident plane of plastic scintillation, which takes into account the presence of air. Simulation work is also carried out in Geant4, and the calculation results are compared with the simulation results, which show that the two methods are consistent. The results show that for the practical pinhole geometry, due to the long distance of pinhole imaging, the attenuation and scattering of neutrons by air not only cannot be ignored, but also becomes the main contribution of scattering intensity. For a point neutron source, the scattering intensity distribution due to pinhole attenuation is basically uniform, which has no negative effect on the image diagnosis. However, the scattering neutron intensity due to air attenuation is not evenly distributed and its shape is similar to the through-view aperture of the point source. In addition, we found that the relative scattering intensity caused by pinhole attenuation was inversely proportional to the square of the image distance, such as changing the image distance from 1m to 16m the scattering intensity is changed from 5.74×10^{-7} to 1.83×10^{-9} , while the relative scattering intensity caused by air attenuation does not change with the image distance and it is almost stable at 3.42×10^{-6} . Further studies indicate that the scattering intensity received by the incident plane of scintillation is almost all from the scattering of air within the first half meter of plastic scintillation. In order to reduce the influence of air scattering on neutron pinhole image diagnosis, one possible method is to put the image diagnosis system in a vacuum chamber. The results of this paper are instructive for the scattering evaluation and shielding of neutron pinhole image.

Keywords: scattering intensity distribution, neutron pinhole image, air attenuation, novel calculation program, Geant4 simulation

Pulse Research Reactor IBR-3 – New Reflector Concept

Hassan A.A.^{1,2}, Shabalin E.P.¹

¹Joint Institute for Nuclear Research (JINR), Dubna, Moscow Region, 141980, Russia

²National Research Nuclear University "MEPhI," Moscow, Russia

Periodic Pulsed research reactors IBR-2 type in Dubna is the most effective source of slow neutrons extracted beams for studying various structures by diffraction, small-angle scattering, reflectometer, inelastic scattering and neutron diffraction, due to a short neutron pulse and a high average flux of up to $10^{14} \text{ cm}^{-2} \cdot \text{s}^{-1}$. At the same time, due to the specificity of the kinetics, fluctuations in the power energy of pulses in such a reactor are tens of times higher than in stationary reactors and create problems for the control of the apparatus. This paper proposes and substantiates a method for a significant reduction in the level of fluctuations in power pulses of such reactors using the example of the IBR-3 (NEPTUNE) pulsed reactor project with the threshold Np-237 isotope as a nuclear fuel.

ASSESSMENT OF HEAVY METAL ABSORPTION BY RICE PLANTS IN CONTAMINATED WATER

Mustafa Hussein^a, Wael Badawy^{b,c}, Andrey Dmitriev^b

^aChemistry Department, Faculty of Science, Cairo University, 1 Gamaa Street, Giza, P.O. Box 12613, Egypt

^bFrank Laboratory of Neutron Physics, Joint Institute for Nuclear Research, Dubna 141980, Russia

^cRadiation Protection and Civil Defense Department, Nuclear Research Centre, Egyptian Atomic Energy Authority, Cairo 13759, Egypt

The presence of heavy metals in groundwater and surface water used for agriculture has become a significant environmental problem. Industrial activities that release heavy metals into the environment through the discharge of industrial effluents are one of the sources responsible for this problem. Heavy metals such as Fe, Mn, Cr, Zn, and Al, which are present in food crops, can have a negative impact on human health. Neutron activation analysis (NAA) was used in this study to examine the uptake of these heavy metals by rice plants in contaminated water at two different pH values, i.e., pH 1 and pH 7. The concentration of heavy metals in the contaminated water was measured using ICP-MS to ensure that the heavy metals were transferred to the soil or rice plants during the five-day period. The rice plants were then separated into roots and shoots, and neutron activation analysis was used to examine the distribution of heavy metals in the components studied. The average heavy metal concentration in the shoots at pH 1 was $\text{Fe} > \text{Mn} > \text{Al} > \text{Zn} > \text{Cr}$, while at pH 7 it was $\text{Mn} > \text{Al} > \text{Fe} > \text{Zn} > \text{Cr}$. Of these, Mn had the highest TF (transfer factor) value of 0.88 at pH 1, while Cr had the lowest TF value of 0.02. Similarly, Mn had the highest TF value of 0.39 at pH 7, while Cr had the lowest TF value of 0.01. The study concludes that heavy metals mobility depends on water pH which direct effect on soil pH, so neutral water should be preferred for rice plants to prevent transferring of heavy metals to the plant, which could lead to health risks.

Keywords: industrial activities, heavy metals, pollution (water, soil, plant), rice plants, neutron activation analysis.

Natural-Based Microspheres for Heavy Metal Remediation from Industrial Wastewater

Medhat A. Ibrahim

Molecular Spectroscopy and Modeling Unit, Spectroscopy Department, National Research Centre, 33 El-Bohouth St., 12622, Dokki, Giza, Egypt

Email: ma.khalek@nrc.sci.eg

Pollutants such as heavy metals find its way to water canals in Egypt according to both transport and insufficient treatment of industrial wastewater. To control this problem, it is important for continuous monitoring of the pollutants in the environment, this process is an essential process among many other steps for environmental impact assessment strategy EIAS. Various spectroscopy tools could be used in addition to some nuclear facilities, such as neutron activation analyses to determine the concentration of pollutants in the environment. In this presentation, the problem of heavy metals in the aquatic environment of the Nile is pointed out with a possible solution based on natural resources.

Consequently, cost effective, ecofriendly natural materials such as bio-polymers and aquatic plants are suggested after a certain treatment to control heavy metal from polluted water. Such materials are recognized as beads and/or microsphere.

The overall aim of such microsphere is to be applied for controlling industrial discharge to permit their possible transport of pollutants into the aquatic environment. Furthermore, compact device has been designed and implemented to deliver mass production of these microspheres.

Keywords: Spectroscopy, Neutron activation analyses, Microsphere; Bio-polymers; Heavy metals; Remediation.

CHARACTERIZATION OF NANO-SIZED TITANIUM DIOXIDE

¹Gunel Imanova, ¹Sevinj Melikova, ¹Anar Aliyev, ¹Zaur Mansimov,
^{1,2}Matlab Mirzayev, ¹Salimkhan Aliyev

¹*Institute of Radiation Problems, Ministry of Science and Education of the Republic of Azerbaijan, Baku AZ-1143, B. Vahabzade 9, Azerbaijan*

²*Joint Institute for Nuclear Research, Dubna, Russia*

Titanium dioxide pigments are finely divided white powders which are chemically inert or unreactive, in contrast to all commonly used materials for paper filling or coating systems, and are used to increase opacity. There are three naturally occurring crystallographic forms of titanium dioxide: anatase, brookite and rutile. Rutile is the most common and stable form. Its structure, shown in Figure 1 (a), is based on a slightly distorted hexagonal close-packing of oxygen atoms with the titanium atoms occupying half of the octahedral interstices. Anatase and brookite are both based on cubic packing of the oxygen atoms, but the coordination of the titanium is again octahedral.

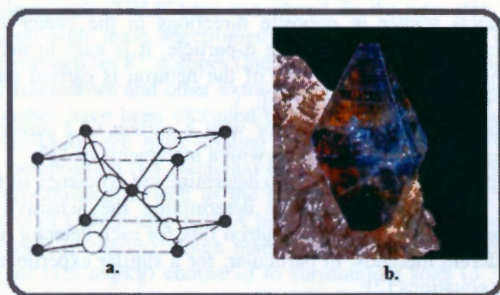


Figure 1. a) Unit cell of rutile. Black circles: titanium atoms; open circles: oxygen atoms. b) Photograph of a crystal of anatase

Anatase, a natural mineral, is one of the polymorph of TiO_2 . The name “anatase” is derived from the Greek word “ana,” which means “elongated” and refers to the mineral crystal's shape (Figure 1 (b)). Using Wulff construction and calculated surface energies, the equilibrium shape of a TiO_2 anatase crystal has been predicted to consist of a truncated octahedron, which agrees with experimental observations. The role of anions during solution-based synthesis of inorganic compounds is multiple. Depending on their complexing ability toward cations, anions can drive the nucleation/crystallization toward a specific crystal structure. They can also adsorb onto surfaces thus orienting, in a particular direction, the growth of particles.

Determination of the Efficiency of Neutron Detectors in the Experiment of Inelastic Neutron Scattering on ^{12}C

Ionkin V.K.* and TANGRA Collaboration

Lomonosov Moscow State University, Faculty of Physics, Moscow, Russia

*E-mail: ionkin.vk19@physics.msu.ru
(Student, 4th year of Bachelor's degree)

Information about neutron-nuclear interactions is extremely important for applied and fundamental physics. Since the neutron has no electric charge, it has a high penetrating power, which can be used, in particular, to research the structure of matter.

As part of the TANGRA collaboration, an experiment is being conducted to study the reaction of inelastic neutron scattering on a carbon nucleus $^{12}\text{C}(n, n')^{12}\text{C}^*$ using the method of labeled neutrons. It is planned to obtain the values of the differential neutron scattering cross sections of 14.16 MeV in the angle range from 0 to 2π .

The method of labeled neutrons implies registration of events (in our case, inelastic collision of neutrons with carbon nuclei ^{12}C), in coincidences with α -particles formed in a neutron generator in the reaction of deuterium and tritium synthesis:



The reaction products scatter in opposite directions in the center-of-mass system, so that knowing the direction of departure of the α -particle, it is easy to determine the direction of departure of the neutron. The "marking" of the neutron is carried out by a pixel α -detector located in body of the neutron generator [1].

The installation is a neutron generator with a carbon C12 screen located in front of it, surrounded by detectors at different angles with a increments of 15° .

An important part of data analysis is to determine the efficiency of the detectors used in the experiment. This is important both for determining the sensitivity limits of measuring instruments and for estimating the total neutron flux for each detector. Efficiency estimates can be made using different methods, in particular, for a similar experiment V. Valkovich's group used the following equations [2]:

$$\begin{aligned} \varepsilon(0thr) &= \frac{N_H \sigma_H}{N_H \sigma_H + N_C \sigma_C} (1 - e^{-d(N_H \sigma_H + N_C \sigma_C)}) \\ \varepsilon(E_{thr}) &= \varepsilon(0thr) \left(1 - \frac{E_{thr}}{E_{neutron}}\right), \end{aligned} \quad (1)$$

where, N_H is density of hydrogen atoms, N_C is density of carbon atoms, σ_H and σ_C – total cross sections for scattering of neutrons having energy E_n on H and C, $d = 8\text{cm}$.

As a result of this work were obtained estimates for the efficiency of neutron detectors, performed their calibration, and constructed dependences for efficiency on the energy of the incoming neutron were.

Literature

1. V.M. Bystritsky, V. Valkovich, D.N. Grozdanov, A.O. Zontikov, I.J. Ivanov, Yu.N. Kopach, A.R. Krylov, Yu.N. Rogov, I.N. Ruskov, M.G. Sapozhnikov, V.R. Skoi, V.N. Shvetsov, Letters to EPAN 12, 486 (2015) [Phys. Part. Nucl. Lett. 12, 325 (2015)].
2. V. Valkovic. 14 MeV Neutrons. Physics and Applications. CRC Press, New York. 2015.

SAMPLE ANALYSIS BY LASER SPECTROSCOPY, ICP-MS, RIMS AND INAA

I.N. Izosimov¹, B.D. Saidullaev², I. Strashnov³, A. Vasidov²

¹Joint Institute for Nuclear Research, 141980 Dubna, Russia

²Nuclear Physics Institute, Tashkent, Uzbekistan

³University of Manchester, School of Natural Sciences, UK

Among the modern analytical methods, laser spectroscopy, Instrumental Neutron Activation Analysis (INAA) and mass spectrometry are the leading techniques for the detection of trace amounts of different isotopes in complex matrices providing the breadth of information about the elemental and isotope composition [1–7]. Combination of the INAA, Inductively Coupled Plasma Mass Spectrometry (ICP-MS), and laser spectroscopy (TRLIF, TRLIC, RIMS) may be very efficient both for element and isotope composition analysis of the samples. We report on chemiluminescence of plutonium, uranium, and samarium in solutions. The details of multi-step excitation of species and time-resolved detection of resulting luminescence (TRLIF) and chemiluminescence (TRLIC) are considered. In the next step, we combine the atomic laser spectroscopy with mass spectrometry detection (RIMS). The trace amount detection has been demonstrated for Kr isotopes (including ^{81}Kr) of radiogenic (nuclear power plants) and cosmogenic (meteorites and other extra-terrestrial material) origin [3,4]. Several multi-step RIMS approaches have been extended to uranium and other radioisotopes from solid and liquid samples [3,4]. We have applied both INAA and ICP-MS methods and analysed the elemental composition (64 elements) of bones of dinosaurs, South mammoths, prehistoric bear and archanthropus as well as the samples of surrounding soils; everything collected in different parts of Uzbekistan [5,7]. A high concentration of uranium we detected in the bones of dinosaurs (122 mg/kg), South mammoth (220 mg/kg), prehistoric bear (24 mg/kg) and archanthropus (1.5 mg/kg) compared to surrounding soils (3.7–7.8 mg/kg) and standard bones (<0.01 mg/kg) is a bit of a puzzle [7]. We plan to solve this puzzle by measuring the isotopic composition of the samples. Some results of isotopic composition measurements will be presented.

1. I.N. Izosimov, *Procedia Chemistry*, **21**, 473(2016).
2. I.N. Izosimov, *Environmental Radiochemical Analysis VI*, pp. 115-130, Royal Society of Chemistry Publishing, 2019. DOI: 10.1039/9781788017732-00115
3. I. Strashnov, et al., *J. Anal. Atom. Spectroscopy*, **34**,1630(2019).
4. I. Strashnov, et al., *J. of Radioanalytical and Nuclear Chemistry*, **322**, 1437(2019).
5. A. Vasidov, et al., *J. of Radioanalytical and Nuclear Chemistry*, **310**, 953(2016).
6. I.N. Izosimov, *Environmental Radiochemical Analysis VI*, pp. 115-130, Royal Society of Chemistry Publishing, 2019. DOI: 10.1039/9781788017732-00115.
7. I.N. Izosimov, et al., *Czech Chemical Society Symposium Series*, **20**, 116(2022).

PRODUCTION OF MOLECULAR HYDROGEN
(AN ENVIRONMENTALLY FRIENDLY FUEL) BY THE INTERACTION
OF γ -RAYS WITH THE BeO/H₂O SYSTEM

Y.D. Jafarov, N.K. Abbasova

*Institute of Radiation Problems, Ministry of Science and Education of the Republic
of Azerbaijan, Baku AZ-1143, Azerbaijan*

Conducted studies showed that radiation-chemical yield of molecular hydrogen, under radiation-catalytic influence by γ -quanta on some metals or metal oxides, especially beryllium and beryllium oxide, in contact with water, is much higher. We investigated the radiation-chemical yield of molecular hydrogen obtained by the radiation-heterogeneous transformation of water under the influence of gamma rays (⁶⁰Co, P=18.17 rad/sec, T=300K) on beryllium oxide system with particle sizes $d < 4 \mu\text{m}$, 32–53 μm and 75–106 μm + adsorbed water and by suspending particles in water. Table compares experimental and model values of the energy yield of molecular hydrogen obtained during the radiolysis of water adsorbed ($\theta=4$) on BeO surface with particle size of $d < 4 \mu\text{m}$, $d=32\text{--}53$, 75–106 μm .

Table

Comparison of values obtained from experimental and model-based calculations of molecular hydrogen energy yields in the BeO+H₂O system

$d < 4 \mu\text{m}$	32–53 μm	75–106 μm	$G_n(h^+e^-)$	$G_n(L_{1v})$	$G_n(H_2)$
Energy yield of H ₂ , $G_t(H_2)$ molecule/(100 eV)			Values based on the model		
6.4	3.81	2.8	9.1–4.23	3.89–0.9	6.5–2.57

The maximum radiation-chemical yield of molecular hydrogen obtained from the radiation-catalytic decomposition of water in systems BeO/H₂O with particle sizes $d < 4 \mu\text{m}$, $d=32\text{--}53$ and 75–106 μm ($\theta=4$) under the γ -quanta influence are $G(H_2)=6.4$; 3.81 and 1.83 molecule/100 eV accordingly. The acquisition of molecular hydrogen is explained according to the recombination and exciton mechanism, which corresponds to the theoretical values ($G_n(H_2)=6.5\text{--}2.57$).

INVESTIGATION OF MOLECULAR HYDROGEN IN THE NANO-SiO₂
($d=15\text{--}20 \text{ nm}$)/H₂O SYSTEM UNDER THE INFLUENCE OF γ -QUANTA

Y.D. Jafarov¹, S.M. Bashirova², G.T. Imanova¹, S.M. Aliyev¹

¹*Institute of Radiation Problems, Ministry of Science and Education of the Republic
of Azerbaijan, Baku AZ-1143, B. Vahabzade 9, Azerbaijan*

²*MDI NASA of Space Research of Natural Resources, S.S. Akhuzade, 1, AZ 1115, Baku*

Recently, in various researches conducted by us and other researchers around the world, the study of products obtained from the radiolysis process of liquids, especially water in contact with metal or metal oxides under the influence of ionizing rays (γ -quanta, electrons, protons, neutrons, α -particles, high-energy ions, etc.) is of great importance both scientifically and energetically. The dependence of the radiation-chemical yield of the products obtained from the experiments on the particle size of metal or metal oxides (size effect), on their mass in suspended systems (mass effect) and on their type was observed. This effect is more pronounced in nanoscale metal or metal oxides.

In the presented work, under the influence of γ -quanta (⁶⁰Co, P=9.276 rad/sec, T=300K), the mass of water ($m=0.001$, 0.8 g), the amount, formation rate and radiation-chemical yields of molecular hydrogen obtained from the radiolysis processes in nano-SiO₂/H₂O systems with a mass of $m=0.2$ g and a particle size of $d=15\text{--}20 \text{ nm}$ were studied.

In those systems, the formation rates of molecular hydrogen obtained from the water radiation-catalytic decomposition determined for the water (2), total system (3) and nano-SiO₂ (4) are given in table.

The formation rates of molecular hydrogen obtained from radiation-catalytic decomposition of water in the systems created by the addition of water with the mass of $m=0.001$, 0.003, 0.01, 0.02, 0.04, 0.08, 0.2, 0.4 and 0.8 g to the nano-SiO₂ with the mass of $m=0.2$ g and particle size of $d=15\text{--}20 \text{ nm}$ under the influence of γ -quanta (⁶⁰Co, P=9.276 rad/sec, T=300K)

$G(H_2)$, molecule/(100 eV)	m_{H_2O} , g								
	0,001	0,003	0,01	0,02	0,04	0,08	0,2	0,4	0,8
$G_{SiO_2}(H_2)$	0,35	0,51	0,72	0,98	1,58	2,58	4,08	4,48	5,58
$G_{H_2O}(H_2)$	28,4	19,1	14,3	11	8,6	6,1	4,3	2,4	1,41
$G_{tot}(H_2)$	0,32	0,47	0,65	0,95	1,31	1,7	1,97	1,55	1,1

It is known from the research that: under the influence of γ -quanta (⁶⁰Co, P=9.276 rad/sec, T=300K), the radiation-chemical yield of molecular hydrogen obtained from radiolysis processes occurring with a change in water mass $m_{H_2O}=0.001\text{--}0.8 \text{ g}$ in created nano-SiO₂/H₂O systems with a mass of $m=0.2$ g and a particle size of $d=15\text{--}20 \text{ nm}$:

- ✓ decreases $G(H_2)=22.5\text{--}1.11$ molecule /100eV if determined for the water
- ✓ increases $G(H_2)=0.29\text{--}4.45$ molecule /100eV if determined for the nano-silica
- ✓ increases $G(H_2)=0.27\text{--}1.47$ molecule /100eV at a value of water mass $0.001\text{g} \leq m_{H_2O} < 0.2\text{g}$, reaches maximum $G(H_2)=1.66$ molecule /100eV at a value of water mass $m_{H_2O}=0.2\text{g}$, gradually decreases $G(H_2)=1.26\text{--}0.89$ molecule/100eV at a value of water mass $0.2\text{g} < m_{H_2O} \leq 0.2\text{g}$ if determined for the total system.

NATURAL AND ANTHROPOGENIC CONTAMINATION ANALYSIS OF
THE SEDIMENTS COLLECTED AROUND NOVAYA ZEMLYA

Jakhu R.¹, Yushin N.¹, Chaligava O.^{1,2}, Grozdov D.¹, Zinicovscaia I.^{1,3}

¹Joint Institute for Nuclear Research, Joliot-Curie 6, 141980 Dubna, Russia

²Faculty of Informatics and Control Systems, Georgian Technical University, 77
MerabKostava Street, 0171 Tbilisi, Georgia

³Horia Hulubei National Institute for R&D in Physics and Nuclear Engineering, 30
Reactorului Str., Magurele, Romania

The Dispersal profile of the radioisotopes (²²⁶Ra, ²³²Th, ²³⁵U, ⁴⁰K, ¹³⁷Cs) along with potentially toxic elements (Cd, Co, Cr, Cu, Ni, Pb, V, Zn, Hg) in the sediments around the Novaya Zemlya were determined. The task was fulfilled with the aid of HPGe gamma detector, inductively coupled plasma optical emission spectroscopy, DMA-80 Direct Mercury Analysis System, X-ray diffraction and statistical tools. At most of the locations, the radionuclide activity is higher than the world average activity concentration for the respective nuclei, ⁴⁰K being the most abundant. From all the potentially toxic elements detected, Cr and Ni were usually observed on very higher levels compared to their background values, indicating the probability of the detrimental biological effects. Thus, the present situation at the studied area might be a threat to the neighboring marine life.

Keywords: Sediments; Radionuclides; Potentially toxic elements; ¹³⁷Cs; Pollution source

THEORETICAL APPROACH THAT SIMULTANEOUSLY DESCRIBES
P-EVEN T-ODD ASYMMETRIES IN NUCLEAR FISSION REACTIONS BY
POLARIZED NEUTRONS WITH THE EMISSION OF DIFFERENT LIGHT
PARTICLES

S.G. Kadmsky, D.E. Lubashevsky

Voronezh State University, Voronezh, Russia

E-mail: kadmsky@phys.vsu.ru

In [1, 2], the coefficients $D_{nf,p}^{exp}(\theta)$ of P-even T-odd asymmetries in the cross sections of the reactions under consideration with the emission of precession and evaporative light particles p were found, expressed in terms of the experimental count rates $N_p^{\pm}(\theta)$ of particles p in coincidence with light fission fragments for the directions of the polarization vector σ_n^+ or σ_n^- along or against the Y axis of the l.c.s. The differential cross sections of the reactions under consideration were represented [1] by equation $d\sigma_{nf,p}(\theta)/d\Omega = d\sigma_{nf,p}^{(0)}(\theta)/d\Omega + d\sigma_{nf,p}^{(1)}(\theta)/d\Omega$ (1), where the first term $d\sigma_{nf,p}^{(0)}(\theta)/d\Omega = \sigma_{nf,p}^{(0)} P_p^{(0)}(\theta)$ corresponds to the case of unpolarized neutrons, and $P_p^{(0)}(\theta)$ is the angular distribution of light particles p . The second term, linearly dependent on the vector σ_n , corresponds to the components of the analyzed asymmetries and is presented [1] in terms of the sum of ternary and quintuple correlators $(d\sigma_{nf,p}^{(1)}(\theta)/d\Omega)_{3(5)} = (d\sigma_{nf,p}^{(1)}(\theta)/d\Omega)_{ev(odd)}$ (2), where the indices ev(odd) correspond to the even (odd) components of the indicated sections with respect to transformation $\theta \rightarrow \pi - \theta$ and can be related with values $(\beta_{nf,p}^{(1)}(\theta))_{3(5)} = (d\sigma_{nf,p}^{(1)}(\theta)/d\Omega)_{ev(odd)} / \sigma_{nf,p}^{(0)}$. For a theoretical description of the quantities $(\beta_{nf,p}^{(1)}(\theta))_{3(5)}$, one can use [1] eq. (3) $(\beta_{nf,p}^{(1)}(\theta))_{3(5)} = \Delta_{p,3(5)} d(P_p^{(0)}(\theta))_{odd(ev)} / d\theta$, which takes into account the rotation at an angle $\Delta_{p,3(5)}$, between the directions of emission of a particle p and a light fission fragment under the action of the Coriolis interaction associated with the rotation of the fissile system around an axis perpendicular to its symmetry axis. The experimental values of the quantities $(\beta_{nf,p}^{(1)}(\theta))_{3(5)}$ can be found as $(\beta_{nf,p}^{(1)}(\theta))_{3(5)} = (D_{nf,p}^{exp}(\theta) P_p^{(0)}(\theta))_{ev(odd)}$, using the results of [1], and the results of [2, 3] in which the quantity expressed in terms of the experimental count rates $N_p^{\pm}(\theta)$ of particles p is introduced. Within the framework of the semiclassical approach, the rotation angles $\Delta_{p,3(5)}$, in (3) were calculated using the method of trajectory calculations developed in [2], which always have positive values. It is demonstrated that within the framework of the quantum approach, taking into account only the Coriolis interaction in the case of an axially symmetric fissile system, due to the complexity of the detailed calculation of the rotation angles $\Delta_{p,3(5)}$, taking into account interference effects, it is natural to use the maximum likelihood method to determine them. Due to this, it is possible to simultaneously describe the indicated asymmetries in the case of various light particles p for the ²³⁵U, ²³⁹Pu, and ²⁴¹Pu nuclei at positive values of $\Delta_{p,3(5)}$, as well as for quintuple correlators in the case of α -particles, evaporation neutrons, and γ -quanta for the ²³³U nucleus at negative values of $\Delta_{n(\gamma),\alpha,5}$. Adding a constant to the triple correlator related [1] to axial symmetry breaking leads to agreement in the case of α -particles for the ²³³U nucleus. Therefore, within the framework of the quantum approach, taking into account the conditions presented above, it is possible to simultaneously describe P-even T-odd asymmetries in the cross section of the reactions under consideration with the emission of various light particles p for the case of all target nuclei ²³³U, ²³⁵U, ²³⁹Pu and ²⁴¹Pu.

1. Kadmsky S.G., Bunakov V.E., et al. // Bull. Russ. Acad. Sci.: Phys. 2019. V. 83. P. 1128.
2. Gagarski A., Goennenwein F., Guseva I., et al. // Phys. Rev C. 2016. V.93. P. 054619.
3. Danilyan G.V., Klenke J., Kopach Y.N., et al. // Nucl. Phys. 2014. V. 77. P. 677.

Status and Prospects of Studies of (γ , f) Reactions at MT-25 Microtron

Kamanin D.V.¹, Pyakov Yu.V.^{1,2}, Solodov A.N.¹, Zhuchko V.E.¹, Goryainova Z.I.¹,
Strekalovsky O.V.¹, Kuznetsova E.A.¹, Zhukova A.O.¹

¹Joint Institute for Nuclear Research, Dubna, Russia

²National Research Nuclear University "MEPhI", Moscow, Russia

E-mail: solodov@jinr.ru

The experiments were performed at the beam of the MT-25 microtron, FLNR, JINR, using the VEGA (V-E Guide based Array) setup. Fission fragments (FFs) from the $^{235,238}\text{U}$ (γ , f) and ^{232}Th (γ , f) reactions were captured by an electrostatic guide system (EGS). The guide is a cylindrical capacitor of four meters long with a thin wire as a central electrode. Some part of the ions emitted from the target at one end of the guide become involved in the spiral-like movement along the guide axis [1]. By this way the FFs are transported to the time-of-flight mass-spectrometer that consists of a microchannel-plates based timing detector and a mosaic of four PIN diodes. The mean time-of-flight of the FFs in the EGS exceeds 400 ns. The peculiarities of the experimental two dimensional FFs mass correlation distributions allowed us to suggest the following nature of such peculiarities (linear structures) [2]: due to inelastic Coulomb scattering, a very deformed FF from binary (γ , f) reaction undergoes a break-up while crossing a Lexan foil of the time detector. It is possible if the fragment is born in the shape isomer state with a typical life time of more than 400 ns. The experimental data at the MT-25 microtrone suffer from an intensive noise generated by the accelerator. In order to improve the experimental conditions, we are upgrading the VEGA setup by moving the detector module into the noise protected chamber six meters away from the target.

References

1. N.C. Oakey, P.D. McFarlane, NIM. 49, 220 (1967).
2. Yu.V. Pyatkov, D.V. Kamanin, A.A. Alexandrov, et al., Proceedings of the 27th International Seminar on Interaction of Neutrons with Nuclei, Dubna, Russia, 10-14 June 2019. Dubna 2020, p. 249.

REVISION OF THE ANALYTICAL PROPERTIES OF REACTION AMPLITUDE NEAR THRESHOLDS ON THE EXAMPLE OF MUON-INDUCED PROMPT FISSION

F.F. Karpeshin

D.I. Mendeleev Institute for Metrology, Saint-Petersburg, Russia

E-mail: fkarpeshin@gmail.com

In muonic atoms of ^{238}U , the nuclei can undergo fission caused by non-radiative transitions of the muon: $2p - 1s$, $3p - 1s$, $3d - 1s$ etc. [1]. This kind of fission is called prompt fission, in contrast with delayed fission, which occurs as a result of the muonic K -capture. Main features of the fission dynamics are studied in prompt fission: augmentation of the barrier, dynamics of the saddle-to-scission descent, muonic conversion and characteristic X-rays from fission fragments supply information on the multipolarity of electromagnetic transitions and charge distribution, structure of nuclear transition currents. Our present purpose is to revise the concept, which considers the thresholds in nuclear reactions as the singular branching points of the analytic reaction amplitude, the cross-section increasing with increasing incoming energy just before the thresholds.

Probability of the non-radiative nuclear excitation in the muonic transition $i \rightarrow f$ can be expressed in terms of the photoexcitation cross-section $\sigma_\gamma(0 \rightarrow \omega)$ as follows [2]:

$$\alpha_\mu^{(d)}(i \rightarrow f)(\pi\omega)^2 \sigma_\gamma(0 \rightarrow \omega), \quad (1)$$

where $\alpha_\mu^{(d)}(i \rightarrow f)$ is analogue of the muonic conversion coefficient, ω – the nuclear transition energy. Satisfactory agreement is attained with experiment [3] for non-radiative transition widths in ^{238}U . Analysis is deployed around comparison of the non-radiative probabilities in ^{235}U and ^{238}U . Energy of the $2p - 1s$ transition is the same in both cases: 6.3 MeV. This is above the (γ , n) and (γ , f) thresholds in both cases. The difference is that the nuclear levels of the compound nucleus in one case overlap with one another, in the other they do not overlap. Moreover, due to augmentation of the fission barrier, prompt-fission channel is equally suppressed in the both cases. At the same time, the total photoexcitation cross-section, which includes both neutron and fission channels, is much bigger than that which includes only neutron exit channel. The question naturally arises which cross-section should be substituted in the Eq. (1) above. Discussion is deployed around these peculiarities.

References

1. M.Ya. Balatz, L.N. Kondrat'ev, L.G. Landsberg, P.I. Lebedev, Yu.V. Obukhov, B. Pontecorvo // Sov. Phys. JETP, 1960. V. 38. P.1715; 1961. V. 39. P.1168.
2. Karpeshin F.F. and Nesterenko V.O. // J.Phys.G: Nucl. Part. Phys.1991. V. 17. P.705.
3. H. Haenscheid, P. David, H. Foiger, J. Konijn et al., Z. Phys. A – Hadrons and Nucl. 342, 111 (1992).

OBSERVATION OF STRUCTURAL GAMMA QUANTA IN NEUTRON RADIATIVE DECAY

Khafizov R.U.^{a,*}, Kolesnikov I.A.^a, Nikolenko M.V.^a, Tarnovitsky S.A.^a,
Tolokonnikov S.V.^a, Torokhov V.D.^a, Trifonov G.M.^a, Solovei V.A.^a,
Kolkhidashvili M.R.^a, Konorov I.V.^b

^a NRC «Kurchatov Institute», Russia

^b Technical University of Munich, Munich, Germany

*khafizov_ru@nrcki.ru

The purpose of the study of neutron radiative decay is to further advance the atomic project for which the «Kurchatov Institute» was established. In the last experiment when we first detected radiative decay events, the value of its main characteristic, decay branching ratio (BR) significantly exceeded the one calculated according to the Standard Model of Electroweak Interaction. In this experiment we were the first to measure the branching ratio (B.R.) of radiative neutron decay $B.R. = (3.2 \pm 1.6)10^{-3}$ (where C.L. = 99.7% and gamma quanta energy threshold is equal to 35 Kev) [1]. On the other hand, theoretical calculations of this value according to the Standard Model give 1.5 times lower value [2]. Thus, in our experiment we recorded additional gamma quanta which are structural gamma quanta emitted by the quarks that a neutron consists of.

1. Khafizov R.U., et al., JETP Letters, **83**(1) (2006)5.
2. Gaponov Yu.V., Khafizov. R.U., Phys. Lett. B **379**(1996)7.

Chromium and Zinc Accumulation and Translocation in Root and Leafy Vegetables Irrigated with Industrial Effluents — a Laboratory Study

Kravtsova A.V.^a, Zinicovscaia I.I.^{a,b,c}, Peshkova A.A.^{a,d}, Yushin N.S.^{a,d}

^a Joint Institute for Nuclear Research, 6 Joliot-Curie Str., 141980 Dubna, Russia;
alexkravtsova@yandex.ru

^b Laboratory of Quantum Chemistry, Chemical Cynetics and Magnetic Resonance, Institute of Chemistry of the Academy of Sciences of Moldova, 3, Academiei Str., MD-2028 Chisinau, R. Moldova;
zinikovskaia@mail.ru

^c Department of Nuclear Physics, Horia Hulubei National Institute for R&D in Physics and Nuclear Engineering, 30 Reactorului Str. MG-6, 077125 Magurele, Romania;

^d Doctoral School of Biological, Geonomic, Chemical and Technological Sciences, State University of Moldova, A. Mateevich Str., 60, MD-2009, Chisinau, R. Moldova; peshkova.alexandra92@gmail.com;
ynik_62@mail.ru

The industrial effluents and wastewaters, which are often used for irrigation purposes, contain heavy metals such as Fe, Mn, Zn, Cr, Ni, and others. Since heavy metals have the capability of translocation from soil to the edible parts of food crop, it leads to their accumulation in the food chain and can negative effect on human health. It is known that vegetables, especially some leafy vegetables grown on contaminated soils, contain higher metal concentrations than vegetables grown on uncontaminated sites. Therefore, a laboratory study was performed to assess the accumulation and translocation of chromium and zinc in the edible and non-edible parts of radish (*Raphanus sativus*), lettuce (*Lactuca sativa*) and green onion (*Allium fistulosum* L.) irrigated with filtered water and industrial effluents. The concentration of metals in effluents, soil and vegetables was determined by inductively coupled plasma optical emission spectrometry (ICP-OES).

The highest concentrations of zinc in the edible parts of vegetables were determined in lettuce (up to 833 ± 131 mg/kg), and the minimum content (up to 396 ± 38.5 mg/kg) - in radish. The opposite pattern was observed in the accumulation of chromium: the lowest content of metal was determined in leafy vegetables (7.50 ± 0.16 mg/kg), and the maximum level - in the edible radish roots (12.1 ± 3.13 mg/kg).

To study the features of metal accumulation by vegetable roots and their transfer to other parts of the plant, the bioaccumulation and translocation factors were calculated. The values of bioaccumulation factor for zinc in radish and lettuce decreased with increasing of metal concentrations in the industrial effluents. Conversely, the bioaccumulation factor of chromium for all vegetables was higher when irrigated with wastewater.

The levels of chromium and zinc in the parts of radish, lettuce and soil followed the order: soil \geq roots > edible part. The different order of metals translocation was observed for onion: roots \geq soil > edible part.

Since the main source of human exposure to heavy metals is via oral ingestion, the estimated daily intake (EDI) of chromium and zinc was determined based on their average concentration in the edible part of vegetables and the daily intake of radish, lettuce and onion. The maximum EDI of chromium and zinc resulted from the consumption of radish > lettuce > onion and lettuce > onion > radish, respectively, irrigated with industrial effluents. The obtained values were by an order of magnitude lower than the reference doses established for zinc (0.3 mg/kg bw/day) and chromium (0.003 mg/kg bw/day).

The Cross-Section Function for the $^{115}\text{In}(\gamma,2n)^{113\text{m}}\text{In}$ Reaction Determined in the Energy Range up to 23 MeV

M. Krmar¹, N. Jovancevic¹, D. Maletic², Y. Teterev³, S. Mitrofanov³, D. Knezevic², Z. Medic²

¹Physics Department, Faculty of Sciences, University of Novi Sad, Novi Sad, Serbia

²Institute of Physics, Belgrade, Serbia

³Flerov Laboratory of Nuclear Reactions, Joint Institute for Nuclear Research, Dubna, Russia

The cross-section function for the $^{115}\text{In}(\gamma,2n)^{113\text{m}}\text{In}$ reaction was determined in the energy range up to 23 MeV. Measurement was done using the bremsstrahlung facility at the MT25 Microtron, JINR, Dubna. 7 Indium disks were irradiated with bremsstrahlung spectra at endpoint energies of 17 MeV, 18 MeV, 19 MeV, 20 MeV, 21 MeV, 22 MeV and 23 MeV. Induced saturated activity of $^{113\text{m}}\text{In}$ was obtained with gamma spectroscopic measurement. To determine the cross-section function in the wide-energy photon beam the unfolding technique was applied. The obtained results were compared with TALYS 1.9 calculations and existing experimental data.

OBTAINING OF INITIAL FORMS FOR SYNTHETIC SELECTION OF DROUGHT-RESISTANT RICE CROPS USING RADIATION MUTAGENESIS ON FAST NEUTRONS

A.I. Kruglyak^{1*}, Y.V. Aleksiyenak¹, K.B. Bakiruly², N.O. Appazov³, A.S. Doroshkevich¹

¹Joint Institute for Nuclear Research, Dubna, Russia

²Kazakh Research Institute of Rice named after I. Zhakhaev, Kyzylorda, Kazakhstan

³Korkyt Ata Kyzylorda University, Kyzylorda, Kazakhstan

* Anastasiya.Kruglyak@nf.jinr.ru

It is known that viruses and cosmic rays make a decisive contribution to the evolution of biological species on Earth, participating in their transformation at the genetic level, largely determining the processes of selection [1].

Rice (*Oryza sativa* L.) is the world's most important food crop [2]. Also, rice represents a key model for studying the genomics of agroecosystems, due to the relative simplicity of its genome [3]. The use of neutrons as a mutagen leads to an increase in the diversity of mutant forms and makes it possible to solve the urgent problems of a declining amount of fresh water resources, soil salinization, and the increasing aggressiveness of flora and fauna pathogens.

This work is conducted to the mechanism study of the cosmogenic neutron radiation effect on the mutagenesis of biological objects on the example of rice cultures.

Within the framework of the project of the Ministry of Agriculture of the Republic of Kazakhstan No. BR10765056, along with the Kazakh Research Institute of Rice named after Zhakhaev (Kyzylorda, Kazakhstan), Budker Institute of Nuclear Physics (Novosibirsk) as a result of irradiation of rice seeds with fast neutrons mutant forms of rice varieties Aikerim, Leader and Syr Suluy were obtained. They are resistant to salinity, drought and both stress factors at the same time.

The largest number of mutant lines resistant to stress factors were obtained in the Syr Suluy variety (98 pcs.), other varieties gave fewer mutant plants – for the Leader varieties it was 44 pcs. and Aikerim – 16 pcs. All the isolated M1 plants differ significantly from the original forms in morphological features – plant height, length and laceration of panicles. Most plants are characterized by stunting and dwarfism (40-80 cm), as well as shortness and high empty-grain (up to 100%) of panicles, which indicates that they are mutant forms that are resistant to salinity, drought or both stress factors.

The obtained plants will be used as initial forms in synthetic breeding to create varieties with agronomically important properties.

References

1. M.V. Ragulskaya (2019), Sun and biosphere, Radiotekhnika, 170 p.
2. R. Mehrotra, et al., J. Plant Physiol., 2014, p. 486–96.
3. V.E. Viana, et al. Mutagenesis in Rice: The Basis for Breeding a New Super Plant // Frontiers in Plant Science, 2019.

Evaluation of a Mistaken Asymmetry in the Projected Experimental Search of Spatial Anisotropy of Gammas from $^{109}\text{Ag}(n,\gamma)$ Reaction at Neutron Energies near 32-eV p-Wave Resonance

Kuznetsov V.L.^{1,2}, Mitsyna L.V.¹, Rebrova N.V.¹, Sedyshev P.V.¹

¹Frank Laboratory of Neutron Physics, JINR, Dubna

²Laboratory of Neutron Research, INR RAS, Troitsk

An experiment is going to be carried out for a detection of forward-backward anisotropy of γ -quanta emission at the radiative decay of ^{110}Ag nucleus after capture of neutrons with energies in the region of 30.6-eV s-wave and 32.7-eV p-wave resonances of ^{109}Ag isotope. At preparatory stage for the experiment, which is planned to run by the time-of-flight method at 10-m flight-path of the IREN facility, Monte-Carlo simulations were made in order to calculate contributions of multiple scattering of neutrons before capture in natural-silver targets of different thicknesses, as well as to obtain a value the distorting kinematic asymmetry of γ -quanta emission in real geometry under condition of γ -emission isotropy.

THEORETICAL STUDY OF RESONANCE ELASTIC SCATTERING OF THERMAL NEUTRONS ON ATOMIC NUCLEI

L.S. Kuznetsova¹, A.S. Bazhin^{1,2}, M.A. Naumenko², V.V. Samarin^{1,2}

¹Dubna State University, Dubna, Russia

²Joint Institute for Nuclear Research, Dubna, Russia

Experimental cross sections for elastic scattering of thermal neutrons on atomic nuclei [1-3] have clearly pronounced maxima for some nuclei, for example, for ^{58}Ni . To explain this effect, the cross sections for elastic scattering of thermal neutrons on a wide set of nuclei have been calculated by numerical solution the Schrödinger equation. The experimental data are explained based on the concept of virtual levels [4]. It is shown that for the nuclei, for which the elastic scattering cross sections increase sharply, the energies of the s-levels of neutrons in the nuclear mean field go to zero.

The calculated radial probability densities for the s-states of thermal neutrons upon elastic scattering on the ^{28}Si and ^{58}Ni nuclei are shown in Fig. 1. The two maxima for silicon correspond to the low-lying 2s-state, three maxima for nickel correspond to the virtual 3s-state. The sharp change in the wave function when going from ^{28}Si to ^{58}Ni explains the resonance nature of elastic scattering of thermal neutrons on the ^{58}Ni nuclei with a cross section of 25 barns, which is an order of magnitude higher than the cross section for ^{28}Si (2 barns). Thus, it is shown that the resonance at the virtual s-level with an energy close to zero leads to a sharp increase in the elastic scattering cross section.

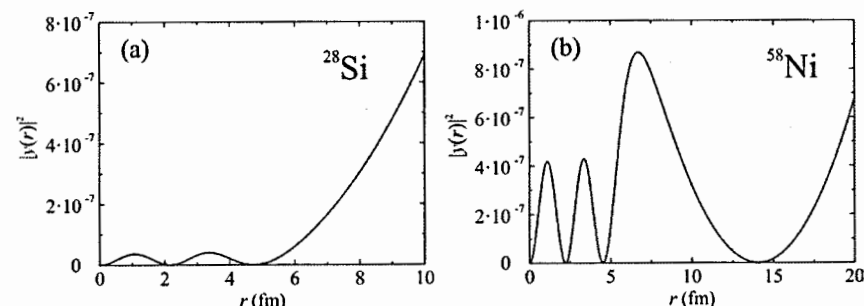


Fig. 1. Radial probability densities for the s-states of thermal neutrons upon elastic scattering on the ^{28}Si (a) and ^{58}Ni (b) nuclei.

References

1. V. I. Zagrebaev, A. S. Denikin, A. V. Karpov, A. P. Alekseev, M. A. Naumenko, V. A. Rachkov, V. V. Samarin, V. V. Saiko, NRV Web Knowledge Base on Low-Energy Nuclear Physics, <http://nrw.jinr.ru/>.
2. A. V. Karpov, A. S. Denikin, M. A. Naumenko, A. P. Alekseev, V. A. Rachkov, V. V. Samarin, V. V. Saiko, V. I. Zagrebaev, NRV Web Knowledge Base on Low-Energy Nuclear Physics, *Nucl. Instrum. Methods Phys. Res. A* 859, 112 (2017).
3. National Nuclear Data Center, <https://www.nndc.bnl.gov/>.
4. L. D. Landau, E. M. Lifshitz, Course of Theoretical Physics. Quantum Mechanics: Non-Relativistic Theory, Vol. 3 (Pergamon Press, 1977).

The Production of the Industrially Significant ^{210}Po Radionuclide Irradiating ^{209}Bi by Neutrons

Solomon Lim
solomonlim210@gmail.com

National University of Singapore High School of Mathematics and Science, Singapore

The production of the industrially significant radionuclide polonium-210 from the neutron irradiation of bismuth metal and the subsequent beta decay of bismuth-210 is highly inefficient due to the small neutron capture cross section of bismuth-209. In this paper, we report a previously undescribed self-sustaining nuclear chain reaction involving self-propagating neutron multiplication in bismuth salts that allow for rapid and cost-effective production of polonium-210. The reaction proceeds in a cycle of three alternating elementary steps – the capture of neutrons by bismuth-209 and the subsequent formation of polonium-210, the emission of high-energy alpha particles by polonium-210, and the production of more neutrons from (α,n) and $(n,2n)$ reactions on light element and bismuth-209 nuclei respectively. Furthermore, the high hydrogen density of the compound also confers it intrinsic neutron moderation properties, increasing the neutron capture cross section of bismuth-209 at thermal neutron energies. The chain reaction was proven to have successfully occurred by irradiating a sample of the bismuth salt with a 80 μCi neutron source and monitoring the activity levels of the reaction. It was found that the activity of the reaction increased exponentially after an initial stable period following a derived formula for polonium production trends for the reaction, thus validating the occurrence of the reaction. Furthermore, alpha spectroscopy confirmed that polonium-210 had been produced by characterizing the 5.41 MeV alpha emission peak of the reaction, further proving that the reaction was successful. Hence, this paper reports the successful initiation and characterization of a novel nuclear chain reaction, and its potential applications offered by a method of rapidly producing large quantities of polonium-210.

Neutronic Chain Reactions in Bismuth Salts

Solomon Lim

National University of Singapore High School of Mathematics and Science, Singapore

The production of the industrially significant radionuclide polonium-210 from the neutron irradiation of bismuth metal and the subsequent beta decay of bismuth-210 is highly inefficient due to the small neutron capture cross section of bismuth-209. In this paper, we report a previously undescribed self-sustaining nuclear chain reaction involving self-propagating neutron multiplication in bismuth salts that allow for rapid and cost-effective production of polonium-210. The reaction proceeds in a cycle of three alternating elementary steps – the capture of neutrons by bismuth-209 and the subsequent formation of polonium-210, the emission of high-energy alpha particles by polonium-210, and the production of more neutrons from (α,n) and $(n,2n)$ reactions on light element and bismuth-209 nuclei respectively. Furthermore, the high hydrogen density of the compound also confers it intrinsic neutron moderation properties, increasing the neutron capture cross section of bismuth-209 at thermal neutron energies. The chain reaction was proven to have successfully occurred by irradiating a sample of the bismuth salt with a 80 μCi neutron source and monitoring the activity levels of the reaction. It was found that the activity of the reaction increased exponentially after an initial stable period following a derived formula for polonium production trends for the reaction, thus validating the occurrence of the reaction. Furthermore, alpha spectroscopy confirmed that polonium-210 had been produced by characterising the 5.41 MeV alpha emission peak of the reaction, further proving that the reaction was successful. Hence, this paper reports the successful initiation and characterisation of a novel nuclear chain reaction, and its potential applications offered by a method of rapidly producing large quantities of polonium-210.

Pneumatic Transport System REGATA-2 for Neutron and Gamma-Activation Analysis at the IREN Facility at FLNP JINR: Implementation and First Results

V.V. Lobachev¹, A.Yu. Dmitriev^{1*}, S.B. Borzakov^{1,2}, A.A. Smirnov¹,
I.S. Zhironkin¹, E.A. Golubkov¹, V.N. Shvetsov¹

¹Frank Laboratory of Neutron Physics, Joint Institute for Nuclear Research, Dubna, Russia
²State University "Dubna", Dubna, Russia

* e-mail: andmitriev@jinr.ru

The IREN facility at the Frank Laboratory of Neutron Physics (FLNP) JINR is a source of neutrons or gamma-quanta fluxes. The fluxes are used for carrying out experiments on neutron activation (NAA) and gamma activation analysis (GAA). The pneumatic transport system (PTS) REGATA-2 was developed in the Bulgarian Academy of Sciences for the automation of NAA and GAA. The project was adapted and modified taking into account the features of the IREN facility, and then was successfully implemented. Later, the PTS was modernized by introducing a touch control panel that completely replaced the electromechanical one, and by establishing information exchange with the activation analysis database.

PTS provides the automated delivery of samples to the irradiation position and back for the analysis of the elemental composition of samples of various origins, including by short-lived isotopes with a half-life of about one minute or more. The study of samples intended for IAEA Proficiency tests was carried out using NAA and showed good agreement with passport data. Archaeological ceramics were studied using NAA by short-lived isotopes, which significantly complemented the previously obtained picture of the elemental composition of samples by medium- and long-lived isotopes. The first experiments were carried out using GAA, some isotopes of elements of irradiated samples were qualitatively determined.

The report will provide an overview of the functional blocks for the PTS, their modification, and implementation on the IREN facility. Furthermore, the results of experiments on NAA and GAA, outcomes of the PTS modernization and implementation of new options, as well as plans for the future will be presented.

Accelerator Version of the Intensive Lithium Antineutrino Source

V.I. Lyashuk

Institute for Nuclear Research of the Russian Academy of Sciences, Moscow, 117312

E-mail: lyashuk@itep.ru

The combination of the decay parameters of the neutron rich β^- -decaying ^8Li isotope (short $T_{1/2} = 0.84$ s) and its hard spectrum ($E_{\nu}^{\max} = 13$ MeV and $\langle E_{\nu} \rangle = 6.5$ MeV) of well-known distribution allows to consider it as the very perspective candidate for the artificial antineutrino source. In comparison with nuclear reactor which traditionally used as an intensive antineutrino source the lithium one is characterized by well-known spectrum that excludes the serious problems arising due to the soft and rapidly decreasing reactor spectrum obtained with significant errors ((4-6)% -precision at energy up to ~ 6 MeV) caused by unknown schemes of decays, time variations, presence of the spent nuclear fuel, that put together cause an unsolved puzzles in precision and interpretation of neutrino oscillation results [1].

The construction of the intensive neutrino sources are possible in different schemes basing on the nuclear reactor (as neutron source for (n, γ)-activation of purified ^7Li), on the preparing (basing on the reactor technology) of the high Ci-activity β^- -source (as in proposal [2]), on the tandem scheme of the accelerator with neutron producing target plus lithium blanket (neutron converter) irradiated by $^7\text{Li}(n,\gamma)^8\text{Li}$ activation [3]. It is possible the dynamical scheme realized in transport regime where an activated ^7Li is pumped in the close cycle through the active zone of the reactor; further (in cycle) it is delivered close to the neutrino detector. Strong advantage of the dynamical scheme is the possibility to decrease the total spectrum errors in order of values [4] and high count rate in the compact ($\sim \text{m}^3$) neutrino detector – $\sim 4 \times 10^4$ of ($\bar{\nu}_e, p$)-events ($\text{m}^{-3} \times \text{day}^{-1} \times \text{GW}^{-1}$) [5].

In the other perspective realization the proton beam strike into the heavy-element-target and produces the significant neutron yield for the lithium blanket irradiation. The scheme is considered for energies up to ~ 600 MeV for different heavy targets (W, Pb, Bi, Ta). The density of ^8Li creation is simulated in details that allowed to propose an effective blanket scheme with central lithium containing volume enclosed by carbon (acting as an effective neutron reflector) and outer thick water layer to diminish the neutron escape. The analysis of ^8Li distribution in the blanket allows to propose an approach of tandem schemes of linear accelerators (with proton energy about several tens of MeV) and construction of small-volume- $\bar{\nu}_e$ -source (of short dimension ~ 70 cm) that is exclusively important for search of sterile neutrinos in case of $\Delta m^2 \sim 1 \text{ eV}^2$ [6].

1. C. Giunti, Y.F. Li, C.A. Ternes, and Z. Xin. [arXiv:2110.06820](https://arxiv.org/abs/2110.06820) (2022).
2. M. Gribier, M. Fechner, T. Lasserre, et. al. Phys. Rev. Lett. 107, 291801 (2011).
3. V.I. Lyashuk & Yu.S. Lutostansky. Bull. Russ. Acad. Sci. Phys. 79, 431–436 (2015). <https://doi.org/10.3103/S106287381504022X>
4. V.I. Lyashuk. Results Phys. 7, 1212 (2017). <https://doi.org/10.1016/j.rinp.2017.03.025>.
5. V.I. Lyashuk. JHEP06 (2019)135. DOI: [10.1007/JHEP06\(2019\)135](https://doi.org/10.1007/JHEP06(2019)135)
6. J. Kopp, M. Maltoni and T. Schwetz, Phys. Rev. Lett. 107, 091801 (2011). DOI:<https://doi.org/10.1103/PhysRevLett.107.091801>

THE EFFECT OF GAMMA-IRRADIATION ON VAC OF GaS MONOCRYSTAL DOPED WITH Yb

Madatov R.S.^{1,2}, Tagiyev T.B.¹, Khaliqzadeh A.Sh.¹, Madadzada A.I.³

¹Institute of Radiation Problems, Ministry of Science and Education of the Republic of Azerbaijan, Baku, Azerbaijan

²National Aviation Academy, Department of Applied and General Physics, Baku, Azerbaijan

³Frank Laboratory of Neutron Physics, Joint Institute for Nuclear Research, Dubna, Russia

GaS monocrystals belonging to layered A^3B^6 compounds are semiconductors with a partially irregular structure. GaS monocrystal has strong anisotropy. The structural feature is due to the presence of covalent bonds between atoms in layered semiconductors, and Van der Waals forces within the layers. The volt-ampere characteristics of GaS and GaS (Yb) monocrystals, as well as the effect of gamma irradiation on their electrical properties. VAC of GaS and GaS (Yb) monocrystals, parameters of local levels in their restricted zone, for example, energy location of local levels in the forbidden zone, price of activation energies of charge carriers at local levels, etc. After studying the VAC of the initial sample to study the effect of gamma radiation on the VAC, the sample was irradiated with gamma rays irradiated by ^{60}Co isotope source at a temperature of 290 K.

Figure 1 shows the volt-ampere characteristics of GaS and GaS (Yb) single crystals at different doses at room temperature, and the results before irradiation are given in curves 1 and 2 to compare the graphs. A comparative analysis of the curves shown in Figure 1 shows that when the GaS single crystal is alloyed with the Yb atom, the current decreases, the ohmic region shifts toward the high voltage region, and at the same time, the transition voltage in the non-trap quadratic region shifts toward the high voltage region.

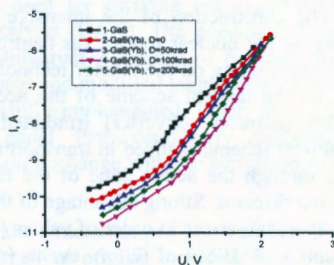


Figure 1. Volt-ampere characteristics of GaS and GaS(Yb) single crystals at different doses ($T=300\text{K}$).

Figure 1 shows that as can be seen from the graph, the VAC of the GaS(Yb) crystal irradiated with γ -quanta is observed with the regularity before irradiation, but the value of the voltage corresponding to ohmic, quadratic ($J-V^2$), a sharp increase in current ($J-V^3$) and finally, non-trap regions corresponding to $\geq 60\text{V}$ shift to the high voltage region. When the GaS (Yb) crystal is irradiated with a dose of $D = 50\text{krad}$ (curve 3), the value of the current passing through the sample decreases compared to the non-irradiated sample, but the nature of the curve does not change. In this case, the value of the transition voltage from the ohmic region to the quadratic region increases. A comparison of the parameters shows that the decrease in current in the irradiated GaS (Yb) crystal at a dose of 50 krad is due to a decrease in the concentration of free charge carriers. Curve 4 shows that when irradiating GaS(Yb) single crystal with a dose of $D=100\text{krad}$, the value of the current passing through the sample decreases again, and non-trap quadratic region is not observed in the subsequent increase in voltage ($U \geq 100\text{V}$). Such a change in current may be due to the formation of deep levels that collect the charge carriers involved in the conduction. When irradiating a GaS(Yb) crystal with a dose of $D=200\text{krad}$, the value of current increases in the whole voltage region ($U=8 \cdot 10^{-1} \div 10^2$), and after $U \geq 60\text{V}$, a non-trap quadratic region is observed. As a result of dissociation of the $[\text{V}_{\text{Ga}} \text{I}_{\text{Yb}}]$ complex at radiation doses $\Phi > 100\text{krad}$, an increase in the concentration of free charge carriers (relative to the pre-irradiation concentration) is observed, the VAC of the crystal shifts to a low voltage region.

ANISOTROPY IN PRE-FISSION NEUTRON SPECTRA OF $^{235}\text{U}(n, f)$

V.M. Maslov

Slobodskoy proezd 4, 220025 Minsk, Belarus

Angular anisotropy of secondary neutrons was evidenced in neutron emission spectra (NES) [1], and prompt fission neutron spectra (PFNS) [2]. In case of NES that is due to pre-equilibrium/semi-direct mechanism of emission of first neutron in $(n, nX)^1$ reaction, while in case of PFNS by exclusive spectra of pre-fission neutrons of $(n, xn)^1$ [3]. In $^{239}\text{Pu}(n, xn)^{1\dots x}$ and $^{235}\text{U}(n, xn)^{1\dots x}$ reactions observed PFNS demonstrate differing response to the emission of first pre-fission neutron in forward and backward semi-spheres. Mean energies of $(n, nf)^1$ neutrons depends on its angle of emission θ with respect to the incident beam. The average prompt fission neutron number, fission cross section, TKE depend on θ as well. Exclusive spectra of $(n, xn)^{1\dots x}$ neutrons at $\theta=90^\circ$ are consistent with $^{235}\text{U}(n, f)$ / $^{235}\text{U}(n, xn)$ and $^{239}\text{Pu}(n, f)$ / $^{239}\text{Pu}(n, xn)$ observed cross sections and neutron emission data at $E_n \sim 0.01\text{--}20$ MeV.

The correlations of the angular anisotropy of PFNS with the relative contribution of the (n, nf) fission chance to the observed fission cross section and angular anisotropy of neutron emission spectra are revealed. The exclusive spectra of $(n, xn)^{1\dots x}$ and $(n, n\gamma)$ and $(n, xn)^{1\dots x}$ reactions are calculated alongside with (n, f) and (n, xn) cross sections within Hauser-Feshbach formalism, the angular anisotropy of $(n, nX)^1$ neutrons being included (Fig. 1). The ratios of mean PFNS energies $\langle E \rangle$ for forward and backward emission of $^{235}\text{U}(n, xn)^1$ pre-fission neutrons (Fig. 2) are consistent with measured data [2].

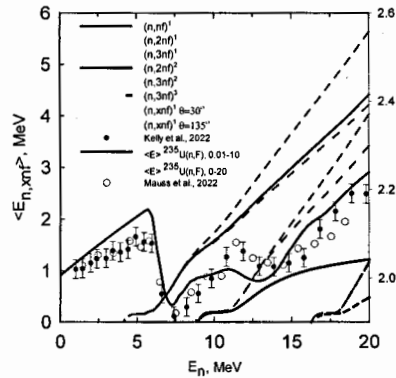


Fig. 1 $\langle E \rangle$ and $\langle E_{n, xn} \rangle$ of $^{235}\text{U}(n, f)$.

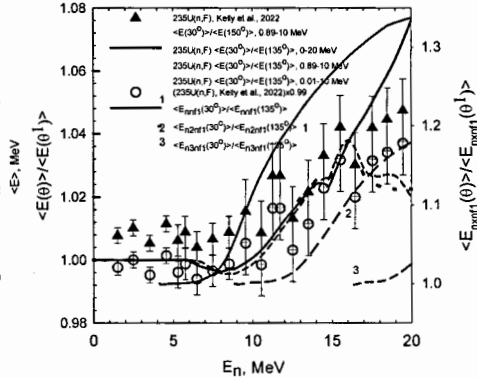


Fig. 2 $^{235}\text{U}(n, f)$ ratios of $\langle E \rangle$, $\langle E_{n, xn} \rangle$ at $30^\circ/135^\circ$.

1. Kammerdiener J.L., UCRL-51232, 1972.
2. Kelly K. J., Gomez J.A., Devlin M. et al, Phys. Rev. C **105**, 044615 (2022).
3. Maslov V.M., LXXII International Conference " NUCLEUS-2022, Fundamental problems and applications", Moscow, July, 11—16, 2022, Book of Abstracts, p.168, <https://events.sinp.msu.ru/event/8/attachments/181/875/nucleus-2022-book-of-abstracts-www.pdf>.
4. Mauss B., Taieb J., Laurent B. et al., https://oe.cd/nea.org/dbdata/nds_jefdoc/jefdoc-2200.pdf, Nuclear Data Week, November, 2022, JEFDOC-2200.

Effect of Angular Momentum Variation in Heavy-Ion Induced Fusion Reaction

Utkarsha Mishra, Punit Dubey, Mahesh Choudhary, Aman Sharma, Namrata Singh, Nitin Dubey and Ajay Kumar

Banaras Hindu University, Varanasi, India

E-mail: utkarshmishra22@bhu.ac.in

In order to examine the nucleus at high spin or high temperature, fusion reactions are useful tool, and the dissipative evolution of compound nuclei is an active area of research in heavy ion induced fusion reactions. In such reactions, the colliding nuclei possess a certain amount of intrinsic angular momentum. In this study, we have calculated the variation of compound nucleus formation time with the angular momentum as shown in Fig. 1 for the two different reactions that make the same compound nucleus [1,2]. Dynamical model code HICOL [3] is employed to calculate the formation time of a compound nucleus at different values of angular momentum.

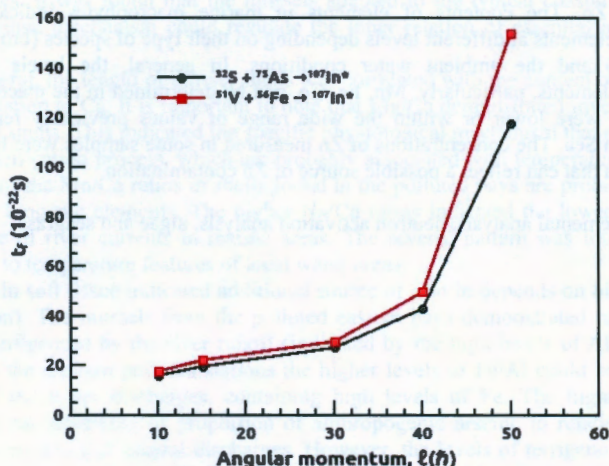


Fig.1: The influence of angular momentum on compound nuclear formation time.

From Fig. 1, it is clear that the compound nucleus ($^{107}\text{In}^*$) formed through $^{51}\text{V} + ^{56}\text{Fe} \rightarrow ^{107}\text{In}^*$ has a long formation time compared to the $^{32}\text{S} + ^{75}\text{As} \rightarrow ^{107}\text{In}^*$ and this indicates the dissipation in the nuclear reaction during compound nuclear formation [4], because angular momentum may prevent the energy from being transferred to other degrees of freedom and nuclei in collision experience more distortion at high angular momentum.

1. Ajay Kumar *et al.*, Phys. Rev. C **68**, 034603 (2003).
2. Ajay Kumar *et al.*, Phys. Rev. C **70**, 044607 (2004).
3. H. Feldmeier *et al.*, Nucl. Phys. A **435**, 229 (1985).
4. N.K. Rai *et al.*, Phys. Rev. C **98**, 024626 (2018).

Environmental Study for Mediterranean Sea Ecosystem Using Seagrass and Algae Samples with Neutron Activation Analysis

Nassar N.¹, Kravtsova A.², Frontasyeva M.², Sherif M.¹

¹Department of Physics, Faculty of Science, Cairo University, 12613, Giza, Egypt

²FLNP JINR, 6, Joliot-Curie str., 141980, Dubna, Russia

Instrumental neutron activation analysis is used to determine the concentrations of Na, Mg, Al, S, Cl, K, Ca, Sc, Ti, V, Mn, Fe, Co, Ni, Zn, As, Se, Br, Rb, Sr, Mo, Ag, Sb, I, Cs, Ba, La, Sm, Tb, Yb, Hf, Ta, Th and U in some types of marine macrophytes (algae and seagrass), collected from 7 stations along the Mediterranean Sea coast of Egypt. INAA was performed in the radio-analytical laboratory at the pulsed fast reactor IBR-2 of the Frank Laboratory of Neutron Physics, JINR, Dubna, Russia. The concentrations of most of these elements were rarely or never studied in this territory as well as the levels of classically investigated Mn, Fe, Co, Ni and Zn. The contents of elements in marine macrophytes indicated that they accumulated elements at different levels depending on their type of species (brown, red, green and seagrass) and the ambient water conditions. In general, the levels of classically investigated elements, particularly, Mn, Fe, Co, and Ni determined in the macrophytes in the present study were lower or within the wide range of values previously reported for the Mediterranean Sea. The concentrations of Zn measured in some samples were higher than the published data that can reflect a possible source of Zn contamination.

Keywords: Elemental analysis, neutron activation analysis, algae and seagrass

Elemental Ratios in Marine Mussels for Assessment of Ecological Characteristics

Pavel Nekhoroshkov

Frank Laboratory of Neutron Physics, Joint Institute for Nuclear Research, Russian Federation
p.nekhoroshkov@gmail.com

The elements in mussel tissues and shells determined by using instrumental neutron activation analysis could provide additional information about accumulation process in the selected aquatic areas. The specific ratios indicate the features of environmental conditions affecting such filtrate organisms. These findings could be used for characterization of the local water areas, biomonitoring studies or ecological state assessment.

The data were obtained during wide period of observation (2013–2020) in different water areas of the South Africa and the Black Sea. According to ratios of elements in shells and soft tissues. It was found that the mussels adapted to the typical coastal conditions by using depositional mechanism could regulate the inner relation of essential and other trace elements.

In general, the length of mussel shells was correlated with the content of Co and Ni in shells with relation to Ca. It is important to note that Mg/Ca demonstrated inverse correlation with length of shells. This indicated the specific physiological mechanism that reduces Mg/Ca during the calcification process, which are probably associated with temperature regime. The higher levels of the Mn/Ca ratios in shells found in the polluted bays are probably associated with entering biogenic elements. The higher Na/Ca ratios indicated the lower salinity bays, with influence of river currents in marine areas. The reverse pattern was found for Mg/Ca corresponded to temperature features of local water areas.

Fe/Al in soft tissue indicated additional source of iron in depends on biological proxy (phytoplankton). The mussels from the polluted eastern bays demonstrated relatively stable Fe/Al levels influenced by the river runoff (indicated by the high levels of Al), while in the mussels from the western polluted stations the higher levels of Fe/Al could be explained by specificity of the water discharges, containing high levels of Fe. The higher As/Sc ratio demonstrated the increasing of proportion of anthropogenic arsenic in relation to the non-volatile Sc in the areas of coastal discharges. However, the levels of terrigenous component, which could be indicated by the Al, Sc, Th et al., should be considered.

The mussels from the Black Sea water areas despite the typical lower salinity levels demonstrated the same patterns of studied ratios in soft tissues and shells. The higher ratios of Mn/Ca such as in polluted South African bays indicated the seasonal increasing of the biogenic elements and phytoplanktonic assemblages.

ELECTROPHYSICAL PROPERTIES OF THIN FILMS Mn_4Si_7

M.T. Normuradov¹, K.T. Dovranov¹, G.T. Imanova^{2,*}, I.R. Bekpulatov³,
D.A. Normurodov¹

¹ Karshi State University, 180103, str. Kuchabog 17, Karshi city, Uzbekistan

² Ministry of Science and Education of the Republic of Azerbaijan, Institute of Radiation Problems, AZ1143, B.Vahabzadeh 9, Baku, Azerbaijan

³ Tashkent State Technical University, 100095, Universitetskaya street 2, Tashkent city, Uzbekistan

* E-mail: gunel_imanova55@mail.ru

(Ph.D. in physics, Associate professor, Gunel Imanova)

$Mn_4Si_7/Si(111)$ films were grown by ion-plasma sputtering using argon ions. Their electrical conductivity and electrical resistance were studied as a function of temperature, and the ratio of HSM thin films was also carried out.

The Mn_4Si_7 film formed by magnetron sputtering is in the amorphous state (Fig. 1a) and the polycrystalline state (Fig. 1b) before thermal heating.

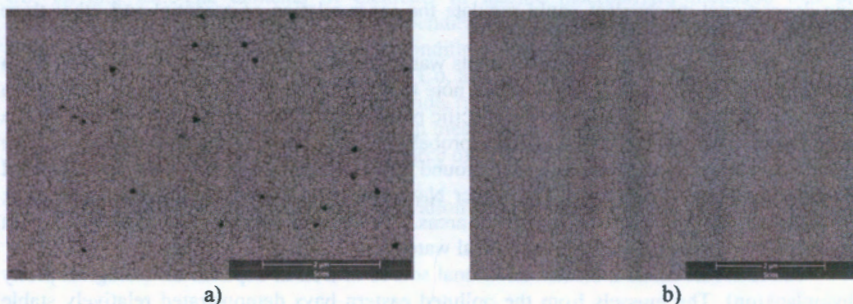


Figure 1. Mn_4Si_7 film before heating (a) and after heating at a pressure of 10^{-3} Pa at a temperature of $T = 800$ K (b).

In the amorphous state, the resistance of the film is greater than the resistance in the polycrystalline state. This is due to the fact that the bond between the manganese and silicon atoms is very weak and there are defects on the surface areas that are not completely covered. The resistance of a HCM film grown on the surface of p -type semiconductor silicon has a non-linear character on the temperature dependence graph, which means that it is, by its nature, semi-metallic. The electrical conductivity of the $Mn_4Si_7/Si(111)$ film 102.3 nm thick, measured at room temperature, is $1078.5 \Omega^{-1} \cdot cm^{-1}$, and the electrical resistance is 111.5 Ω .

Silicon and manganese atoms deposited on silicon oxide almost completely cover the substrate. As a result of experiments with this film, it was found that it has metallic properties.

Thin nanometer $Mn_4Si_7/Si(111)$ layers grown by the ion-plasma method were also formed on various silicon substrates at different growth temperatures. The electrical conductivity, power factor and electrical resistance of the resulting $Mn_4Si_7/Si(111)$ layers of various thicknesses were analyzed in the temperature range of 300 – 600 K. The highest value of the power factor is $1580.5 \mu W/m \cdot K^2$ at 500 K. /Si(111) is 800 K. The results show that the electrical conductivity increases with decreasing film thickness on the silicon surface. This fact can be used to increase the sensitivity of IR receivers.

Angular Distribution in Fast Neutrons Induced Reactions on ^{64}Zn Isotope

C. Oprea¹, A.I. Oprea²

¹County Center for Education, 11 Mihai Eminescu st, 410019, Oradea, Bihor County, Romania

²Frank Laboratory of Neutron Physics (FLNP), Joint Institute for Nuclear Research (JINR),
141980 Dubna, 6 Joliot Curie st, Moscow Region, Russian Federation

Cross sections, angular distributions, forward-backward asymmetry effect and alpha spectra in fast neutrons induced processes on ^{64}Zn nucleus were investigated. Theoretical evaluations were realized using own authors codes and dedicated software for the investigation of the structure of atomic nuclei and nuclear reactions mechanisms. Contributions to the cross sections, angular correlations and alpha spectra of nuclear reactions mechanisms (direct, compound and pre-equilibrium ones) were obtained. Cross sections and angular distributions theoretical evaluations are in good agreement with existing experimental data from literature and those obtained in FLNP. Further, from the comparison of theoretical and experimental data, parameters of Woods-Saxon potential (volume, surface and spin-orbit each with real and imaginary part) were extracted. For neutrons energy of few MeV's, experimental forward-backward effect was observed. For this incident energy of neutrons only compound mechanism is acting and therefore the measured asymmetry cannot be explained by the presence of direct processes. The possible explanations of the existence of measured forward-backward effect are also analyzed.

Applying TalysLib Library for Optimization of Optical Potential Parameters for Neutron Scattering on ^{24}Mg and ^{32}S

G.V. Pampushik¹, N.A. Fedorov²

¹Lomonosov Moscow State University, Moscow, Russia

²Frank Laboratory of Neutron Physics, Joint Institute for Nuclear Research, Dubna, Russia

E-mail: pampushik.g@gmail.com

In the Frank Laboratory of Neutron Physics, the international project TANGRA is being implemented to study the scattering of tagged 14.1 MeV neutrons on atomic nuclei. For the purposes of the theoretical part of the project, the TALYS program is used. It has wide functionality, and also contains nuclear structure database and set of the nuclear reaction models parameters, based on the RIPL-3 library [2]. The main way to describe neutron-nuclear reactions in this program is the optical model, which is used to calculate the elastic and inelastic scattering cross sections. To simplify access to the calculation results and the TALYS database, as well as EXFOR [3] databases, object oriented C++ library, TalysLib is being developed. Using its functional we obtained new sets of optical model parameters for fast neutron scattering on ^{24}Mg and ^{32}S which will be presented. An example of optimizing parameters on ^{32}S is given on Fig. 1. It can be clearly seen what our calculations is better approximate experimental data than default TALYS calculations.

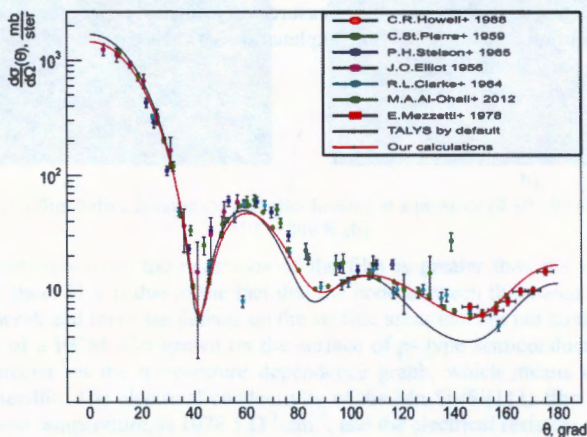


Fig. 1. Results of optical parameters optimization for elastic neutron scattering on ^{32}S . Black line – TALYS by default, red line – our calculations. All experimental data were received from EXFOR by using TalysLib.

1. Koning A. J., Hilaire S., Duijvestijn M. C. «TALYS-1.0» // Proceedings of the International Conference on Nuclear Data for Science and Technology. EDP Sciences, 2007. C. 211–214.
2. IAEA-Tecdoc, RIPL3, Reference Input Parameter Library, <http://www-nds.iaea.org/RIPL-3>
3. Experimental Nuclear Reaction Data (EXFOR), <https://www-nds.iaea.org/exfor>

Examination of Weisskopf–Ewing Approximation for the Determination of (n, α) Reaction Cross-Sections

Jyoti Pandey¹, Bhawna Pandey², H.M. Agrawal², S.V. Suryanarayana³

¹*Inter University Accelerator Centre, Aruna Asaf Ali Marg, New Delhi - 110067, India*

²*Govind Ballabh Pant University of Agriculture and Technology, Pantnagar, Uttarakhand, India*

³*Bhabha Atomic Research Centre, Nuclear Physics Division, Mumbai, Maharashtra 400085, India*

Out of the many neutron-induced reactions that take place inside a fusion reactor, the ones that produce gaseous elements like hydrogen and helium are of utmost importance for the study of the structural integrity of reactor materials. Hydrogen and helium gas production occurs mainly through (n,xp) and (n,x α) reactions. These reactions are induced on the different walls of the fusion reactor mainly the first wall, structural, blanket materials, and others. The production of hydrogen and helium leads to other processes such as atomic displacements and transmutations which can produce microstructural defects and modify the physical properties of the materials. The materials suitable for the reactor structures are stainless steel with Cr, Fe, and Ni as main constituents in SS316(LN)-IG content of (Fe ~ 65%, Ni ~ 12%, Cr ~ 17%). As the neutrons continuously coming from plasma interact with the various walls of the reactor made up of SS, there will be the generation of various long-lived radio-nuclides like ⁵⁵Fe ($T_{1/2}$ = 2.737 years), ⁵⁹Ni ($T_{1/2}$ = 7.6×10^4 years) and many others inside reactor environment. The neutrons coming from plasma interacts with various long-lived radionuclides already generated in the reactor environment during its operation, such types of reactions are called second generation reaction. The cross-sections of the neutron-induced reaction of various radionuclides are not measured and studied till now. So, there is a large gap in the nuclear data library. In the past years, the surrogate method has been used for cross-section measurement. The surrogate method assumes that the reaction takes place through the compound nucleus mechanism only, but at high energies, pre-equilibrium and direct reaction channels also occur. The present study explores the surrogate reaction method by determining the validity of Weisskopf-Ewing approximation for (n, α) reaction on n + ⁵⁶Fe reaction.

Accumulation and Translocation of Copper and Gold Nanoparticles in *Petroselinum Crispum* Segments under Root Irrigation Conditions

Alexandra Peshkova^{1,2}, Inga Zinicovscaia^{1,3,4}, Liliana Cepoi⁵, Ludmila Rudi⁵,
Tatiana Chiriac⁵, Nikita Yushin^{1,2}

¹Joint Institute for Nuclear Research, 6 Joliot-Curie Str., 141980, Dubna, Russia

²Doctoral School of Biological, Geonomic, Chemical and Technological Sciences, State University of Moldova, 60 Alexei Mateevici Str., MD-2009, Chisinau, Moldova

³Horia Hulubei National Institute for R&D in Physics and Nuclear Engineering, 30 Reactorului Str., 077125 Măgurele, Ilfov, Romania

⁴Institute of Chemistry, 3, Academiei Str., MD-2028 Chisinau, Republic of Moldova

⁵Institute of Microbiology and Biotechnology, Technical University of Moldova, 1 Academiei Str., Chisinau, MD-2028, Republic of Moldova

The relevance of studying the effect of metal nanoparticles on different biological objects and possible influence on human health is associated with their active use in various fields. Increasing production and consumption of nanoparticles leads to their release into the environment both with emissions into atmosphere and with wastewater. Accumulation of metal nanoparticles in soils, their translocation to plant segments and further transfer to other trophic levels depend on many conditions, including nanoparticles concentration, size, structure, form and composition. Present study reports the results of copper (CuNPs) and gold (AuNPs) nanoparticles effect on Parsley (*Petroselinum crispum*) under root irrigation. To determine copper and gold content in plants segments and soils ICP-OES/MS were applied. Accumulation of copper and gold in soil and their translocation in roots and leaves was different at their application in the concentration range 1-200 mg/L. Gold was accumulated in soil and transferred to plant's segments. Copper was mainly accumulated in soil and had low uptake in leaves. Both types of nanoparticles caused stress in parsley. At application of all CuNPs concentrations content of carotenoids and total chlorophyll in plants decreased. AuNPs at low concentrations stimulated increase of the content of pigments, but at concentrations higher than 10 mg/L reduced them.

MEASUREMENT AND ANALYSIS OF THE TOTAL THICK TARGET YIELD FROM $^{13}\text{C}(\alpha, n_0)^{16}\text{O}$ REACTION

P. S. Prusachenko¹, T. L. Bobrovsky^{1,2}, M. V. Bokhovko¹, A. F. Gurbich¹

¹Institute for Physics and Power Engineering, Obninsk, Russia;

²National Research Nuclear University "MEPhI", Moscow, Russia

E-mail: prusachenko.pavel@gmail.com

The thick-target neutron spectra from the $^{13}\text{C}(\alpha, n_0)^{16}\text{O}$ reaction were measured for the energy range of 3.0-6.5 MeV at 10 angles in the laboratory angle interval of 0-150°. The thick target yield was determined by integration of the neutron spectra over the neutron energy range corresponding to the $^{13}\text{C}(\alpha, n_0)^{16}\text{O}$ reaction followed by integration of the obtained angular distribution of the differential thick target yield over the solid angle 4π . The content of ^{13}C atoms in the target was determined by ion beam analysis with accuracy of <1%. The obtained thick target yield values support the calculated ones based on the $^{16}\text{O}(n, \alpha_0)^{13}\text{C}$ reaction cross-section evaluation from the ENDF/B-VIII.0 library.

Observation of New Modes of Multi-Body Decays of $^{252}\text{Cf(sf)}$

Yu.V. Pyatkov^{1,2}, D.V. Kamanin², Z.I. Goryainova², E.A. Kuznetsova²,
A.N. Solodov², O.V. Strelakovsky², V.E. Zhuchko³, A.O. Zhukova², S.M. Wyngaardt³

¹National Research Nuclear University "MEPhI", 115409 Moscow, Russia

²Joint Institute for Nuclear Research, 141980 Dubna, Russia

³University of Stellenbosch, Stellenbosch, Western Cape, South Africa

In our previous publications [1-4], we discussed various manifestations of the decay channel of low excited heavy nuclei, called collinear cluster tri-partition (CCT). New modes of ternary and likely quaternary decays of $^{252}\text{Cf(sf)}$ were observed using the "double-hit" approach. The experiments were performed at the COMETA, a double-armed, mosaic, time-of-flight spectrometer of fission fragments [5]. Digital images of all the detector signals were obtained using multichannel fast flash-digitizer. Off-line processing of the recorded data allowed us to select the decay events where two fragments were detected in the same PIN diode during the time-selection gate of 200 ns. For the selected events, the pre-scission configuration of the mother nucleus seems to be a channel consisting of different magic nuclei.

References

1. Yu.V. Pyatkov et al., Eur. Phys. J. A **45**, 29 (2010).
2. Yu.V. Pyatkov et al., Eur. Phys. J. A **48**, 94 (2012).
3. Yu.V. Pyatkov et al., Phys. Rev. C **96** (2017) 064606.
4. Yu.V. Pyatkov et al., Eurasian Journal of Physics and Functional Materials, v.4, №1 (2020) 13–18.
5. Yu.V. Pyatkov et al., Eur. Phys. J. A **48**, 94 (2012).

Investigation of Rhenium by Neutrons

Ruskov I.N.¹, Kopatch Yu.N.², Tretyakova T.Yu.^{2,3,4}, Skoy V.R.², Fedorov N.A.²,
Grozdanov D.N.^{1,2}, Gundorin N.A.², Shvetsov V.N.², Sirakov I.A.¹, Jovančević N.⁵,
Knežević D.⁵, Badawi M.S.^{8,9}, Thabet A.A.¹⁰, Kumar A.⁷, Gandhi A.¹², Sharma A.⁷,
Dongming W.¹¹, Hramco C.², Borzakov S.B.², Zinicovscaia I.², Tzvetkova Ch.⁶,
and TANGRA Collaboration

¹Institute for Nuclear Research and Nuclear Energy, Bulgarian Academy of Sciences, 72,
Tsarigradsko shose Blvd., 1784 Sofia, Bulgaria, ivan.ruskov@gmail.com

²Frank Laboratory of Neutron Physics, Joint Institute for Nuclear Research, 6, Joliot-Curie Str.,
141980 Dubna, Russian Federation, kopatch@nf.jinr.ru, dgrozdanov@mail.ru

³Skobeltsyn Institute of Nuclear Physics (SINP), M.V. Lomonosov Moscow State University,
Vorob'evy Gory, 119992, Moscow, Russian Federation, tretyakova@srd.sinp.msu.ru

⁴Faculty of Physics, M.V. Lomonosov Moscow State University, 1, building 2, GSP-2,
Leninskiye Gory, 119992, Moscow, Russian Federation, na.fedorov@physics.msu.ru

⁵Department of Physics, Faculty of Sciences, University of Novi Sad, 4, Trg Dositeja
Obradovica, 21000 Novi Sad, Serbia, nikola.jovancevic@df.uns.ac.rs, miendor@gmail.com

⁶Institute of General and Inorganic Chemistry, Bulgarian Academy of Sciences, 11,
Acad. Georgi Bonchev Str., 1113 Sofia, Bulgaria, hristi@svr.igic.bas.bg

⁷Department of Physics, Banaras Hindu University, 221 005 Varanasi, India,
ajayvagi@bhu.ac.in, aman.marley1314@gmail.com

⁸Physics Department, Faculty of Science, Alexandria University, Alexandria, Egypt,
ms241178@hotmail.com

⁹Faculty of Advanced Basic Sciences, Alamein International University, Alamein City,
Matrouh Governorate, Egypt

¹⁰Department of Biomedical Equipment Technology, Faculty of Applied Health Sciences
Technology, Pharos University in Alexandria, Egypt, abouzeid.thabet@pua.edu.eg

¹¹School of Energy and Power Engineering, Xi'an Jiaotong University, Xianning Road No. 28,
Shaanxi Province, 710049 Xi'an, China, huasi_lu@mail.xjtu.edu.cn

¹²Horia Hulubei National Institute of Physics and Nuclear Engineering, 409, Atomists Street,
077125 Măgurele, Romania, gandhiaman653@gmail.com

Modern and advanced technologies require the synthesis and use of new materials with improved and well-known properties and characteristics. In recent years, due to the unique properties of rhenium (Re) as one of the other refractory elements (Ta, Mo, W, Ti, Zr, Tc), its use worldwide has increased significantly. Rhenium is used, for example, in the aerospace industry (high-temperature W- and Mo-alloys for jet and rocket engines), the chemical industry, coating and welding, electronics, photography, nuclear medicine, etc. Rhenium is among the rarest metals on Earth and it does not occur uncombined or as a compound in a mineable mineral species. However, it is spread throughout the Earth's crust to the extent of ~0.001ppm. Production of rhenium is by extraction from the flue dusts of molybdenum smelters or by phytoextraction from soils and waters. The EXFOR experimental nuclear data library for the cross sections of (n,γ), (n,n'), (n,2n), (n,3n), (n,p), (n,α) reactions (activation, differential, total), the energy and angular distributions of the reaction products contain not many data. Some of the included datasets significantly differ from each other, others have relatively large experimental error-bars. It is proposed to start a comprehensive study of the nuclear properties of rhenium isotopes using neutrons of various energies at the Frank Laboratory of Neutron Physics (FLNP) of the Joint Institute for Nuclear Research (JINR) in Dubna (Russia). The experimental results obtained can be used to better understand the mechanism of neutron-induced nuclear reactions, as well as for the needs of nuclear, life and environmental sciences.

Forward-Backward Asymmetry Effect in the Slow Neutrons Capture by Silver Nucleus

P.V. Sedyshev¹, A.I. Oprea¹, C. Oprea², V.L. Kuznetsov¹

¹*Frank Laboratory of Neutron Physics (FLNP), Joint Institute for Nuclear Research (JINR), 141980 Dubna, 6 Joliot Curie st, Moscow Region, Russian Federation*

²*County Center for Education, 11 Mihai Eminescu st, 410019, Oradea, Bihor County, Romania*

Forward-backward asymmetry effect in the capture process of slow neutrons on Silver nucleus was investigated. Cross sections, angular distributions, and forward-backward effect were obtained in the frame of the mixing states of compound nucleus with the same spin and opposite parities formalism. Simulated gamma spectra, taking into account different type of target and gamma loss, were also evaluated. Using modeled gamma spectra, the influence of target properties (composition, target thickness) on the investigated effect were analyzed. Forward-backward effect together with other asymmetry and parity breaking effects allow to extract new information on neutrons and gamma reduced partial widths and matrix element of weak non-leptonic interaction.

Theoretical Works of G.C. Wick in Neutron Physics of 30-ies

E.I. Sharapov

Frank Laboratory of Neutron Physics, JINR, Dubna, Russia

The name of the Italian theorist Gian Carlo Wick is well-known in the particle physics. However, in the middle of 30-ies, working in the E.Fermi group he published, in Italian and German, the works on the neutron physics which are little known at present by young physicists. This report deals with the results on the thermal neutrons albedo problem obtained by G.C. Wick as well as with his theory of inelastic neutron scattering by the condensed matter. The history of these printed works, their essence and the relevance for the neutron physics will be discussed.

1. G.C.Wick, Sulla diffusione dei neutron lenti, Atti della Reale Accademia Nazionale dei Lincei, Rendiconti XXIII, 774(1936).
2. G.C.Wick, Uber die Streung langsamen Neutronen und Atomgitters, Physikalische Zeitschrift, 38, 403(1937).

Experimental Validation of Surrogate Ratio Method for the (n,xp) Cross Sections

Aman Sharma^{1,§}, Jyoti Pandey², Punit Dubey¹, Utkarsha Mishra¹, Nitin Dubey¹, Ramandeep Gandhi^{3,4}, A. Pal^{3,4}, A. Baishya^{3,4}, T. Sathosh^{3,4}, P.C. Rout^{3,4}, S. Santra^{3,4}, B.K. Nayak^{3,4}, A. Chakraborty⁵ and A. Kumar¹

¹ Department of Physics, Banaras Hindu University, Varanasi, India

² Inter University Accelerator Centre, Aruna Asaf Ali Marg, New Delhi, India

³ Nuclear Physics Division, Bhabha Atomic Research Centre, Mumbai, India

⁴ Homi Bhabha National Institute, Anushaktinagar, Mumbai, India

⁵ Department of Physics, Siksha Bhavana, Visva-Bharati, Santiniketan, India

§ email: aman.marley1314@gmail.com

For the better estimation of gas production due to activation from fast neutrons in the structural materials of the upcoming fusion reactors, knowledge of (n,xp) cross sections of radionuclide is important [1]. Long-lived radionuclide gets accumulated in the structural material of the reactor during its operation, and (n,xp) reactions from these radionuclide will contribute to the total hydrogen production in the material. Measurements of such cross sections using direct methods are very difficult due to unstable targets. In order to overcome this issue surrogate ratio method (an indirect method) has been used in past few years [1,2]. But validity of surrogate ratio method for (n,xp) cross sections has not been studied yet by comparing the cross sections from surrogate ratio method with that from direct measurements [3]. We have performed an experiment at BARC-TIFR Pelletron accelerator facility in Mumbai, to determine ⁵⁶Fe(n,xp) cross sections using surrogate ratio method and then we compared the cross sections to the available experimental data from the direct methods. We have used ⁵²Cr(n,xp) as our reference reaction, and used ⁶Li(⁵⁵Mn,α)⁵⁷Fe and ⁶Li(⁵¹V,α)⁵³Cr surrogate reactions to populate the desired compound nuclei. The cross sections were calculated using the following ratio equation.

$$\frac{\sigma_{56Fe(n,xp)}(E_{ex})}{\sigma_{52Cr(n,xp)}(E_{ex})} = \frac{\sigma_{CN}^{56Fe+n}(E_{ex})P_{n,xp}^{57Fe}(E_{ex})}{\sigma_{CN}^{52Cr+n}(E_{ex})P_{n,xp}^{53Cr}(E_{ex})} \quad (1)$$

Where cross sections for ⁵²Cr(n,xp) were used from JENDL-3.3 library, and compound nucleus formation cross sections (σ_{CN}) were calculated using optical model calculations and decay probabilities (P^{CN}) were determined experimentally by taking ratio of the coincidence counts to the single counts. The measured cross sections are presented in Fig. 1, and it is observed that the cross sections are in agreement with the available experimental data and the evaluated data. This study established that the surrogate ratio method is valid to determine the (n,xp) cross sections.

References:

1. J. Pandey et al., *Physical Review C*, **99** (2019) 014611.
2. R. Gandhi et al., *Physical Review C*, **100** (2019) 054613.
3. A. Sharma et al., *Physical Review C*, **105** (2022) 014624.

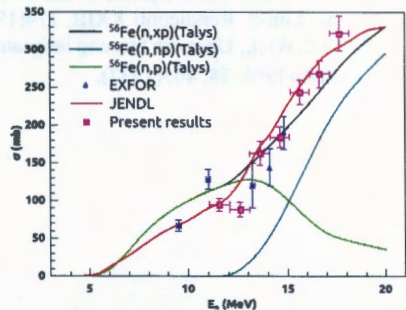


Fig. 1: ⁵⁶Fe(n,xp) cross sections obtained from surrogate ratio method along with the JENDL-3.3 and experimental data from EXFOR and TALYS predictions.

Modified Collimator for Neutron Therapy Applications: Enhancing Narrow Beam Detection of Fast Neutrons

Shehada A.M.

Chechen State Pedagogical University, Grozny, 364037, Russia

E-mail: shihada@tpu.ru

In clinical practice, it is often necessary to concentrate neutrons emitted by a target in 4π space into a mono-directional beam. This process is crucial for increasing the particle flux density and optimizing the beam shape and cross-sectional area, while minimizing neutron absorption in structural elements. A collimator can be used to change the beam shape, significantly narrowing it and achieving optimal results. This paper presents simulation works using the MCNP5 code to investigate the feasibility of applying a narrow beam of fast neutrons, measuring 2 cm or less, in radiotherapy. The simulations were performed on the original design of an 8.5×8.5 cm² collimator for treatment, located in the cyclotron laboratory of Tomsk Polytechnic University. The results show that the neutron energy spectrum remains nearly unchanged in the fast region, while the neutron flux increases by approximately 11% when using the collimator with a 2 cm aperture. The spatial distribution of fast neutrons is significantly narrower at a distance of 10 cm from the aperture compared to the original design of 8.5×8.5 cm². The narrower and more intense neutron beam reduces damage to healthy tissue and decreases the treatment time, making the procedure more comfortable for the patient. Narrow beams offer the potential to make neutron beam radiotherapy safer and more accurate for the treatment of small and irregularly shaped tumors.

Monitoring of Airborne Potentially Toxic Elements Using Moss Bag Technique on Territory of Moscow Parks

Shvetsova M.^{1,*}, Zinicovscaia I.I.^{1,2}, Kamanina I.Z.^{1,3}, Chaligava O.^{1,4},
Nekhoroshkov P.S.¹, Yushin N.S.¹

¹Joint Institute for Nuclear Research, 6 Joliot-Curie Str., 141980, Dubna, Russia

²Horia Hulubei National Institute for R&D in Physics and Nuclear Engineering, 30
Reactorului Str.MG-6, Bucharest-Magurele, Romania

³State University "Dubna", 19 Universitetskaya St., Dubna, 141980, Russia

⁴Faculty of Exact and Natural Sciences, Georgian Technical University, 77 Merab Kostava
Street, 0171 Tbilisi, Georgia

*e-mail: mks@nf.jinr.ru

Active biomonitoring using moss bag technique was applied to examine atmospheric deposition of potentially toxic elements and other elements in recreational areas of Moscow. Moss bags with *Sphagnum girgensohnii* were exposed on territory of seven parks (Elk Island, Victory Park, Ostankino, Sokolniki, Izmailovo, Kuzminki-Lublino, Tsaritsyno) at three locations in each park from June to September 2018. The content of 32 chemical elements: Na, Mg, Al, Cl, K, Ca, Sc, V, Mn, Fe, Co, Zn, As, Br, Rb, Sr, Mo, Sb, Cs, Ba, La, Sm, Tb, Hf, Ta, W, Au, Th, U, Cu, Pb and Cd) in moss samples was determined by instrumental neutron activation analysis and atomic absorption spectrometry. After three-month exposure period in some moss samples high uptake of Sb, U, Th, Sm, La, Mo, Zn, Co, Fe, V, Sc, ect. was noticed. Physiologically active elements Cl, K, and the alkali elements Rb and Cs were depleted from the moss tissue during the time of exposure. The high accumulation of Zn, Pb, Cu, Co, V and Sb in moss samples evidence the anthropogenic impact on parks, mainly associated with road traffic. A set of environmental indexes: contamination factor (CF), enrichment factor EF, total pollution index (TPI) and relative accumulation factor (RAF) were calculated in order to reveal the level of pollution. The highest RAF values were obtained for Sb on the territory of all parks. According to EF the samples were enriched in Al, Fe, U, Pb, Cd, Au, Sb, Th, Ta. The high CF values were obtained for sites located close to road traffic in Elk Island, Izmailovo, Tsaritsyno and Kuzminki-Lublino. According to TPI the level of air pollution on territory of abovementioned parks varies from moderate to high. In order to identify the major sources of pollution correlation and principal components analyses were applied.

PFN MULTIPLICITY VARIATIONS MEASUREMENT AT THE IREN FACILITY

O.V. Sidorova^{1,2}, Sh. Zeynalov¹

¹Joint Institute for Nuclear Research, Dubna, Moscow region, Russia;

²Dubna State University, Dubna, Moscow region, Russia

E-mail: sidorova@jinr.ru

PFN emission of $^{235}\text{U}(n,f)$ reaction are under investigation in JINR for last 20 year. The recent achievements in experimental apparatus simulation are the subject of this presentation. The object of simulation is prompt fission neutron (PFN) detector used for resonance neutron induced fission of U-235. The neutron source was IREN facility and double ionization chamber (DIC) with Frisch grids was used for fission fragment spectroscopy. The PFN detector was multi detector system consisted of 32 BC501 scintillation liquid filled modules from the Sionix (Netherlands) company. Detectors were located on the sphere surface with 50 cm radius. Double Frisch gridded ionization chamber, used as fission spectrometer at the same time generated trigger signal for PFN registration apparatus. For each fission event the following simulated information was recorded: correlated fission fragments time mark, emission angle in respect to the selected coordinate frames along with the pulse heights and shapes of neutron detector signals. Multiple neutron scattering and the cross-talks were taken into account in order to evaluate contribution of those effects in the final results.

Non-Destructive Investigation of Fragments of Mirrors (6th–3th Centuries BCE) from the Necropolis Volna 1 on the Taman Peninsula by Neutron Resonance Capture Analysis

N. Simbirtseva¹, S. Mazhen^{1,2}, A. Yergashov^{1,2,3}, P.V. Sedyshev¹, I.A. Saprykina^{1,4}, R.A. Mimokhod⁴

¹Frank Laboratory of Neutron Physics, Joint Institute for Nuclear Research, Dubna, Russia

²Institute of Nuclear Physics, Almaty, 050032, Republic of Kazakhstan

³L.N. Gumilyov Eurasian National University, 010008 Nur-Sultan, Kazakhstan

⁴Institute of Archaeology of the Russian Academy of Sciences, Moscow, Russia

Neutron Resonance Capture Analysis (NRCA) is known as non-destructive method. The use of neutrons, a highly penetrating particle, with resonance energy, allows one to investigate archeological objects without damaging. NRCA is based on the registration of neutron resonances in radiative capture and the measurement of the yield of reaction products in these resonances [1].

We have applied the method for the analysis of several archeological objects from the necropolis Volna 1 [2]. In this paper, we concentrate on a study of fragments of mirrors.

The mirrors have high vertical ledges, presumably belong to the Borysthenitic type of mirrors. The handle is lost, the remains of the fastening are preserved on the mirror. The metal of the mirror is degraded to a large extent, it is not possible to restore the height of the side and the design of the fastening. Analysis of the elemental composition by the XRF method is difficult. In this regard, data on the elemental composition obtained by the NRCA method are of great importance.

The study was supported by a grant from the RSF № 23-18-00196.

REFERENCES

1. P. V. Sedyshev, N. V. Simbirtseva, A. M. Yergashov, S. T. Mazhen, Yu. D. Mareev, V.N. Shvetsov, M.G. Abramzon and I.A. Saprykina, 2020, *Physics of Particles and Nuclei Letters*, vol.17, No.3, pp.389 – 400.
2. N. Simbirtseva, P.V. Sedyshev, S. Mazhen, A. Yergashov, A. Yu. Dmitriev, I. A. Saprykina, R.A. Mimokhod, “Non-destructive investigation of the Kyathos (6th-4th centuries BCE) from the necropolis Volna 1 on the Taman Peninsula by neutron resonance capture and X-ray fluorescence analysis”, *Acta IMEKO*, 2022, 11(3), 20.

Activation Study of the Metal-Organic Composite Using DT Neutrons

Skorkin V.M.

Institute for Nuclear Research of the Russian Academy of Sciences, Moscow, Russia

The metal-organic composites containing nanoparticles of gold, rare earth elements, lead are used to increase the effectiveness of radiation therapy, diagnostics and personal radiation protection. The composite structures of DNA macromolecules and Gd³⁺ ions were irradiated with neutrons from the source based on NG-400 DT neutron generator and the combined moderator from W, Pd, Bi, CH₂ materials. Samples with gadolinium composite of various weights immobilized on “Sigma” filter were activated by fast neutrons in the moderator with a flux density of 2×10^9 neutron/(cm²·s). The gadolinium radionuclide emitted photons with the energy of 363.6 keV with a half-life of 18.6 h was formed in ¹⁶⁰Gd (*n, 2n*) ¹⁵⁹Gd reaction. The sample activity of was measured with IGC-45 coaxial Ge detector (ORTEC). Determined by fast neutron activation analysis, the average weight concentration of gadolinium in the composite was about 44%. Thus, there are 3 Gd³⁺ ions per 2 DNA nucleotides.

The radiobiological efficiency of the slow neutron capture reaction in Gd composite was also investigated. The composite, containing about 0.5 mg of the natural gadolinium, was injected into the biological samples, containing about 0.1 ml of a cell suspension. The resulting gadolinium concentration is about 5 mg/ml. The biological samples have been irradiated into the cavity by slow neutrons. The integral thermal, epithermal, fast neutron and gamma ray fluxes in the biological samples was estimated using NCNP4B Monte-Carlo program. The neutron flux density measured by the activation method with the help of Mn, Nb and In samples was 1.5×10^8 neutron/(cm²·s) for thermal and 0.3×10^8 neutron/(cm²·s) for fast neutrons, respectively. Irradiation time of the biological samples was about 1 h. When gadolinium composite was present into biological samples, was the killing of all cells when irradiation.

A Study of Selected Rurik Dynasty Burials by the NAA Method

T.E. Strokovskaya^{1*}, N.V. Glombotskaya¹, A.Yu. Dmitriev¹, O.S. Philippova¹,
S.G. Lennik²

¹Frank Laboratory of Neutron Physics of Joint Institute for Nuclear Research, Dubna, Russia

²Institute of Nuclear Physics, Almaty, Kazakhstan

* t.e.strokovskaya@gmail.com

Group of Neutron Activation Analysis of Frank Laboratory of Neutron Physics of Joint Institute for Nuclear Research (FLNP JINR) analyzed unique samples of bone remains of members of the ruled dynasty of Rurik: 1) Princess Maria Borisovna of Tver (1442-1467), first wife of Grand Prince Ivan Vasilievich III of Moscow, and 2) Ivan Vasilievich IV the Terrible (1533-1585), Grand Prince and Sovereign of Moscow, who in 1547 took the title "Tsar".

Princess Maria Borisovna died young. Taking under the attention the political reasons of her marriage with the Grand Prince of Moscow state, in order to strengthen the alliance of the principalities of Tver and Moscow, and further subsequent changes of the political goals of Ivan III, the Princess of Tver became an inconvenient figure. So her death appeared very "timely" even to her contemporaries.

About the death of Ivan the Terrible there is more information from manuscripts, but the elemental analysis of his bone remains, has added some information about the lifetime ailments of the first Russian Tsar. The data obtained can also present in a new perspective the reasons of wide known odious peculiarities of his manners and his character, previously explained by the difficult circumstances of his childhood.

The elemental research was made with the help of neutron activation analysis (NAA). The samples were irradiated using the IBR-2 reactor at the FLNP JINR and the WWR-K reactor at the Institute of Nuclear Physics, Almaty, Kazakhstan.

As a result, the mass fractions of 31 elements were calculated in the samples. In bone samples of both Ivan the Terrible and Maria Borisovna, an excess of Fe was found in comparison with the remains of their contemporaries buried in medieval cemeteries in Denmark. In the remains of Maria Borisovna, an increased content of Zn, Hg, and As was found. In the bones of Ivan the Terrible, the content of magnesium is twice as low as in the bones of Maria Borisovna. The elements found may be of both lifetime and postmortem origin. When interpreting the results, the fact of diagenesis was excluded (or confirmed), and differences in the conditions of burials in the Sobornaya Square of the Kremlin and in the necropolis of the Resurrection nunnery were taken into account. Diffusion of some elements into the skeleton bones from textiles and clothing accessories as well as from soil and precipitations is possible, given the age of the burials and changes in the environment of Moscow Kremlin area in the 19th and 20th cc.

A study based on an interdisciplinary analysis of the different kinds of sources added to the information about the elemental composition of the remains of the Russian medieval elite and opened up new opportunities to revise established comprehensions about lifestyles and diet of nobility. It allowed to assert that members of the ruling dynasty used plenty of medicines and cosmetics based on mercury and arsenic during their lives, and, with a degree of probability, to state the differences for men and women of the royal family in the used materials of costumes, tableware and in their routine court practices. The data obtained allow us to hypothesize on the reasons of death of Maria Borisovna of Tver as a result of deliberate systemic poisoning of small doses of arsenic in cooptation with systemic unintentional abuse of mercury drugs. We also can revise the causes of cognitive traits of famous historical personalities, associated with lifetime imbalance of important microelements in the body.

GROUPING OF NEUTRON RESONANCE POSITIONS

S.I. Sukhoruchkin, Z.N. Soroko, M.S. Sukhoruchkina

Petersburg Nuclear Physics Institute NRC "Kurchatov Institute", 188300 Gatchina

Measurements of the neutron cross sections of heavy nuclei and their analysis at the IAE and ITEP, carried out in the 1950s and later, made it possible to find out deviations from the statistical model in the distributions of positions and spacings of neutron resonance levels [1].

In this work, we check the distinguishing character of resonance positions of target nuclei: ²³⁹Pu (0.296 eV), ²⁴¹Pu (0.264 eV), ²⁴¹Am (0.3051 eV) and ²⁴³Am (0.419 eV).

Stable intervals in the exactly known high-energy nuclear excitations observed in neutron resonance positions and spacings are compared with stable intervals in the low energy spectrum. For example the interval 1500 eV in Sb, Pd, Hf, U and other isotopes is related to stable excitations close to 1293 keV (the nucleon mass splitting) in these nuclei as $\alpha/2\pi$. The same ratio $\alpha/2\pi = 116 \cdot 10^{-5}$ exists between the superfine and fine structure intervals 1.34 eV and 1.2 keV, $2m_e=1022$ keV, $2M_q=882$ MeV and $6 \cdot M_{H^0} = 6 \cdot 125$ GeV [2].

1. S.I. Sukhoruchkin. Electron mass as the base parameter of the Standard Model. These abstracts.
2. S.I. Sukhoruchkin. Electron-based Constituent Quark Model. Nucl. Part. Phys. Proc. 318 - 323 (2022) 142.

ELECTRON MASS AS THE BASE PARAMETER OF THE STANDARD MODEL

S.I. Sukhoruchkin

Petersburg Nuclear Physics Institute NRC "Kurchatov Institute", 188300 Gatchina

Analysis of nonstatistical effects in neutron resonances of heavy nuclei was presented in [1]. In Fig. 1 distribution of resonance positions of all nuclei known in the 1966 is shown. The maximum at $5.5 \text{ eV} = 4\varepsilon''$ (where $\varepsilon'' = 1.34 \text{ eV}$ is a stable interval in ^{137}Nd spectrum) was considered in [2] as a result of the influence of the physical condensate (vacuum), which manifests itself as a radiative correction to the electron mass: $8\varepsilon'' = 11 \text{ eV} = (\alpha/2\pi)^2 \times \delta$, where $\delta = 16m_e = 8.176 \text{ MeV}$ equal to twice the pion mass difference [2].

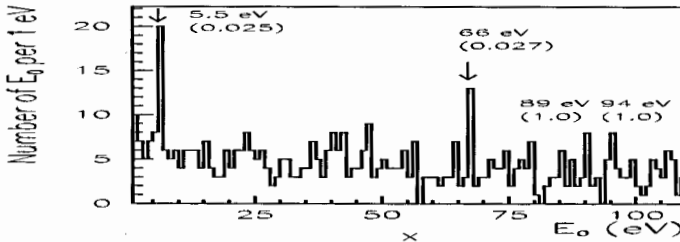


Figure 1: Distribution of resonance positions known in the 1966. The selection of one strongest resonance in the interval 10 eV was used (in parentheses is a random probability).

The pion parameters, parameters of the Constituent Quark Model and baryon masses contain an empirical discreteness parameter $16m_e = \delta$: $f_\pi = 130 \text{ MeV} = 16\delta$, $m_\pi = 140 \text{ MeV} = 17\delta$ and $\Delta M_\Delta = 147 \text{ MeV} = 18\delta$, $M_q = 3\Delta M_\Delta = 441 \text{ MeV} = 54\delta$, $M_q^\omega = 3f_\pi = 391 \text{ MeV} = 48\delta$ and $m_N = 115\delta - m_e + (1/9 \text{ or } 8/9 \text{ of the nucleon mass difference})$. The 3:1 ratio between the electron mass m_e and the scalar boson mass times the square of the QED correction to the electron mass $M_{H^0}(\alpha/2\pi)^2$ is considered. It was found out that the mass of the third lepton $m_\tau = 1777 \text{ MeV}$ differs from the masses of two muons by exactly four M_q^ω .

A symmetry motivated approach to the problem of the particle mass spectrum was used to show the distinguishing role of the electron, its symmetry, and the radiative correction to its mass. The ratio of the electron and nucleons masses is very accurately estimated in the CODATA review. The representation of the nucleon masses in terms of the period $16m_e = \delta$ close to the doubled value of the pion β -decay allows one to check the same representation in the masses of other particles [2].

1. S.I. Sukhoruchkin, Z.N. Soroko, M.S. Sukhoruchkina. Grouping of neutron resonance positions. These abstracts.
2. S.I. Sukhoruchkin. Electron-based Constituent Quark Model. Nucl. Part. Phys. Proc. **318 - 323** (2022) 142.

THERMAL MODEL OF THE IGR RESEARCH REACTOR

Surayev A.S., Vityuk V.A., Vityuk G.A., Irkimbekov R.A., Zhanbolatov O.M.

National Nuclear Center of the Republic of Kazakhstan, Kurchatov, Kazakhstan

The IGR reactor is a research pulsed reactor with a heat-capacitive type graphite core. It is one of the research reactors operated by the National Nuclear Center of the Republic of Kazakhstan. At present, along with irradiation devices testing studies are underway on the neutron-physical and thermophysical characteristics of the IGR core [1]. This requires specialized calculation tools. Therefore, this work aims to create a new high-precision model of the IGR reactor for thermophysical calculations.

The core of the IGR reactor consists of 340 graphite columns formed from graphite blocks, one part of which is impregnated with a uranium solution, and the other is not impregnated and acts as a reflector. Depending on the purpose of the column, the blocks included in its composition differ in design. They have technological holes, lugs, and grooves, which provide the possibility of their mutual fastening (fig.1a). For example, blocks with a cross-section of $\sim 98 \times 98$ mm are used to form fuel columns, and unimpregnated graphite blocks with dimensions of $\sim 197 \times 197$ mm are used for the side reflector. The height of the blocks varies from 140 mm to 148 mm. To accurately describe graphite blocks by finite element methods, grid structures were developed based on which hexahedral finite elements were generated (fig.1b).

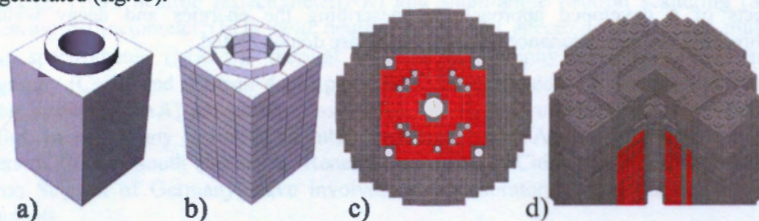


Fig. 1. IGR model: a) block geometry; b) block mesh; c) horizontal section; d) 3D view

The developed thermal model of the IGR reactor is an ordered and structured set of finite elements (fig. 1c), built with the preservation of important geometric parameters of graphite blocks. The model has 4 700 304 nodes, 4 614 328 elements, 8 427 element types, and 3 materials.

A full-scale three-dimensional model of the IGR reactor (fig.1d) is built from structured and optimized finite elements associated with the neutron model of the reactor. Implemented full interaction of models at the element level guarantees the transfer of data from one model to another in an explicit form. The model was created in the VB.NET programming environment for thermal analysis using the ANSYS program. The core temperature measured using thermocouples during the reactor start-up validated the model. The average deviation of the calculated temperature from the measured one was obtained when the core is heated up to 1400 K.

The work was funded by the Science Committee of the Ministry of Science and Higher Education of the Republic of Kazakhstan (Grant No. AP09058353).

[1] E. Batyrbekov, V. Vityuk, A. Vurim, and G. Vityuk. 2023. "Experimental Opportunities and Main Results of the Impulse Graphite Reactor use for Research in Safety Area" *Annals of Nuclear Energy* 182. doi:10.1016/j.anucene.2022.109582.

Ab Initio Study of Energies and Decay Widths of Neutron Resonances

Tchuvil'sky Yu.M.¹, Rodkin D.M.^{1,2}

¹*Skobel'syn Institute of Nuclear Physics, Lomonosov Moscow State University, Moscow 119991, Russia*

²*Dukhov Research Institute for Automatics, 127055, Moscow, Russia*

The modern theory of the light nuclei structure is being actively developed due to the introduction of ab initio methods for describing nuclear systems. An important place among these methods is occupied by various versions of the No-Core Shell Model (NCSM), which use realistic NN-potentials to describe the interaction of nucleons and bases of multinucleon states, the dimensions of which reach $10^{10} \times 10^{10}$. As a rule, the discussed potentials are constructed within the framework of the chiral effective field theory. Such methods make it possible to describe the spectra of the lower states of nuclei up to masses $A \sim 16$, their moments, and the probabilities of electromagnetic transitions.

The talk presents an ab initio approach that extends the possibilities of NCSM - the method of orthogonal functions of nucleon and cluster channels - which allows one to calculate the widths of real and virtual decays of nuclear states into nucleon and cluster channels. The prospects of a developed approach for describing the energies and decay widths of near-threshold neutron resonances of light nuclei are demonstrated.

Neutron Facilities and Their Applications at China Advanced Research Reactor

Tianfu Li, Kai Sun, Dongfeng Chen

China Institute of Atomic Energy

*Author email: litianfu.li@163.com, ksun@sina.com, dongfeng@ciae.ac.cn

The China Advanced Research Reactor (CARR) is a high-flux and multipurpose reactor, located at the campus of China Institute of Atomic Energy (CIAE) in Beijing. This reactor is a tank-in-pool inverse neutron trap type reactor with a maximum power of 60MW. The peak flux in a heavy-water reflector is about 8.0×10^{14} n/cm²/s. The main applications of the CARR are neutron scattering experiments, radioisotopes production, material irradiation, neutron transmutation doping silicon, neutron activation analysis, etc.

Up to date, fifteen neutron instruments have been successfully installed at CARR. They are high resolution powder diffractometer (HRPD), high intensity powder diffractometer (HIPD), residual stress diffractometer (RSD), texture diffractometer (TD), single crystal diffractometer (SCD), thermal neutron triple axis spectrometer (TAS), triple axis spectrometer (IOP-CIAE TAS), neutron reflectometer (NR) and small-angle neutron scattering (SANS), engineering diffractometer (ED), cold neutron triple axis spectrometer (CTAS), multi axis crystal spectrometer (MACS), thermal neutron radiography (TNR), cold neutron radiography (CNR) and neutron depth profiling (NDP). In addition, the neutron activation analysis systems (NAA) are under construction. These neutron instruments are open user facilities. In fact, many research institutes, including China Academy of Sciences, Peking University, Central South University, Renmin University of China and the Juelich Center for Neutron Science of Germany, have involved as collaborators in the construction of the instruments.

By using these instruments, many researches have been carried out. In this talk, some research examples on battery materials, magnetism, structural materials, archaeology samples and industry applications will also be briefly introduced.

ACCOMPANIED BY ALPHA-PARTICLES TERNARY FISSION OF ACTINIDES INDUCED BY THERMAL NEUTRONS

L.V. Titova, S.G. Kadmsky, E.S. Petrykina

Voronezh State University, Voronezh, Russia

E-mail: titova_lv@phys.vsu.ru

In [1-3] the virtual mechanism of ternary fission of the compound nucleus (A, Z) , formed by the capture of the thermal neutron by target-nucleus $(A-1, Z)$ as the two-stage process was suggested. At the first stage long-ranged α -particle with kinetic energy T_α close to the Coulomb barrier height is emitted from the nucleus (A, Z) with the forming of the virtual state of the intermediate nucleus $(A-4, Z-2)$ with internal energy lower than its ground state energy and undergoing binary fission at the second stage. The yield N_α of the α -particles and the energy distribution $W_{af}(T_\alpha)$ related to one act of the binary fission are defined as [1-3]

$$N_\alpha = \int W_{af}(T_\alpha) dT_\alpha = \frac{\Gamma_{af}}{\Gamma_f^A}, \quad (1)$$

$$W_{af}(T_\alpha) = \frac{1}{2\pi} \frac{(\Gamma_\alpha^A(T_\alpha))^0}{(Q_\alpha + |B_n| - T_\alpha)^2} = \omega_\alpha \frac{\hbar c \sqrt{2T_\alpha}}{2R_{neck} \sqrt{\mu c^2}} P(T_\alpha), \quad (2)$$

where Γ_{af} and Γ_f^A is the widths of the ternary and binary fission of compound nucleus (A, Z) , consequently, $(\Gamma_\alpha^A(T_\alpha))^0$ is the width of the virtual α -decay of the nucleus (A, Z) from the deformed transition fission state corresponding to the configuration (0) of these nuclei with the neck radius R_{neck} between two fission prefragments, Q_α is the heat of the true α -decay of the nucleus (A, Z) , B_n is neutron binding energy in (A, Z) , $P(T_\alpha)$ is α -particle penetrability factor of the Coulomb barrier formed by the sum of the non-spherical nuclear $V_n(\bar{r})$ and Coulomb $V_c(\bar{r})$ potentials of the α -particle interaction with nucleus $(A-4, Z-2)$, ω_α is the probability of α -particle formation in the nucleus (A, Z) , μ is the reduced mass of α -particle and nucleus $(A-4, Z-2)$. Using the experimental energy distributions $W_{af}(T_\alpha)$ [4-6] the estimations of the R_{neck} from (2) were obtained, taking into account that $P(T_\alpha) \approx 1$ at the maximal energies of the emitted α -particles T_α . The values of the neck radius R_{neck} are 2.37 fm for target-nuclei U^{233} , 2.66 fm for ^{235}U , 2.87 fm for ^{241}Pu and 2.54 for ^{251}Cf in fission induced by thermal neutrons and are in good agreement with R_{neck} from [7] and demonstrates that α -particle in ternary fission is escapes from the compound nucleus neck.

1. S.G. Kadmsky et al. PEPAN 63, 620 (2022)
2. S.G. Kadmsky, L.V. Titova, D.E. Lyubashevsky Phys. At. Nucl. 83, 326 (2020)
3. L.V. Titova, Bulletin MSU. Ser. 3: Physics. Astronomy. № 5, 64 (2021)
4. Yu.N. Kopatch et. al. // CP798 Nuclear Fission and fission spectroscopy, p. 115 (2005)
5. O. Serot et al. // CP769 Int. Conf, in Nucl. Data for Science and Technology, p. 857 (2005)
6. S. Vermote et al. Nuclear Physics A 837, 176 (2010)
7. O.Serot, N.Carjan, C.Wagemans, Eur. Phys. J. A. 8, 187 (2000)

Determining of Thermal and Resonance Neutron Fluxes Distribution for Research of Nuclear Data of Isotopes at the IREN Facility

Tran Minh Nhat Le¹, S.B. Borzakov¹, A.Yu. Dmitriev¹, Hong Khiem Le²,
Duc Cong Vu^{1,2}, Ngoc Toan Tran¹

¹Joint Institute for Nuclear Research, Dubna, Russia

²Institute of Physics, Viet Nam Academy of Science and Technology,
Ha Noi, Viet Nam

*e-mail: andmitriev@jinr.ru

The nuclear data is important values not only for fundamental nuclear physics but also for applications. Nowadays, many physical methods have applied to research one of which is Neutron Activation Analysis (NAA), so the updating demand for these data are always crucial for global nuclear data library. In Frank Laboratory of Neutron Physic JINR, NAA method is carried out at the IREN facility. The IREN facility is the pulsed intensive resonance neutron source, combining of a linear electron accelerator LUE-200, a Wolfram-Ni-Iron alloy target (90% W) and the water moderator. Since the flux of neutrons emitted from the target is uneven, it is necessary to reveal the dependence of flux to the irradiation position on the moderator's surface.

In this work, we used 6 pairs of flux monitors: Cu (in a cadmium shell) – Cu (without the shell) with same size. The monitors were placed at 1, 3, 5, 7, 9 cm top-down from the upper edge of the moderator. Also the same size 11 pairs of Cu flux monitors were placed around of 43 cm perimeter of moderator at 5 cm mark from the top-down. All monitors were irradiated in two phases for 5 hours for each. The IREN control modes were follows: burst frequency – 25 Hz, beam current – 1.6 A, electron energy – 110 MeV and average electron's current – 4.5 μ A approximately. Spectrometric data were collected for 2 hours for each sample, using an automatic system, which includes a samples changer and the Canberra GC 4018 HPGe detector with relative efficiency 40%, resolution 1.8 keV at 1.33 MeV. GENIE-2000 software was used for spectra processing. Cadmium-difference method was applied for calculating the neutron fluxes. As a result, the maximal value of the thermal neutron flux is equal to $2 \cdot 10^8$ n \cdot cm⁻²·sec⁻¹ at 5 cm from the top-down. The changes in fluxes distribution around the perimeter of the moderator were minor.

We plan to use obtained data for determination both thermal neutron capture cross-section and resonance integral of some important isotopes, using in different physic fields.

Optical Properties and Chemical Composition of Native-Oxide Layer on the Surface of GaAs Irradiated with Noble Gases

P.L. Tuan^{1,2}, A.I. Madadzada^{1,3}, M. Kulik⁴, A.Sh. Khaligzadeh⁵, T.V. Phuc^{6,7}, D. Kolodynska⁸, L.H. Khiem^{6,7}, K. Siemek⁹

¹Frank Laboratory of Neutron Physics, Joint Institute for Nuclear Research, Dubna, Russia

²Hanoi Irradiation Center, Vietnam Atomic Energy Institute, Hanoi, Viet Nam

³Department of Nuclear Research, Innovation and Digital Development Agency, AZ 0100 Baku, Azerbaijan

⁴Institute of Physics, Maria Curie-Skłodowska University, pl. M. Curie-Skłodowskiej 1, 20-031 Lublin, Poland

⁵Institute of Radiation Problems of the Ministry of Science and Education of the Republic of Azerbaijan, Baku, Azerbaijan

⁶Graduate University of Science and Technology, Vietnam Academy of Science and Technology, Ha Noi, Viet Nam

⁷Institute of Physics, 10 Dao Tan, Ba Dinh, Ha Noi, Viet Nam

⁸Chemical Department, Maria Curie-Skłodowska University, pl. M. Curie-Skłodowskiej 2, 20-031, Lublin, Poland

⁹Institute of Nuclear Physics, Polish Academy of Sciences, PL-31342 Krakow, Poland

Monocrystalline (100) semi-insulating gallium arsenide (GaAs) samples were irradiated by noble gases (He⁺, Ne⁺, Ar⁺, Kr⁺ and Xe⁺) ion beam. The energies of the ion beams were 100, 150 and 200 keV, respectively. The irradiation was performed at a room temperature using a fluence of 1×10^{16} ions/cm². Because, noble gases have complete valence shells and do not form any new chemical bonds with the target atoms (Ga and As), the interaction with implanted atoms does not result in the production of any new chemical compounds. This is why noble gases were used in this research. To investigate the formation and growth of native oxide layers on samples before and after implanting, the spectroscopic ellipsometry (SE) method and X-ray photoelectron spectroscopy (XPS) method were used. The SE method demonstrates that the optical properties of the native oxide layer on the surface of GaAs samples vary with ions and energy. We found that the mass of the ion used in the implantation process has an effect on both the shape and the values of the imaginary part of the optical properties. XPS approach, which reveals the chemical composition of native oxide layer on the surface of GaAs samples, confirms that the native oxide layer on GaAs samples is a mixing of Ga₂O₃, As₂O₃, As₂O₅ and GaAs compound. The concentration of these compound various with ion mass.

Corresponding author: madadzada@jinr.ru

Using Rutherford Backscattering Spectroscopy to Investigate ErF₃ Doped CaF₂ Samples

P.L. Tuan^{1,2,*}, M. Kulik³, M. Stef⁴, T.V. Phuc^{5,6}, N.T.B. My^{1,7}, N.N. Anh^{8,9}, T.Y. Zelenyak¹, G. Buse⁴, A. Racu⁴, A. Doroshkevich¹, L.H. Khiem^{5,6}, V.D. Cong^{1,5}

¹Frank Laboratory of Neutron Physics, Joint Institute for Nuclear Research, Dubna, 141980, Russia;

²Hanoi Irradiation Center, Vietnam Atomic Energy Institute, Hanoi, 129000, Viet Nam;

³Institute of Physics, Maria Curie-Skłodowska University, Pl. Marii Curie-Skłodowskiej 1, 20-031 Lublin, Poland;

⁴Faculty of Physics, West University of Timisoara, 300223 Timisoara, Romania;

⁵Institute of Physics, Vietnam Academy of Science and Technology, 10 Dao Tan, Ba Dinh, Hanoi, 118500, Viet Nam;

⁶Graduate University for Science and Technology, Vietnam Academy of Science and Technology, 18 Hoang Quoc Viet, Cau Giay, Hanoi, 122100, Viet Nam;

⁷Institute for Nuclear Science and Technology, Vietnam Atomic Energy Institute, Hanoi, 122100, Viet Nam;

⁸Faculty of Fundamental Science, PHENIKAA University, Yen Nghia, Ha Dong, Hanoi 12116, Viet Nam;

⁹PHENIKAA Research and Technology Institute (PRATI), A&A Green Phoenix Group JSC, No.167 Hoang Ngan, Trung Hoa, Cau Giay, Hanoi 11313, Viet Nam

Using the vertical Bridgman method, we grow ErF₃ doped calcium fluoride (CaF₂) crystals with various concentrations. These samples are investigated using the Rutherford backscattering spectroscopy (RBS) method, which determines the depth profile of Ca, F, and Er (Fig. 1). The obtained results allow us to identify the correlated changes in the concentration of element of the crystals as Er³⁺ ions are doping. In addition, we build several trial models using the SIMNRA computer code to simulate the RBS spectra of all the investigated samples with different incident angle. Because the simulated spectra agree well with the experimental spectra, we can use these models to determine the depth profile of elements obtained directly from the RBS experiment spectra, the homogeneity of samples, and the possibility of layer porosity in ErF₃ doped CaF₂ crystals, where the concentration of Er may also play an important part (Fig. 2).

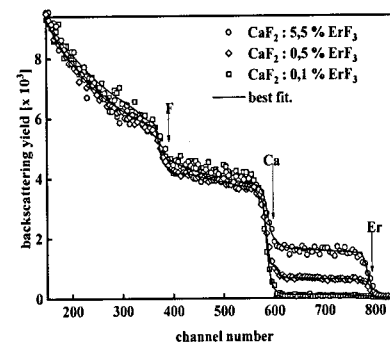


Fig. 1

Keywords: calcium fluoride; RBS; ErF₃; depth profile; porosity

*Corresponding author: phanluongtuan@gmail.com

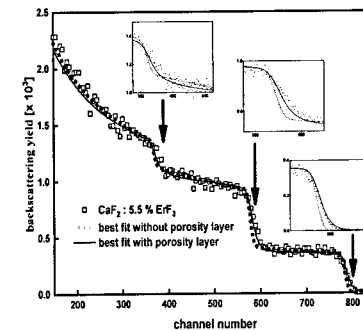


Fig. 2

Moss Survey-2020/2021 in the Regions of Central Russia

Vergel K.^{1,2*}, Zinicovscaia I.^{1,4}, Yushin N.¹, Chaligava O.^{1,2}, Cepoi L.^{2,3}

¹*Sector of Neutron Activation Analysis and Applied Research, Division of Nuclear Physics, FLNP, Joint Institute for Nuclear Research, Dubna, Moscow Region, Russian Federation*

²*Doctoral School of Biological, Geonomic, Chemical and Technological Sciences, Moldova State University, Chisinau, Republic of Moldova*

³*Institute of Microbiology and Biotechnology, Technical University of Moldova, Chisinau, Republic of Moldova*

⁴*Horia Hulubei National Institute for R&D in Physics and Nuclear Engineering, 30 Reactorului Str. MG-6, Bucharest - Magurele, Romania*

**e-mail: vergel@jinr.ru*

Results of the study of heavy metals atmospheric deposition in the regions of Central Russia: Moscow, Vladimir, Yaroslavl and Tver regions based on moss analysis are presented. Moss samples were collected during summers in the period 2019-2021 at 425 sample sites evenly distributed over the region in accordance with the guidelines of the UNECE ICP Vegetation. Investigated territory covered an area of 193 000 km². Neutron activation analysis was used for determination of up to 40 elements in samples collected in Moscow, Vladimir and Yaroslavl regions and ICP-OES for detection of 16 elements in Tver region. Multivariate statistical analysis has been applied to reveal possible pollution sources. Using GIS software were created distribution maps. The main air pollution source in all investigated regions is transport, while industrial enterprises contributed to local contamination of the environment.

Experimental Measurement of Neutronic Performance at Neutron Beam Line in CSNS

Song Lin WANG, Bin ZHOU, Tian Cheng YI, Fei SHEN, Tian Jiao LIANG

Institute of High Energy Physics, Chinese Academy of Sciences, Beijing 100049, China

China Spallation Neutron Source (CSNS) passed its national acceptance on August 23, 2018, and was officially open to worldwide users in various disciplines. Three neutron beam lines of target station, BL06, BL09 and BL20, have been constructed in the spectrometers room at CSNS. A primary mission of three beamlines is to study the neutronic performance of CSNS. This paper describes detailed objectives and experimental techniques to be adopted in the experiments.



Fig.1 Three neutron beam lines of target station, BL06, BL09 and BL20.

The neutronic performance measurements are crucial for commissioning and operation to demonstrate that target stations are working properly to produce neutrons at a satisfactory level, it's also helpful to validate the MC simulation. The Current mode Time of Flight (CTOF) is chosen to measure the neutron spectrum during commissioning, this can be helpful to reduce the activity of target station components during commissioning due to the high detection efficiency. The experimental measurements agree well with the simulation results.

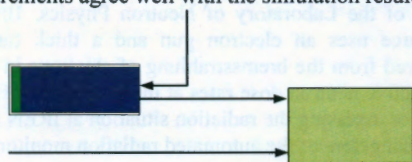


Fig.2 The electronic circuit diagram of CTOF technique.

The pulse shape of neutrons emitted from the moderator as a function of energy is essential for the design of instruments. A crystal monochromator and detector arrangement as shown in figure 3 is chosen to measure the pulse shape of serial neutrons whose energy fulfills the Bragg law. The neutron pulse shape experimental measurements of BL06 and BL09 agree well with the simulation results.



Fig.3 The schematic view of experimental arrangement for pulse shape measurement.

Neutron Fields Measurements at IREN Facility behind Biological Shielding

Yakubov T.R., Timoshenko G.N., Shvetsov V.N.

Department of Radiation Safety and Frank Laboratory of Neutron Physics, Joint Institute for Nuclear Research, Dubna 141980, Russia

The radiation fields behind the shields of the JINR nuclear facilities are formed mainly by neutrons of a wide energy spectrum. Radiation control in the fields of mixed (neutrons and gamma rays) and scattered radiation is a difficult task, especially in cases where the upper neutron energy exceeds 15–20 MeV. This is due to the fact that the mechanisms of interaction of neutrons with matter (and, accordingly, the sensitivity of neutron dosimeters) change strongly with an increase in their energies from thermal to tens and hundreds of MeV. The most adequate technique for determining the values of the effective dose of neutrons is associated with the measurement of their energy distribution and the use of calculated fluence-effective dose conversion factors in the geometry of human irradiation typical for the measurement site. To measure the spectrum of scattered neutrons in a wide energy range, a multisphere spectrometer is used, according to the readings of which the neutron spectrum at the measurement point is then restored.

This paper describes the results of measuring neutron spectra at two points at the Resonance Neutron Source (IREN) of the Laboratory of Neutron Physics, JINR. To obtain powerful neutron fluxes, this source uses an electron gun and a thick tungsten target, in which photoneutrons are produced from the bremsstrahlung of electrons in the target. Based on the obtained spectra, the effective neutron dose rates at the measurement points were determined, which is important both for assessing the radiation situation at IREN and for comparison with the readings of neutron dosimeters of the automated radiation monitoring system.

Application of the Yeast *Saccharomyces cerevisiae* for the Removal of Heavy Metals from Industrial Wastewater

Yushin N.¹, Zinicovscaia I.^{1,2}

¹Joint Institute for Nuclear Research, Joliot-Curie Str., 6, 141980 Dubna, Russia

²Horia Hulubei National Institute for R&D in Physics and Nuclear Engineering, 30, Reactorului Str., 077125 Magurele (Ilfov), Romania

The waste of the yeast *Saccharomyces cerevisiae* biomass originated from beer fermentation industry, was used to remove metal ions from four synthetic nickel-containing effluents. Biosorbent was characterized using scanning electron microscopy and Fourier-transform infrared spectroscopy. The effect of pH, nickel concentration, contact time, and temperature on metal biosorption was investigated. Characterisation of biosorption equilibrium was evaluated employing the Langmuir, Freundlich and Temkin models. The kinetics of the biosorption was described using pseudo-first order, pseudo-second order, Elovich model and the intra-particle Weber and Morris diffusion models. According to the thermodynamic parameters the biosorption can be described as a spontaneous process. The effect of pH and sorbent dosage on metal removal from real industrial effluent was investigated. The two-stage sequential scheme of Ni(II) removal from effluent by the addition of different dosage of new sorbent was proposed.

NEUTRON ACTIVATION ANALYSIS IN MEDICAL DIAGNOSIS: CURRENT STATE AND PROSPECTS FOR THE FUTURE

Zaichick V.¹, Kolotov V.²

¹Medical Radiological Research Centre, Obninsk, Russia, E-mail: vzaichick@gmail.com

²Vernadsky Institute of Geochemistry and Analytical Chemistry of Russian Academy of Sciences,
Moscow, Russia

E-mail: kolotov@geokhi.ru

The first studies of the possibilities of using neutron activation analysis (NAA) in medical diagnostics date back to the middle of the last century. This was facilitated both by the appearance of various neutron sources and by the development of spectrometric technology, at first based on scintillation and then on semiconductor detectors. The scientific foundation for conducting such studies is the idea of the presence of elemental homeostasis of living organisms in a normal state. As a result of violations of elemental homeostasis, pathological conditions can occur, and, conversely, pathological conditions can significantly deform elemental homeostasis. In ongoing research, one should distinguish between two major areas: *in vivo* and *in vitro* analysis. These two directions differ significantly, since *in vivo* examination of a person involves obtaining useful medical information with minimal discomfort and harmful effects for both the subject and medical personnel. Such examinations of the human body are strictly regulated by the permissible radiation dose and require the construction of special installations for neutron irradiation and highly sensitive low-background spectrometric equipment. Within *in vivo* studies, two subgroups can be distinguished: *in vivo* determination of the content of chemical elements in the whole human body and partial analysis, when only a certain part of the body or organ is examined. With partial examination, the allowable radiation doses can be higher, which expands the possibilities of NAA, and the irradiation and measurement installations are more compact than with *in vivo* NAA of the whole body.

NAA *in vitro* medical material also has its own peculiarities. First of all, they are associated with the presence of a multicomponent organic matrix and a low, and often ultra-low, content of trace elements. Another feature is associated with restrictions on the mass of the test sample. The modern level of surgery and anesthesiology makes it possible to obtain milligram amounts of tissue from almost any organ of the human body by biopsy, which is widely used in oncology for morphological studies. Such kind of samples can be also used and for NAA.

The report will consider the current possibilities of using NAA *in vivo* and *in vitro* in medicine and give specific examples of the use of the results obtained in assessing the state of the human body. Further development of this direction will largely depend on the rate of accumulation of our knowledge about the elemental composition of the whole human body, its organs, tissues and fluids, both in normal (healthy) and in pathological conditions, taking into account gender, age, race, nationality, place of residence (climate, geochemical factors, the level of regional ecological well-being), nutritional habits, areas of activity (professional factors) and the presence of bad habits.

A New Experiment on Study Non-Stationary Neutron Diffraction by Surface Acoustic Waves

M.A. Zakharov¹, G.V. Kulin¹, A.I. Frank¹, N.V. Rebrova¹, Ph. Gutfreund²,
Yu.N. Khaydukov^{3,4,5}, L. Ortega⁶, D.V. Roshchupkin⁷

¹Joint Institute for Nuclear Research, Dubna, Russia

²Institut Laue-Langevin, Grenoble, France

³Lomonosov Moscow State University, Moscow, Russia

⁴Max-Planck-Institut für Festkörperforschung, Stuttgart, Germany

⁵Max Planck Society Outstation at the MLZ, Garching, Germany

⁶Laboratoire de Physique des Solides, Université Paris-Sud, CNRS, Orsay, France

⁷Institute of Microelectronics Technology and High Purity Materials RAS, Chernogolovka,
Russia

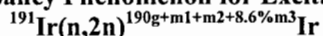
Neutron diffraction by a traveling surface acoustic wave (SAW) is a non-stationary quantum process leading to the transfer of an energy quantum to a neutron $\Delta E = n\hbar\Omega$, where n is an integer, \hbar is Planck's constant, Ω is a frequency of the wave.

The first and until recently the only one experiment on the observation of neutron diffraction by SAW was carried out by Hamilton et al. [1]. In [2], we presented the results of an experimental investigation of this phenomenon and an approach to its theoretical description. In the experiment, the neutron wavelength remained fixed at a variable angle of incidence.

The report will present the results of a new experiment on the study of neutron diffraction by SAW and a comparison with theoretical predictions. In contrast to the experiments [1, 2], the new measurements were carried out at a fixed angle of incidence and in the time-of-flight mode. This made it possible to study the diffraction pattern in a wide range of wavelengths.

1. W.A. Hamilton, A.G. Klein, G.I. Opat and P.A. Timmins., Phys. Rev. Lett., **58**, 2770 (1987).
2. G.V. Kulin, A.I. Frank, V.A. Bushuev, Yu.N. Khaydukov, D.V. Roshchupkin, S. Vadilonga, A.P. Sergeev, Phys. Rev. B, **101**, 165419 (2020).

Study of Discrepancy Phenomenon for Excitation Function of



Zhang Changfan, Hu Guangchun, Xiang Yongchun, Wenjie, Zhou Haojun, Heyao,
Gong Jian

China Academy of Engineering Physics, Institute of Nuclear Physics and Chemistry,
Mianyang city 621900, China

Accurate $^{191}\text{Ir}(n,2n)^{190g+m1+m2+8.6\%m3}\text{Ir}$ cross-section data are of great importance for the ICF medium- and high-energy neutron diagnostics and nuclear structure studies. Numerous integration experiments carried out to check the accuracy of the $^{191}\text{Ir}(n,2n)^{190g+m1+m2+8.6\%m3}\text{Ir}$ cross-section data indicated that the calculated-to-experimental ratios based on ENDF/B-VII.1 evaluation data are large deviations at devices with a large portion of fission neutrons. A new excitation curve Hybrid combining ENDF/B-VII.1 evaluation data with TALYS-1.96 program was constructed, which is in better agreement with the microscopic cross-sectional measurement data above 12 MeV. Several calculation models for the integration test were constructed based on both experiments and literatures, including the Cf source, CFBR-II pulsed reactor, Jezebel, Flattop25, Bigten and Bethe Spheres. A detailed analysis of the deviation between the experiments and calculation was conducted, and it was concluded that the current evaluation data of $^{191}\text{Ir}(n,2n)^{190g+m1+m2+8.6\%m3}\text{Ir}$ are overestimated in the whole range of 8~20 MeV, where the evaluation in 8~12 MeV will lead to a fission neutron diagnosis bias of ~10%, and that in 12~14 MeV will lead to a fusion neutron diagnosis bias of ~5%.

Experimental Introduction to Parity Violation and Time Reversal Asymmetry in NOPTREX

Mofan Zhang¹, William Micheal Snow¹, Ruirui Fan^{2,3}, Xin Tong^{2,3}

¹Indiana University, Indiana IN, 47405, USA

²中国科学院高能物理研究所, 北京市石景山区玉泉路19号乙, 100049

³散裂中子源科学中心, 广东省东莞市大朗镇中子源路1号, 523803

Finding new sources of time reversal asymmetry is of great significance in both particle physics and cosmology. The discovery of any time reversal asymmetry will not only break the Standard Model, but also provide clues to the asymmetry of matter and antimatter in the Big Bang cosmology [1]. The NOPTREX collaboration will search for three types of symmetry violation in nucleon interactions in the P-wave resonance of key nuclei, including: parity-odd/time-even (P-odd/T-even) interactions, parity-odd/time-odd (P-odd/T-odd) interactions, and parity-even/time-odd (P-even/T-odd) interactions in forward transmission of polarized neutrons through polarized/aligned nuclear targets. Parity violation (PV) phenomena on p-wave resonances is amplified by a factor of 10^3 - 10^6 , and theory suggests that P-even/T-odd and P-odd/T-odd interactions in the p-wave resonance will also be amplified by factors of 10^3 - 10^6 .

Parity-odd/Time-reversal-even(P-odd/T-even) interaction

We can relate the P-odd/T-even asymmetry (or in another word PV) with the P-odd/T-odd asymmetry in the same p-wave resonance using the following equation:

$$\Delta\sigma_{TP} = \kappa(J) \frac{w}{v} \Delta\sigma_P$$

$\Delta\sigma_{TP}$ denotes the P-odd/T-odd cross section difference, $\Delta\sigma_P$ denotes the P-odd/T-even cross section difference, w/v is the ratio between the P-odd/T-odd and P-odd/T-even matrix elements, $k(J)$ is a spectroscopic factor of a specific P-wave resonance which can be determined by measuring the angular distribution of gamma rays from neutron capture radiative decay [2,3].

Parity-odd/Time-reversal-odd (P-odd/T-odd) interaction

Compound nuclear resonances can amplify a P-odd/T-odd NN interaction amplitude in the P-wave resonance peak by a factor of 10^6 [4,5,6]. This makes it possible to measure something that was previously impossible with existing scientific technologies. The NOPTREX collaboration is preparing for this experiment by measurement of PV effects in a series of nuclei with different P-wave resonance peaks, the measurement of neutron capture gamma-ray angular distribution to obtain $k(J)$, and the P-even/T-odd measurement mentioned below.

Parity-even/Time-reversal-odd (P-even/T-odd)

Time-reversal symmetry (T) can be broken through parity-even/time-reversal-odd interactions. If a non-zero electric dipole moment (EDM) is measured in a nucleon system, there are two possible explanations: (1) the discovery of a new P-odd/T-odd interaction beyond the standard model, or (2) a combination of a P-even/T-odd interaction with known P-odd interactions in the standard model. Many experiments are vigorously searching for EDMs in many nucleon, nucleus, atom, and molecule systems. If a non-zero EDM is found, distinguishing between (1) and (2) will be very important as they imply different types of beyond standard model physics. The compound nucleus resonance amplification mechanism can amplify the P-even/T-odd NN interaction amplitude in the p-wave resonance peak by a factor of 10^3 [4, 5, 6]. Exploration of P-even/T-odd in neutron-nucleon interactions (NN) systems will complement research on EDM and clarify experimental phenomena found in other nucleon systems. No active experiments in the world are dedicated to search for P-even/T-odd interactions between nucleons or in atomic nuclei, so NOPTREX's efforts in this area will be unique worldwide.

1. A.D. Sakharov, *JETP Lett.* 5, 24-27, 1967.
2. Vladimir Gudkov and Hirohiko M. Shimizu. *Phys. Rev. C*, 065502, 97 (2018).
3. T. Okudaira, et al, *Phys. Rev. C*, 034622, 97 (2018).
4. V. E. Bunakov and V. P. Gudkov, *Nucl. Phys. A401*, 93 (1983).
5. V. P. Gudkov, *Phys. Rept.* 212, 77 (1992).
6. V. P. Gudkov and Y-H. Song, *Hyperfine Interact.* 214, 105 (2013).
7. Chupp et al, *Rev. Mod. Phys.* 91, 015001 (2019).

Measurement of the $^{159}\text{Tb}(n, \gamma)$ Cross Section at the CSNS Back-n Facility

S. Zhang^{1,2}, M. Huang^{1,2}, D.X. Wang^{1,2}, D.D. Niu^{1,2}, X.Li^{1,2}, G. Li^{1,2}, M. Gu^{1,2},
Y.S. Huang^{1,2}, Y. Bai^{1,2}, Z.L. Wang^{1,2}

¹College of Mathematics and Physics, Inner Mongolia Minzu University,
Tongliao 028000, China

²Inner Mongolia Joint Laboratory of Nuclear and Radiation Detection,
Tongliao 028000, China

The stellar (n, γ) cross section data for the mass numbers around $A \approx 160$ are of key importance to nucleosynthesis in the main component of the slow neutron capture process, which occurs in the thermally pulsing asymptotic giant branch (TP-AGB). The new measurement of (n, γ) cross sections for ^{159}Tb was performed using the C_6D_6 detector system at the back streaming white neutron beam line (Back-n) of the China spallation neutron source (CSNS) with neutron energies ranging from 1 eV to 1 MeV. Experimental resonance capture kernels are reported up to 1.2 keV neutron energy with this capture measurement. Maxwellian-averaged cross sections (MACS) are derived from the measured $^{159}\text{Tb}(n, \gamma)$ cross sections at $kT = 5 \sim 100$ keV and are in good agreement with the recommended data of KADoNiS-v0.3 and JEFF-3.3, while KADoNiS-v1.0 and ENDF-VIII.0 significantly overestimate the present MACS up to 40% and 20%, respectively. A sensitive test of the s-process nucleosynthesis is also performed with the stellar evolution code MESA. Significant changes in abundances around $A \approx 160$ are observed between the ENDF/B-VIII.0 and present measured rate of $^{159}\text{Tb}(n, \gamma)$ ^{160}Tb in the MESA simulation.

References

1. S. Zhang, et al. arXiv preprint arXiv:2212.01820 (PRC accepted)
2. R. Reifarth, C. Lederer, and F. Kappeler, *J. Phys. G: Nucl. Part. Phys.* 41, 053101 (2014).
3. F.-K. Thielemann, et al., *Prog. Part. Nuc. Phys.* 66, 346 (2011).
4. E. Burbidge, G. Burbidge, W. Fowler and F. Hoyle, *Rev. Mod. Phys.* 29, 547 (1957).
5. A. Cameron, Technical Report CRLC41 (Chalk River: Atomic Energy of Canada, Ltd.), 1957.
6. M. Arnould, S. Goriely, *Phys. Rep.* 384, 1 (2003).
7. S.E. Woosley, D.H. Hartmann, R.D. Hoffman, and W.C. Haxton, *Astrophys. J.* 356, 272 (1990).

Design and Calibration of Large Field of View Dual-Particle Time-Encoded Imager Based on Depth of Interaction Detector

Zhao Dong¹, Liang Xuwen¹, Hei Daqian², Jia Wenbao¹

¹Nanjing University of Aeronautics and Astronautics, Nanjing 210000, China

²Lanzhou University, Lanzhou 730000, China

Global concern for the illicit transportation and trafficking of nuclear materials and other radioactive sources is on the rise, with efficient and rapid security and non-proliferation technologies in more demand than ever. This issue highlights the importance of the effective control of nuclear and radiation materials at national and international cross points such as borders, ports and airports. Time-encoded imaging could be useful for searching potential radioactive sources for preventing illicit transportation and trafficking of nuclear materials.

A 2-D, dual-particle, time-encoded imager based on depth of interaction (DOI) detector was developed for gamma-ray and neutron source imaging. The imager mainly consists of a central detector, a cylindrical coded mask and a drive unit. An EJ276 plastic scintillator (Size: $\Phi 3 \text{ cm} \times 15 \text{ cm}$) couple to two silicon photomultiplier was designed as a depth of interaction detector for neutrons and gamma-rays. The position resolution of the DOI detector was approximately 4.4 cm. The cylindrical coded mask consisted of the polyethylene (PE) and brass to shield the fast neutron and gamma-ray. The thickness of the brass for gamma-ray modulation and PE for fast neutron modulation was 0.9 cm and 6 cm, respectively. The order of the mask was 61×19 and the open fraction was about 50% (589 mask elements and 570 apertures). The height of each layer was about 1.63 cm. For easy processing, the 19 layers of mask designed to be identical according to the Uniform Redundant Array (URA). Each layer is rotated at different angles (horizontal unit) from each other, randomly. The cylindrical mask was fixed on a rotation table and driven by a step motor.

The response function of the time-encoded imager was simulated using MCNP 5. In the simulation, the horizontal and vertical field of view range was $0^\circ \sim 360^\circ$ and $-60^\circ \sim 60^\circ$, respectively; the neutron and gamma-ray sources were set as Cf-252 and Cs-137 at three meters from the detector. The classical Maximum Likelihood Expectation Maximization (MLEM) method was used in image reconstruction. The 'multi-detector' filtering method was proposed to denoise for this imager. The rotation speed of the mask was set as 200 s/revolution during the measurement. A Na-22 gamma-ray source was placed in different position to determine the field of view (H: $0^\circ \sim 360^\circ$; V: $-55^\circ \sim 55^\circ$); A shielded DT neutron source at 20.4 meters standoff was detected to verify the performance of the imager. The source could be located within 2400s (Approx. 2800 counts) and the angular resolution was better than 3.5° .

ASSESSMENT OF AIR POLLUTION IN ULAANBAATAR USING ACTIVE MOSS BIOMONITORING TECHNIQUE

I. Zinicovskaia^{1,2,3}, J. Narmandakh⁴, N. Yushin¹, A. Peshkova¹, O. Chaligava^{1,5},
T. Tsendsuren⁴, B. Tserendorj⁴, Ts. Tsogbadrakh⁶

¹Joint Institute for Nuclear Research, 6 Joliot-Curie Str., 141980, Dubna, Russia,
zinikovskaia@mail.ru

²Horia Hulubei National Institute for R&D in Physics and Nuclear Engineering, 30
Reactorului Str., MG-6, Bucharest - Magurele, Romania

³Institute of Chemistry, Academiei Str. 3, MD-2028, Chisinau, Republic of Moldova

⁴Institute of Physics and Technology, Mongolian Academy of Sciences, Peace Ave 54B,
Ulaanbaatar, 13330, Mongolia

⁵Faculty of Informatics and Control Systems, Georgian Technical University, 77 Merab
Kostava Street, 0171 Tbilisi, Georgia

⁶Department of Metropolitan Air and Environmental Pollution Control, Ulaanbaatar, 17100,
Mongolia

Moss biomonitoring technique widely applied in many countries, for the first time, was applied to assess the air quality in Ulaanbaatar. Moss *Sphagnum girgensohnii* Russow was exposed for three different periods: December-February, March-May, and December-May at 13 Government stations for air quality monitoring. The content of Al, Ba, Co, Cd, Cr, Cu, Fe, Mn, P, Pb, Sr, S, V, As and Zn was determined using inductively coupled plasma-optical emission spectrometry, while a direct mercury analyzer was used to determine Hg content in samples. Significant differences in elements accumulation between seasons were noticed, the remarkable fact is that accumulation of Al, Ba, As, Co, Cr, Fe, Pb, V and Zn was higher in the spring, while P and S were more actively accumulated in moss samples exposed during the winter period. Several indices, namely the Relative accumulation factor, Contamination factor, Pollution load index, and Enrichment factor were calculated in order to evaluate the level of air pollution and the possible origin of elements. Substantial contributions to air pollution are making Zn, Fe, As, V, Cr and Al. Factor and correlation analysis were applied to highlight the association of elements and to link them with possible sources of emission. Soil particles, dust originating from combustion burning, transport, and coal burning can be designated as main air pollution sources.

Acknowledgment

Present study was supported by the GRANT № NABOG - 02 - 50

Research on Position Resolution Method of Scintillation Signal Based on CNN+LSTM Network

Wei Cheng¹, Chengfeng Liu¹, Wenbao Jia¹, Weiwei Qu², Yongsheng Lin¹

¹Department of Nuclear Science and Technology, Nanjing University of Aeronautics and
Astronautics, Nanjing, 211106, China

²State Key Laboratory of Radiation Medicine and Protection, School of Radiation Medicine
and Protection, Soochow University, Suzhou 215123, China

This study investigates the application of silicon photomultiplier (SiPM) in plastic scintillator detectors, and develops a SiPM based position-sensitive detection system. When neutrons or gamma rays enter the scintillator from the end face, the scintillator emits light. By placing multiple SiPMs on the side of the scintillator and utilizing the difference in spatial angle and distance of each SiPM corresponding to the emitting point, the relationship between the readout signal and the particle incidence position can be established. The light signal distribution generated by 1MeV neutrons in an EJ230 scintillator at different positions was simulated using Geant4, and the signal was received by four SiPMs with a size of 12 mm × 12mm. To avoid the problem of uneven response caused by the luminescence of the edge and too weak signals of individual SiPMs, the SiPMs were biased a certain distance relative to the central axis, and a total of five spatial layouts were designed. By comparing the influence of the bias distance on the inversion results, the size of the bias distance was determined. This paper designs a neural network model that outputs corresponding two-dimensional position signals when four-dimensional detector signals are input. The neural network model includes three hidden layers, and the hyperparameters such as the units per layer, learning rate, and batch size are adjusted according to the Bayesian optimization and hyper band (BOHB) algorithm. The analysis of 34,093 sets of data collected from Geant4 simulation shows that using a detector position further away from the central axis is more advantageous to improve the reconstruction accuracy. Experiments were conducted using a collimated Cs-137 radiation source, and data were reconstructed using sequence analysis algorithm and CNN+LSTM network. The experimental results show that the average absolute error of the neural network in reconstructing the incident particle position is about 8mm, which proves the feasibility of using a neural network to reconstruct the incident particle position.

Group Delay Time in Neutron Optics and Neutron Wave Reflection Time

A.I. Frank¹, V.A. Bushuev²

¹Joint Institute for Nuclear Research, Frank Laboratory of Neutron Physics, 6, Joliot Curie str, 141980 Dubna, Moscow region, Russia

²M.V. Lomonosov Moscow State University, Faculty of Physics, Lewinski gory 1, str. 2, GSP-1, 119991 Moscow, Russia

Using the example of the reflection of a neutron pulse (wave packet) from two - and three-layer planar structures, it was previously shown that the formation of the reflected pulse occurs with a certain time delay relative to the incident pulse [1]. This is obviously due to the fact that some time is spent on the penetration of the wave into the medium and its exit back, which is the physical reason for the well-known Goos-Hänchen effect. In the first approximation, this delay is determined by the so-called group delay time (GDT) [2,3], equal to the energy derivative of the phase from the amplitude reflection coefficient.

The report considers a simpler case, namely the reflection of neutrons from a semi-infinite homogeneous medium. As is known, the amplitude of the mirror reflection and the distribution of the field (or wave function) in the medium are described by the exact Fresnel formulas. With their help, it is easy to obtain expressions for the amplitude of reflection, the structure of the field and the depth of penetration of radiation into the medium, but they do not give any answer about the thickness of the near-surface layer in which the reflected wave is formed.

The report discusses the relationship between GDT and the depth of the formation of a neutron wave mirrored from a semi-infinite homogeneous medium. Calculations show that in the region below the threshold of total external reflection (TER), this depth of formation is exactly equal to the depth of penetration of an exponentially decaying wave. However, in the region above the threshold TER, where the penetration depth of radiation increases significantly, both the GDT and the depth of reflected wave formation obtained on the basis of this value, on the contrary, decrease. For a weakly absorbing medium, the estimate of the depth of formation of the reflected wave obtained in this way leads to a non-physical result consisting in a subnanometer depth of this layer.

Attempts to determine the relationship between the depth of reflection formation and GDT in the region above the TER threshold lead to contradictions. In particular, this applies to the results obtained, on the one hand, on the basis of the first Born approximation, and on the other hand, on the basis of calculations of the reflection time of wave packets using the Green function.

In conclusion, the probable reasons for this discrepancy are briefly discussed, as well as possible experimental approaches to measuring the reflection time of a neutron wave.

References

1. V.A. Bushuev, A.I. Frank, *Physics – Uspekhi*, **61** (2018) 952.
2. D. Bohm, *Quantum Theory* (New York: Prentice-Hall, 1951).
3. E.P. Wigner, *Phys. Rev.* **98** (1955) 145.

The Concept of an UCN Source for Periodic Pulsed Reactor

A.I. Frank, G.V. Kulin, V.A. Kurylev, A.A. Popov, M.A. Zakharov

Frank Laboratory of Neutron Physics, JINR, Dubna

Since the discovery of ultracold neutrons (UCN) [1], a number of intense UCN sources have appeared in the world, and several more of them are under construction. There is no UCN source in Dubna, which is largely due to the peculiarities of the JINR IBR-2 pulsed reactor. Its average power of 2 MW is relatively low for creating a continuous UCN source. However, the pulsed thermal neutron flux of this reactor is very high, since the interval between pulses is hundreds of times greater than their duration.

Apparently, the only way to create a sufficiently intense UCN source at a pulsed reactor of moderate power is to implement Shapiro's idea of pulsed filling of a UCN trap [2] in combination with the principle of neutron focusing in time [3]. The first experience of the practical implementation of this idea is reported in [4].

Recently, the idea of pulsed filling of a UCN trap has been actively discussed in the literature. In recent works [5, 6], some approaches to the time focusing of neutrons and methods for deceleration very cold neutrons (VCN) to UCN energies have been analyzed. It was shown in [7] that when a flipper decelerator with a sufficiently high magnetic field is used, the resulting UCN flux should have a distinct pulsed structure even in the absence of a time lens.

The report discusses the concept of a UCN source based on a pulsed reactor based on a combination of a magnetic time lens and a magnetic resonance device that decelerate neutrons. Estimates of the expected neutron density in the trap are given. The proposed concept opens up the possibility of creating a UCN source at JINR with parameters corresponding to the modern world level.

1. V.I. Luschnikov, Y.N. Pokotilovsky, A.V. Strelkov, F.L. Shapiro, *JETP Letters* **9** (1) (1969) 23–26.
2. F.L. Shapiro, *PEPAN* **2** (4) (1971) 975–979.
3. Frank A.I., Gähler R. *Proc. of ISINN-4. Dubna* (1996) 308; A.I. Frank and R. Gähler. *Phys. At. Nuclei*, **63** (2000) 545.
4. Y. Arimoto, P. Gertenbort, S. Imajo et al. *Phys. Rev. A* **86** (2012) 023843.
5. A.I. Frank, G.V. Kulin, N.V. Rebrova, M.A. Zakharov. *Phys. Part. Nuclei* **53** (2022) 33–44.
6. V.V. Nesvizhevsky, A.O. Sidorin. *Phys. Part. Nuclei Letters* **19** (2022) 162–175.
7. A.I. Frank, G.V. Kulin, M.A. Zakharov. *JINR Comm.* P3-2022-66, Dubna (2022).

THE VIRTUAL CHARACTER OF SPONTANEOUS AND INDUCED
(WITH THE PARTICIPATION OF THERMAL NEUTRONS)
TERNARY FISSION OF NUCLEI WITH THE EMISSION OF PRECISSION
NUCLEONS AND LIGHT NUCLEI

S.G. Kadmsky, Y.O. Otvodenko

Voronezh State University, Voronezh, Russia

E-mail: kadmensky@phys.vsu.ru

In elementary particle physics there are known virtual reactions and decays associated with the appearance in their amplitudes of Green's functions of intermediate particles corresponding to their virtual states, whose energies and momenta are not related by Einstein's relativistic formula. Such processes include, for example, Compton scattering of γ - quanta on free electrons [1]. In nuclear physics, it is also possible to identify [2] virtual reactions and decays, when intermediate nuclei appear in their amplitudes of Green functions associated with their virtual states, lying in energies outside the mass surfaces of the processes under consideration. These decays include the double β - decay of atomic nuclei [3]. It was demonstrated in [4-5] that two-proton decay [4] and ternary nuclear fission with the emission of alpha-particles [5] can also be described using the conception of their virtuality.

Using the results of [6-7] it is shown that the conception of the virtuality of spontaneous and induced (with the participation of thermal neutrons) ternary nuclear fission with the emission as third particles not only of alpha-particles, but also of precession neutrons, protons, and light nuclei (d, t, ^3He) allows us to successfully describe the most important characteristics of these processes (yields, angular and energy distributions of third particles).

1. A.I. Akhiezer, V.B. Berestetskii, Quantum Electrodynamics (Fizmatgiz, Moscow, 1959).
2. S.G. Kadmsky, A.O. Bulychev, Bull. Russ. Acad. Sci., Phys. **80**, 1009, (2016).
3. L.A. Sliv, JETP **20**, 1035 (1950).
4. S.G. Kadmsky, U.V. Ivankov, Phys. At. Nucl. **77**, 1019 (2014).
5. S.G. Kadmsky, U.V. Ivankov, Phys. At. Nucl. **77**, 1532 (2014).
6. S.G. Kadmsky, L.V. Titova, Bull. Russ. Acad. Sci., Phys. **85** 732 (2021).
7. S.G. Kadmsky, S.V. Kufaev, Y.O. Otvodenko, Bull. Russ. Acad. Sci., Phys. **86** 1332, (2022).

ACTIVE BRYOMONITORING OF INDUSTRIAL ATMOSPHERIC
FALLOUT USING DIFFERENT SPECIES OF MOSSES

Gorelova S.V.¹, Yushin N.², Peshkova A.², Vergel K.², Zinicovscaia I.²

¹Department of Biology, Natural Sciences Institute, TSU, Tula, Russia

²FLNP JINR, Dubna, Russia

A study of atmospheric deposition of chemical elements in the area affected by metallurgical enterprises and highways was carried out using the active bryomonitoring technique by applying two species of Bryaceae and one species of sphagnum moss: *Pleurozium schreberi*, *Dicranum polysetum* and *Sphagnum fallax*. The moss bags were exposed for three months from November to February at a distance of 200-600 m from large metallurgical enterprises Kosogorsk metallurgical plant (production of ferromanganese and steels), Tulachermet, Evraz vanadium - Tula and Polema (production of alloyed steels, cast iron, ferrovanadium and vanadium pentoxide, high-purity chromium, molybdenum, tungsten, metal powders and composite materials) and also at a distance of 2-5 m from the central highways of the city. The concentrations of elements in mosses were determined using ICP-AES.

All the studied species of mosses showed a high level of accumulation of individual elements - pollutants of each metallurgical production. However, the species differed in the degree of accumulation of individual elements. Thus, *Dicranum polysetum* and *Sphagnum fallax* differed in the accumulation of Al, Fe, Mn, V, Cr in the zone of emissions from metallurgical industries. Pb and Hg were actively accumulated by green (Bryaceae) mosses. *Pleurozium schreberi* showed greater sensitivity to the pollution with S, Ni, and Zn. Actively and regardless of the degree of Cu pollution, the element accumulated was accumulated by *Sphagnum fallax*.

The amount of accumulated metals in the area of impact of metallurgical production decreased in the following order: *Dicranum polysetum* > *Pleurozium schreberi* > *Sphagnum fallax*.

Pleurozium schreberi accumulated elements most actively in the area affected by motor vehicle emissions. In the zone of the most active and severe pollution from several sources, a greater degree of accumulation was characteristic for *Dicranum polysetum*. According to the sum of accumulated elements-pollutants, it can be concluded that among the studied species of mosses *Dicranum polysetum* is the most suitable for active bryomonitoring of atmospheric deposition in technogenically polluted urban ecosystems with a high level of industrial pollution.

Analysis of Multichannel Resonances with Unitary Breit–Wigner and K-Matrix Approaches and with Effective Range M-Matrix Method

V. Henner

Department of Theoretical Physics, Perm State University, 614990 Perm, Russia

We discuss three methods to obtain the parameters of multichannel resonances from data. The K -matrix method guarantees the unitarity of the S -matrix, but its parameters can be considered as resonances masses and widths only for well-spaced states. It also does not allow to separate the resonant and background contributions in scattering amplitudes. The unitarity of the S -matrix can be guaranteed if Breit-Wigner terms are taken with the proper interference phases. A background can be added to the BW amplitudes in the standard way by using background phases. The multichannel effective range approach is a part of M-matrix method. All these methods can be applied to study NN systems.

Status and Prospects of China Spallation Neutron Source CSNS

Tianjiao Liang^{1,2}

¹*Institute of High Energy Physics, Chinese Academy of Sciences, Beijing, 100049, China*

²*Spallation Neutron Source Science Center, Dongguan, 523803, China*

The current status of the CSNS facility is described covering operations, application and development. After three neutron scattering instruments opened to users in October 2018, CSNS ramped the beam power from 20 kW to 140 kW and consistently achieved an availability of more than 95%. Eight neutron instruments are under construction since 2018 and will complete this year, which the total scattering instrument MPI opened to user at 2021 and five instruments start commissioning since last year. The design and performance of these instruments is outlined. The plan of CSNS-II project that would increase the proton beam power to 500 kW and 11 more neutron instruments is also described.

The Application of Tagged Neutron Method for Elemental Analysis of Material on Conveyors

V.Yu. Alexakhin^{1,2}, I.K.Komarov¹, A.I. Lichkunova¹, E.A. Razinkov¹,
Yu.N. Rogov^{1,2}, M.G. Sapozhnikov^{1,2}, I.E.Chirikov-Zorin^{1,2}

¹*Diamant LLC – Dubna, Russia*

²*JINR – Dubna, Russia*

The results of the application of the tagged neutron method (TNM) for elemental analysis of the sinter on the conveyor are discussed. The tagged neutron method consists in irradiation of the substance under study by fast neutrons with an energy of 14 MeV and registration of the induced characteristic gamma radiation. Neutron tagging is carried out by an alpha detector built in a neutron generator.

The analyser provides the results of the elemental analysis of sinter each 40-60 c without taking the probe. It gives possibility to correct elemental content of the sinter to provide its stability. Large penetrating power of the 14 MeV neutrons provides information of the elemental content of large layer of the substance up to 300 mm. The results of the year data taking will be presented.

202

Научное издание

**FUNDAMENTAL INTERACTIONS & NEUTRONS, NUCLEAR STRUCTURE,
ULTRACOLD NEUTRONS, RELATED TOPICS**

XXIX International Seminar on Interaction of Neutrons with Nuclei

Abstracts

**ФУНДАМЕНТАЛЬНЫЕ ВЗАИМОДЕЙСТВИЯ И НЕЙТРОНЫ,
СТРУКТУРА ЯДРА, УЛЬТРАХОЛОДНЫЕ НЕЙТРОНЫ
И СВЯЗАННЫЕ ВОПРОСЫ**

XXIX Международный семинар по взаимодействию нейтронов с ядрами

Тезисы докладов

Ответственная за подготовку сборника к печати *Л. В. Мицына*.

Сборник отпечатан методом прямого репродуцирования с оригиналов,
предоставленных оргкомитетом.

E3-2023-16

Подписано в печать 16.05.2023

Формат 60×90/16. Бумага офсетная. Печать цифровая
Усл. печ. л. 7,75. Уч.-изд. л. 13,53. Тираж 150 экз. Заказ № 60651

Издательский отдел Объединенного института ядерных исследований
141980, г. Дубна, Московская обл., ул. Жолио-Кюри, 6.

E-mail: publish@jinr.ru

www.jinr.ru/publish/